RUAN MALONI TEIXEIRA

ACTIVATION OF THE NIK1/RPL10/LIMYB SIGNALING CIRCUIT BY BIOTIC AND ABIOTIC SIGNALS AND REGULATION OF DEFENSE AND GROWTH PARAMETERS

Thesis submitted to the Applied Biochemistry Graduate Program of the Universidade Federal de Viçosa in partial fulfillment of the requirements for the degree of *Doctor Scientiae*.

Adviser: Elizabeth Pacheco Batista Fontes

Co-advisers: Christiane Eliza M. Duarte
Pedro Augusto Braga dos Reis
Virgílio Adriano Pereira Loriato

VIÇOSA – MINAS GERAIS
2022

Ficha catalográfica elaborada pela Biblioteca Central da Universidade Federal de Viçosa - Campus Viçosa

T
T266
a2022

Teixeira, Ruan Maloni, 1990-
Activation of the NIK1/RPL10/LIMYB signaling circuit by bioticand abiotic signals and regulation of defense and growth parameters / Ruan Maloni Teixeira. - Viçosa, MG, 2022.
1 tese eletrônica (128 f.): il. (algumas color.).

Texto em inglês.
Orientador: Elizabeth Pacheco Batista Fontes.
Tese (doutorado) - Universidade Federal de Viçosa, Departamento de Bioquímica e Biologia Molecular, 2022.
Inclui bibliografia.
DOI: https://doi.org/10.47328/ufvbbt.2022.191
Modo de acesso: World Wide Web.

1. Biologia Molecular. 2. Plantas - Resistência a doenças e pragas.
3. Stress (Fisiologia). 4. Regulação de expressão gênica. 5. Lignina.
I. Fontes, Elizabeth Pacheco Batista, 1957-. II. Universidade Federal de Viçosa. Departamento de Bioquímica e Biologia Molecular. Programade Pós-Graduação em Bioquímica Aplicada.
III. Título.

CDD 22. ed. 572.865

Bibliotecário(a) responsável: Renata de Fátima Alves CRB6/2578

RUAN MALONI TEIXEIRA

ACTIVATION OF THE NIK1/RPL10/LIMYB SIGNALING CIRCUIT BY BIOTIC AND ABIOTIC SIGNALS AND REGULATION OF DEFENSE AND GROWTH PARAMETERS

Thesis submitted to the Applied Biochemistry Graduate Program of the Universidade Federal de Viçosa in partial fulfillment of the requirements for the degree of *Doctor Scientiae*.

APPROVED: January 28, 2022.

Assent:

Ruan Maloni Teixeira
Author

Elizabeth Pacheco Batista Fontes
Adviser

ACKNOWLEDGMENTS

Primeiramente agradeço a Deus, por me guiar até aqui e me dar forças para seguir em frente, mostrando-me que sempre há mais luz do que trevas. Até aqui nos ajudou o senhor! Agradeço a Virgem Santíssima, Nossa Senhora Aparecida pela intercessão a mim sempre cedida.

Agradeço aos meus Pais, Sebastião e Eliane que sempre lutaram para que eu possa prosseguir com meus sonhos, me dando educação, amor, apoio e preparo para os desafios no caminho. Sempre com muita humildade e fé.

Agradeço a minha orientadora Professora Elizabeth P.B. Fontes, pela contribuição para o meu crescimento profissional, me guiando por caminhos rumo a excelência. Agradeço também pela oportunidade de trabalho que me foi concedida e todo aprendizado e formação até aqui.

Agradeço ao Gabriel Saraiva por toda contribuição com este trabalho e pela amizade que estabelecemos. Ao Otto Fraga e ao Eduardo Bassi pela ajuda em momentos impares e pela amizade que designou este “quarteto”.

Agradeço ao Marco Aurélio pela amizade e parceria que exercemos e por toda ajuda neste trabalho ao qual foi tão presente.

Cleyssinho pela amizade, contribuição com este trabalho e incentivo de sempre. Ao Otávio por toda contribuição com este trabalho. Agradeço aos dois pela condução das análises de bioinformática.

Agradeço aos meus Coorientadores, Professora Christiane E.M. Duarte (UEMG), Professor Pedro A.B. Reis e Virgílio A.P. Loriato. Agradeço toda contribuição em prol de minha formação. Agradeço aos queridos estudantes de iniciação que me acompanharam em parte desta jornada, Nathália e Igor pela dedicação e prestatividade de sempre.

A toda equipe do Laboratório de Biologia Molecular de Plantas, em especial aos companheiros Sâmera, Thaina e Nivea.

Agradeço ao Professor Humberto Ramos e sua equipe por todo suporte em especial, Lucas Leal (lukinha), Flaviane, Angélica, Danilo e Valquíria.

Agradeço a Rose por todo apoio que me deu durante estes anos e pelo incentivo em prol deste trabalho.

Agradeço também a Analu Zanotti, pela parceria eterna construída em Alegre para o resto da vida. E pela condução das análises histológicas de tecidos vegetais.

À Universidade Federal de Viçosa pela oportunidade de crescimento em uma instituição de excelência. Ao Núcleo de Análises de Biomoléculas (Nubiomol) pelo uso de equipamentos necessários a realização deste projeto.

À coordenação de aperfeiçoamento de pessoal de nível superior (CAPES) O presente trabalho foi realizado com apoio da Coordenação de Aperfeiçoamento de Pessoal de Nível Superior – Brasil (CAPES) – Código de Financiamento 001.

Agradeço à FAPEMIG pelo suporte financeiro para realização deste projeto.

Ao Conselho Nacional de Desenvolvimento Científico e Tecnológico (CNPq).

ABSTRACT

TEIXEIRA, Ruan Maloni, D.Sc., Universidade Federal de Viçosa, January, 2022. **Activation of the NIK1/RPL10/LIMYB signaling circuit by biotic and abiotic signals and regulation of defense and growth parameters.** Adviser: Elizabeth Pacheco Batista Fontes. Co-advisers: Christiane Eliza Motta Duarte, Pedro Augusto Braga dos Reis and Virgílio Adriano Pereira Loriato.

Plants are constantly exposed to different microorganisms such as viral pathogens. Geminiviruses are circular DNA viruses encapsidated in geminate virion particles, which infect many crops and cause significant agricultural restrictions. Geminiviruses developed strategies to evade a potent plant antiviral immune system maintaining their broad spectrum of hosts and establishing successful infections. For this, it is necessary that these viruses overcome a multilayered perception system represented by RNA interference sensors and effectors, pattern recognition receptors (PRR) and resistance proteins (R). This recognition system leads to the activation of conserved defense responses that protect plants against different viral and non-viral pathogens existing in nature. Furthermore, a specific antiviral cell surface receptor signaling is activated early in geminivirus infection to suppress global translation. In this investigation, we first presented a review of the layers of virus perception and host defenses and the mechanisms developed by geminiviruses to overcome the plant's antiviral immunity mechanisms. Plant immunity depends on recognition of viral components or effectors by host receptors. This system is composed of two defense layers; the first one occurs from the recognition of molecular patterns associated with pathogens (PAMPs), designated PAMP-triggered immunity (PTI) and effector-triggered immunity (ETI). Emerging evidence in the literature has included classic PTI in the innate antiviral immune arsenal of plant cells. Therefore, our understanding of PAMPs has expanded to include not only classical PAMPs such as bacterial flagellin or fungal chitin, but also virus-derived nucleic acids that can also activate PAMP recognition receptors as documented for mammalian viruses. In our second review, we discussed the understanding that plant viruses can activate classical PTI, leading to both unique antiviral responses and conserved responses to pathogens. We also present evidence that PAMPs derived from viral nucleic acids can trigger the NUCLEAR SHUTTLE PROTEIN-INTERACTING KINASE 1 (NIK1)-mediated antiviral immunity. The NIK1 immune pathway is initiated after perception that leads to receptor phosphorylation, triggering a signaling cascade that phosphorylates the *ribosomal protein L10* (RPL10), which is translocated to the nucleus and interacts with the factor *L10*-

INTERACTING MYB DOMAIN-CONTAINING PROTEIN (LIMYB) to suppress host global translation. Transcriptome studies by overexpressing LIMYB in Arabidopsis also demonstrated that LIMYB, in addition to translation-related genes, represses the expression of photosynthetic apparatus-related genes. Photosynthesis and translation are targets of metabolic control and development in plants; however, how stress signals coordinately regulate these opposing energy production and consumption processes remains enigmatic. Here, we delineate a growth control circuit that links photosynthetic function to translational control in response to biotic and abiotic signals. We first showed that the downstream component of the NIK1/RPL10 antiviral signaling circuit, LIMYB, which represses the expression of translation machinery-related genes, also represses the expression of transcriptional repression activity of LIMYB was the main determinant for the decrease in electron transport rate, gas exchange parameters, quantum efficiency and water use efficiency in the LIMYB-ectopic expressing lines. Decreased photosynthetic activity was linked to NIK1 antiviral signaling and stunted growth. NIK1 activation by viral or bacterial PAMPs, or by expressing a constitutively activated NIK1mutant, T474D, inhibited photosynthetic function in control lines, but not in *limyb* knockout plants. We have also shown that heat and osmotic stress activate the NIK1/RPL10/LIMYB signaling circuit. Coordinated inhibition of photosynthesis and translation via the stress-activated NIK1/RPL10/LIMYB signaling module can adjust the plant's growth pattern in response to the changing environment. Finally, the RNA-seq and ChIP-seq analyses also defined a set of genes upregulated by LIMYB. Among them, phenylpropanoid biosynthesis genes were remarkably enriched. NIK1 activation by begomovirus-derived nucleic acids induced genes involved in lignin synthesis. As a result, the transgenic lines LIMYB and T474D displayed higher lignin content than the control lines. As a plant defense mechanism, the attack by pathogens leads to the thickening of the cell wall by lignification to prevent the entry of microorganisms, a process typically controlled by MYB-type transcription factors. Consequently, the results of this investigation extended the transcriptional function of LIMYB, demonstrating that it also targets photosynthesis and lignin synthesis. They indicated that the NIK1/RPL10/LIMYB signaling module, initially described as an antiviral signal transducer, controls plant growth under biotic and abiotic stress conditions and may also define another layer of defense against non-viral pathogens via lignin accumulation.

Keywords: Molecular Biology. Plants. Transcriptome. LIMYB. plant immunity. viral PAMPs. NIK1. Heat Stress. Osmotic Stress. Phenylpropanoids. Lignin Synthesis.

RESUMO

TEIXEIRA, Ruan Maloni, D.Sc., Universidade Federal de Viçosa, janeiro de 2022. **Ativação do circuito de sinalização NIK1/RPL10/LIMYB por sinais bióticos e abióticos e regulação de parâmetros de defesa e crescimento.** Orientadora: Elizabeth Pacheco Batista Fontes. Coorientadores: Christiane Eliza Motta Duarte, Pedro Augusto Braga dos Reis e Virgílio Adriano Pereira Loriato.

Plantas estão constantemente expostas a diferentes microrganismos, como patógenos virais. Geminivirus são vírus de DNA circular encapsidados em partículas virais geminadas, que infectam muitas variedades de culturas vegetais, causando restrições agrícolas expressivas mundialmente. Os geminivirus desenvolveram estratégias para contornar um potente sistema imunológico antiviral vegetal, e assim manter seu amplo espectro de hospedeiros e estabelecer infecções bem-sucedidas. Para isso, foi necessário que estes vírus superassem um sistema de percepção em multicamadas representadas por sensores e efetores de RNA de interferência, receptores de reconhecimento de padrões moleculares de patógenos (PRR) e proteínas de resistência (R). Este sistema de reconhecimento leva à ativação de respostas de defesa conservadas que protegem as plantas contra diferentes patógenos virais e não-virais. Além disso, uma sinalização específica de receptor de superfície celular antiviral é ativada no início da infecção por geminivírus para suprimir a tradução global. Nesta investigação, foram inicialmente discutidas camadas de percepção e defesas do hospedeiro contra vírus e os mecanismos desenvolvidos pelos geminivírus para superar os mecanismos de imunidade antiviral da planta. A imunidade das plantas depende do reconhecimento de componentes virais ou efetores virais por receptores hospedeiros. Este sistema é composto por duas camadas de defesa, a primeira ocorre a partir do reconhecimento de padrões moleculares associados a patógenos (PAMPs), denominada imunidade desencadeada por PAMPs (PTI) e imunidade desencadeada por efetores (ETI). Evidências emergentes na literatura incluíram o PTI clássico no arsenal imunológico inato antiviral das células vegetais. Portanto, nosso entendimento dos PAMPs expandiu-se para incluir não apenas PAMPS clássicos, como a flagelina bacteriana ou quitina fúngica, mas também ácidos nucleicos derivados de vírus que também podem ativar receptores de reconhecimento PAMPs como os fenômenos documentados em vírus de mamíferos. Em uma segunda revisão, foi apresentado evidências de que os vírus vegetais podem ativar a PTI clássica, levando tanto a respostas antivirais únicas, quanto respostas conservadas a patógenos. Também foi demonstrado de que PAMPs derivados de ácidos nucleicos virais ativam a via de imunidade antiviral mediada pelo receptor NIK1 ("NUCLEAR

SHUTTLEPROTEIN-INTERACTING KINASE 1"). A via de imunidade de NIK1 é iniciada após a percepção de PAMPs virais por um receptor ainda desconhecido o que leva à fosforilação e ativação de NIK1, desencadeando uma cascata de sinalização que fosforila a proteína ribossomal L10 (RPL10). RPL10 fosforilada é translocada do citoplasma para o núcleo, onde interage com o fator LIMYB ("L10-INTERACTING MYB DOMAIN-CONTAINING PROTEIN"*)* para reprimir a expressão de genes da maquinaria de tradução resultando em supressão global do hospedeiro. Nesta investigação, foi determinado o transcriptoma induzido pela superexpressão de LIMYB em Arabidopsis demonstrando que LIMYB também reprime a expressão de componentes do aparato fotossintético. Fotossíntese e tradução são alvos de controle e desenvolvimento metabólico em plantas; no entanto, o mecanismo pelo qual os sinais de estresse regulam coordenadamente esses processos opostos de produção e consumo de energia permanece enigmático. Os resultados definiram um circuito de controle de crescimento que liga a função fotossintética ao controle traducional em resposta a sinais bióticos e abióticos. Inicialmente, uma análise conjunta de RNA-seq e ChIP-seq de linhagens overexpressando LIMYB demonstrou que este componente a jusante do circuito de sinalização antiviral NIK1/RPL10, que reprime a expressão gênica de genes relacionados à maquinaria de tradução, também liga a promotores e reprime a expressão de genes relacionados ao aparato fotossintético, levando à inibição da função fotossintética. A atividade transcricional de repressão de LIMYB foi o principal determinante para a diminuição da taxa de transporte de elétrons, parâmetros de trocas gasosas, eficiência quântica e eficiência do uso da água nas linhagens expressando ectopicamente LIMYB. A diminuição da atividade fotossintética foi associada com a sinalização antiviral de NIK1 e crescimento atrofiado. A ativação de NIK1 por PAMPs virais ou bacterianos, ou a expressão de um mutante NIK1 constitutivamente ativado, T474D, inibiram a função fotossintética em linhagens de controle, mas não em plantas nocaute *limyb*. Também foi demonstrado que o calor e o estresse osmótico ativam o circuito de sinalização NIK1/RPL10/LIMYB. A inibição coordenada da fotossíntese e da tradução por meio do módulo de sinalização NIK1/RPL10/LIMYB ativado por estresse pode ajustar o padrão de crescimento da planta em resposta a mudanças no meio ambiente. Finalmente, as análises de RNA-seq e ChIP-seq também definiram um conjunto de genes regulados positivamente por LIMYB. Entreeles, os genes da biossíntese de fenilpropanóides foram notavelmente enriquecidos. A ativação de NIK1 por ácidos nucleicos derivados de begomovírus induziu genes envolvidos na síntese de lignina. Como resultado, as linhagens transgênicas LIMYB e T474D apresentaram maior teor de lignina total do que as linhagens controle. Como mecanismo de defesa da planta, o ataque de patógenos leva ao espessamento da parede celular por lignificação

para impedir a entrada de microrganismos, processo tipicamente controlado por fatores de transcrição do tipo MYB. Consequentemente, os resultados desta investigação estenderam a função transcricional de LIMYB, demonstrando que também tem como alvo a fotossíntese e a síntese de lignina. Eles indicaram que o módulo de sinalização NIK1/RPL10/LIMYB, inicialmente descrito como um transmissor de sinal antiviral, controla o crescimento de plantas sob condições de estresses biótico e abiótico e também pode definir outra camada de defesa contra patógenos não virais através do acúmulo de lignina.

Palavras-chave: Biologia Molecular de Plantas. Transcriptoma. LIMYB. Imunidade Vegetal. PAMPs virais. NIK1. Estresse Térmico. Estresse Osmótico. Fenilpropanoides. Síntese de Lignina.

SUMMARY

General Introduction

Plants are constantly subjected to biotic and abiotic stresses, respectively caused by pathogens, water stress or unpredictable changes in ambient light. Changes in luminosity are predictable in terms of plant perception of the day and night cycle, however, there are limitations in responses related to weather effects, shading by competitors, herbivory and infectious agents (Belbin et al., 2016). During plant development, metabolic processes are dependent on light conditions, which are perceived by a complex signaling network that involves photoreceptors and mainly transcription factors that act to promote adaptation (Bae and Choi, 2008). Frequent modifications in light availability require a fine modulation of electron capture and electron transfer reactions in order to avoid the opposition between light conversion and metabolic relationships, which may lead to inefficient assimilation, as well as the production of reactive oxygen species (Chaux, 2017).

The attack by pathogens is another important factor that causes considerable losses to agricultural productivity. The phytopathogens infection results in the induction of defense reactions as well as the downregulation of genes involved in photosynthesis (Berger et al., 2004; Qi et al., 2018). A common response to pathogens is the reduction of the photosynthetic rate in infected leaves (Bilgin et al., 2010). Since plants are constantly under attack by viral, bacterial or fungal agents, for example, the host is trapped in an evolutionary arms race, which impulses the development of a series of defense strategies. Once an attack is perceived, the plant metabolism must potentialize the balance of resource allocation to support defense and the conditions for cell maintenance, growth and reproduction (Zangerl and Berenbaum 1997, 2003; Berger, Sinha and Roitsch 2007).

The plant perception of diverse molecular patterns associated with pathogens (PAMPs) characterizes a sophisticated first layer of defense, denominated PAMP- triggered immunity (PTI) (Jones and Dangl, 2006; Ausubel, 2005; Tian et al., 2003; Zavala and Baldwin, 2004; Tian et al., 2017). The recognition of these elicitors occurs through pattern recognition receptors (PRRs) of the kinase type in the plasma membrane, thus initiating the defense process (Ben Khaled, Postma and Robatzek, 2015; Boller and Felix, 2009; Monaghan and Zipfel, 2012; Dangl et al., 2013). Nonetheless, several virulent agents managed to overcome this first layer of defense through the secretion of effectors to interfere with the signals triggered by these membrane receptors. Consequently, plants evolved and generated resistance proteins, designated NUCLEOTIDE BINDING SITE-LEUCINE RICH REPEATS (NBS-LRR), capable of recognizing virulence effectors, then triggering a second line of defense, termed

effector triggered immunity (ETI), which activates the hypersensitive response and programmed cell death (Dodds and Rathejen, 2010; Stotz et al., 2014).

The defense strategies generated from PTI and ETI overlap a series of processes to combat pathogens, including transcriptional reprogramming, ion flow, activation of kinase sets, and remodeling of the cell wall by lignification (Nicholson and Hammerschmidt, 1992; Torres, 2010; Tsuda and Katagiri, 2010). The increase in lignin deposition in response to biotic stresses plays an important role in the support of resistance(Nicholson and Hammerschmidt, 1992; Sattler and Funnell-Harris, 2013). The cell wall thickening strategy has great importance against the action of herbirvors, which can be vectors for many infectious agents, in addition to the injuriousness against these predators, the progression of invasive pathogens is hindered.(Humphrey, 2007; Cantu et al., 2008; Hematy et al., 2009).

Attack by predators leads to induction of lignification, through the increase of the synthesis of monolignols, which make up the polymer (Boerjan et al., 2003; Vogt, 2010;Chezem et al., 2017). This mechanism is controlled by MYB factors, which commonly modulate the transcription of genes related to phenylpropanoid biosynthesis, which from its production pathway, are precursor substrates of composition of the lignin chain (Dubos et al., 2010). MYB factors are important regulators that widely act in primary and secondary metabolism, having important roles in the development and defense of plants against biotic and abiotic stresses (Liu, Osbourn and Ma, 2015).

The MYB-type factors also regulate processes coordinated with photosynthesis, such as the circadian cycle, through the regulation of light-harvesting complex proteins (Lhcb), that are directly involved in light capture. The fine-tuning between the photoperiod and the internal clock aids the correct transduction of signals to genes linked to developmental processes (Anon,2018; Fukuda et al., 2018).

Recent studies have identified a new transcription factor that belongs to the R2R3- Myb group, termed L10-INTERACTING MYB DOMAIN-CONTAINING PROTEIN (LIMYB), which participates in an antiviral defense pathway, that when activated represses the transcription of ribosomal protein genes and translation factors, leading to the global suppression of translation (Zorzatto et al., 2015). The identification of LIMYB occurred through researches on plant defense strategies against viruses carried out in Arabidopsis thaliana, in which the elucidation of an antiviral defense pathway was initiated. It was reported that the viral protein NSP (Nuclear shuttle protein) from Begomovirus, a genus of the Geminiviridae family, was found to interact with a membrane receptor kinase, designated NSP-INTERACTING KINASE (NIK1), which triggers a cascade of defense against

begomoviruses (Mariano et al., 2004; Fontes et al., 2004). NSP binds to the cytoplasmic portion of NIK1, in its activation loop, and inhibits kinase activity, preventing the defense pathway, thus benefitingviral propagation (Fontes et al., 2004).

During viral infection, after perception of PAMPs derived from viral nucleic acids, NIK1oligomerizes with itself or with another unknown receptor, enabling phosphorylation at threonine residue 474, which activates antiviral defense signaling. Activated NIK1 mediates the phosphorylation of the ribosomal protein (RP) RPL10, which is then directed to the nucleus(Fontes et al., 2004; Rocha et al., 2008; Santos, et al., 2009; Teixeira et al., 2019). In the nucleus, RPL10 interacts with LIMYB in order to repress genes involved in the translation machinery culminating in global suppression of protein synthesis (Zorzatto et al., 2015). It has recently been shown that NIK1 antiviral signaling can communicate with the antibacterial immunity (Li et al., 2019). NIK1 interacts with the pattern recognition receptor (PRR) FLAGELLIN-SENSITIVE 2 (FLS2) and its co-receptor BRASSINOSTEROID INSENSITIVE1 (BRI1)-ASSOCIATED KINASE 1 (BAK1) to modulate the PAMP-induced (flagellin) FLS2- BAK1 immune complex formation, and thereby regulating an extent of PTI activation that could affect growth (Li et al., 2019). In spite of that, the activation of the FLS2-BAK1 immune complex results in phosphorylation of NIK1 and its signaling is initiated, which phosphorylates RPL10, which then translocates to the nucleus and interacts with the factor LIMYB, leading to global translation suppression (Zorzatto et al., 2015 ; Li et al., 2019). LIMYB is recognized for its role in NIK1-mediated antiviral defense, but its developmental role has not been described. LIMYB has two Myb/SANT-like domains in its structure. Myb/SANT proteins can interact with DNA and act as transcription factors or, in the case of SANT domains, control the chromatin remodeling by association with histones (Bartholomew, 2014). In the scope of identifying and understanding biological processesregulated by this factor, we conducted analyzes of ChIP-Seq that identified its binding to not only ribosomal protein gene promoters, but also photosynthetic apparatus and phenylpropanoid pathway genes. The promoter sequences were evaluated for the presence of cis-regulatoryelements, and three consensus sequences were noted, C[A/C/T]AA[A/C/G]C, AAGAA[A/G][A/C and a conserved element [A/G]TATAT[A/G] which may be the main LIMYB recognition sites.

The integrative analysis in plants overexpressing LIMYB, by analyzing the accumulation of transcripts via RNA-Seq and identifying the binding to the respective promoters by ChIP-Seq, demonstrated that this factor is possibly capable of modulating

pathways in different ways, reducing or intensifying gene expression. In this context, we proceeded with functional analysis to understand how these processes are regulated. Plants have multifunctional components, implying that a protein or a structural fold can regulate several partners, resulting in different biological outputs, whether to proceed with developmental processes, as well as to activate a line of defense during the response against pathogens (Grosse-Holz et al., 2016). This management is often initiated by kinase membrane receptors, which can act by directing responses according to the perception of the environment, or by recognizing pathogens in the innate immune defense, which allows communication with the outside of the cell to initiate the adaptive intracellular response (Torii, 2018).

LIMYB plays an essential role in the antiviral defense pathway triggered by NIK1, and thecomplete understanding of its function becomes even more relevant due to the increased incidence and aggravation of Geminivirus diseases (Zorzatto, et al., 2015; Mansoor, Zafar and Briddon, 2006; Navas-Castillo, Fiallo-Olivé and Sánchez-Campos, 2011). During the coevolution between plants and pathogens, viruses of the Geminiviridae family excel in their competence to overcome defense strategies and in terms of host diversification (Scholthof et al., 2011; Hanley-Bowdoin et al., 2013). Besides its relevance in plant immune defense, LIMYB belongs to a promising group of MYB factors, which participate at different metabolic levels (Xie et al., 2010). The elucidation of the signals that activate the NIK1/RPL10/LIMYB immune circuit, and their resulting effects were the focus of this work. Initially, this research aimed to carry out functional studies of this circuit on developmental processes, coordinating the global inhibition of translation with the regulation of photosynthetic activity, under biotic stress conditions, based on the perception of viral elicitors; or due to abiotic stresses like heat and osmotic stress. In addition, it was also intended to verify the influence of LIMYB in the defense process against pathogens, which includes cell wall thickening by increasing lignification. In order to legitimize these hypotheses, this investigation was organized into fourchapters. The First chapter focuses on the RNA silencing mechanisms and innate antiviral immunity that are implemented by plants to counter infections by viral pathogens and the strategies that geminiviruses have evolved to overcome these defense barriers. The Chapter I was publishedin the journal Microorganisms, and is entitled “Geminiviral Triggers and Suppressors of PlantAntiviral Immunity” (Teixeira et al., 2021). The third chapter was submitted to the journal ThePlant Cell, and is entitled "A molecular link between photosynthesis and translation under biotic and abiotic stresses". The

second chapter presents a review that discusses the knowledge of plant viruses activating classical PTI, leading both to unique antiviral defenses and conserved responses to pathogens. In search of further evidence, we present findings that PAMPs from viral nucleic acids activate the NIK1-mediated antiviral signaling pathway that transduces an antiviral signalto suppress the host's global translation. This chapter entitled “Virus perception at the cell surface: revisiting the roles of receptor-like kinases as viral pattern recognition receptors” (Teixeira et al., 2019) was published in the Molecular Plant Pathology journal. The chapter III investigated the decrease in photosynthesis throughtranscriptional regulation of LIMYB, presenting evidence of repression in target promoters of genes that code for proteins of the photosynthetic apparatus and how this mechanism might belinked to the NIK1 pathway in development processes and responses to biotic and abiotic stresses. In chapter IV, entitled “LIMYB induces lignin accumulation via NIK1 antiviral signaling”, we investigated LIMYB as a positive regulator lignin biosynthesis, which acts in target gene promoters of the phenylpropanoids pathway, that directly participate in the processing of substrates of this pathway.

We showed that treatment of plants with DNA and RNA from begomovirus- infected plants activates the NIK1-mediated antiviral pathway, monitored by analyzing the nucleic acid- induced repression of ribosomal protein genes and phosphorylation of NIK1 and RPL10. Our results indicate that begomoviral RNA and DNA function as PAMPs to activate the NIK1- mediated antiviral signaling pathway. A more direct link between translational repression andphotosynthesis inhibition is also demonstrated as the viral PAMPs also induce repression of the photosynthetic apparatus components. Subsequently, heat and osmotic stress caused repression of the translation-associated and photosynthesis-associated marker genes in Col-0, nik1-1 and nik2-1, but not in nik1- 1/nik2-1 mutant. These results indicate that abiotic stress- mediated repression of the marker genes required NIK1 or NIK2 function. Therefore, abiotic stress conditions may also activate the NIK1-mediated signaling pathway to coordinately downregulate translation and photosynthesis. Additionally, it was shown that LIMYB not only acts as a repressor, but also as a modulator that upregulates genes involved in the lignification process, that belong to the phenylpropanoids biosynthesis pathway.

References

Albrecht, C.; Russinova, E.; Kemmerling, B.; Kwaaitaal, M. and De Vries, S. C. (2008). Arabidopsis somatic embryogenesis receptor kinase proteins serve brassinosteroid – dependent and independent signaling pathways. Plant Physiology.**148**: 611- 619.

Anon. (2018). The green site of TRANSFAC: Gene regulation controlled by MYB related factors in plants. Available at: http://gene-regulation.com/info/plant.html.

Ausubel, F.M. (2005). Are innate immune signaling pathways in plants and animals conserved? Nat Immunol. **6**: 973–979.

Bae, G. and Choi, G. (2008). Decoding of light signals by plant phytochromes and their interacting proteins. Annu Rev Plant Biol. **59**: 281-311.

Bartholomew, B. (2014). ISWI Chromatin Remodeling: One primary actor or a coordinated effort? Curr Opin Struct Biol. **24:** 150–155.

Belbin, F.E., Noordally, Z.B., Wetherill, S.J., Atkins, K.A., Franklin, K.A. and Dodd, A.N. (2016). Integration of light and circadian signals that regulate chloroplast transcription bya nuclear-encoded sigma factor. New Phytologist. **213:** 727–738.

Ben, Khaled., S., Postma, J., Robatzek, S. (2015). A Moving View: Subcellular Trafficking Processes in Pattern Recognition Receptor-Triggered Plant Immunity. Annu. Rev. Phytopathol. **53**: 379-402.

Berger, S., Papadopoulos, M., Schreiber, U., Kaiser, W. and Roitsch, T. (2004). Complex regulation of gene expression, photosynthesis and sugar levels by pathogen infection in tomato. Physiol Plant. **122**: 419–428.

Berger, S., Sinha, A.K. and Roitsch, T. (2007). Plant physiology meets phytopathology: plantprimary metabolism and plant-pathogen interactions. J. Exp. Bot. **58**: 4019–4026.

Bilgin, D.D., Zavala, J.A., Zhu, J., Clough, S.J., Ort, D.R. and Delucia, E.H. (2010).Biotic stress globally downregulates photosynthesis genes. Plant Cell Environ. **33**: 1597–1613.

Boerjan, W., Ralph J. and Baucher, M. (2003). Lignin biosynthesis. Annu Rev Plant Biol.**54**,519–546.

Boller, T. and Felix, G. (2009). A renaissance of elicitors: perception of microbe associated molecular patterns and danger signals by pattern-recognition receptors. Annual Review ofPlant Biology. **60**, 379–406.

Brustolini, O., Machado, J., Condori-Apfata, J.A., Coco, D., Deguchi, M., Loriato, V., Pereira, W.A., et al. (2015). Sustained NIK-mediated antiviral signaling confers broad-spectrum tolerance to begomoviruses in cultivated plants. Plant Biotechnol J. **13**: 1300-1311.

Cantu D., Vicente A. R., Labavitch J. M., Bennett A. B. and Powell A. L. (2008). Strangersin the matrix: plant cell walls and pathogen susceptibility. Trends Plant Sci. **13**: 610–617.

Carvalho, C.M., Santos, A.A., Pires, S.R., Rocha, C.S., Saraiva, D.I., Machado, J.P.B., Mattos, E.C., Fietto, L.G., and Fontes, E.P.B. (2008). Regulated nuclear trafficking of rpL10A mediated by NIK1 represents a defense strategy of plant cells against virus. PLoSPathog. **4**: e1000247.

Chaux, F., Johnson, X., Auroy, P., Beyly-Adriano, A., Te, I., Cuiné, S., et al. (2017).PGRL1 and LHCSR3 Compensate for Each Other in Controlling Photosynthesis and Avoiding Photosystem I Photoinhibition during High Light Acclimation of Chlamydomonas Cells.Mol Plant. **10**: 216–218.

Chezem, W. R., Memon, A., Li, F. S., Weng, J. K., & Clay, N. K. (2017). SG2-Type R2R3-MYB Transcription Factor MYB15 Controls Defense-Induced Lignification and BasalImmunity in Arabidopsis. The Plant cell. 8: 1907–1926.

Dangl, J.L., Horvath, D.M. and Staskawicz, B.J. (2013). Pivoting the plant immune systemfrom dissection to deployment. Science. **341**: 746–751.

Dodds, P.N. and Rathjen, J.P. (2010). Plant immunity: towards an integrated view of plant-pathogen interactions. Nat Rev Gene. **11**: 539–548.

Dubos, C., Stracke, R., Grotewold, E., Weisshaar, B., Martin, C. and Lepiniec, L. (2010). MYB transcription factors in Arabidopsis. Trends Plant Sci. **15**: 573–581.

Fontes, E.P.B., Santos, A.A., Luz, D.F., Waclawovsky, A.J., and Chory, J. (2004). The geminivirus nuclear shuttle protein is a virulence factor that suppresses transmembrane receptor kinase activity. Genes Dev. **18**: 2545–2556.

Fukuda, S., Hirasawa, E., Takemura, T., Takahashi, S., Chokshi, K., Pancha, I., Tanaka, K. and Imamura, S. (2018). Accelerated triacylglycerol production without growth inhibition by overexpression of a glycerol-3-phosphate acyltransferase in the unicellular red alga Cyanidioschyzon merolae. Sci Rep. **8**: 12410.

Grosse-Holz, F.M. and Renier, A.L. Van Der Hoorn. (2016). Juggling jobs: roles and mechanisms of multifunctional protease inhibitors in plants. New Phytol. **210**: 794– 807.

Hanley-Bowdoin L., Bejarano, E.R., Robertson D. and Mansoor, S. (2013). Geminiviruses: masters at redirecting and reprogramming plant processes. Nat Rev Microbiol. **11**: 777–88.

Hematy, K., Cherk, C. and Somerville, S. (2009). Host–pathogen warfare at the plant cell wall. Curr. Opin. Plant Biol. **12**: 406–413.

Humphrey, T.V., Bonetta, D.T. and Goring, D.R. (2007). Sentinels at the wall: cell wall receptors and sensors. New Phytol. **176**: 7–21.

Jones, J.D.G. and Dangl, J.L. (2006). The plant immune system. Nature, **444**: 323-329.

Liu, J., Osbourn, A. and Ma, P. (2015). MYB Transcription Factors as Regulators of Phenylpropanoid Metabolism in Plants. Mol Plant. **8**: 689–708.

Mansoor, S., Zafar, Y. and Briddon, R.W. (2006). Geminivirus disease complexes: thethreatisspreading. Trends Plant Sci. **11**: 209–212.

Mariano, A.C., Andrade, M.O., Santos, A.A., Carolino, S.M.B., Oliveira, M.L., Baracat- Pereira, M.C., Brommonshenkel, S.H., and Fontes, E.P.B. (2004). Identification of a novel receptor-like protein kinase that interacts with a geminivirus nuclear shuttle protein.Virology. **318**: 24–31.

Monaghan, J. and Zipfel, C. (2012). Plant pattern recognition receptor complexes at the plasmamembrane. Curr Opin Plant Biol. **15**: 349–357.

Navas-Castillo, J., Fiallo-Olivé, E. and Sánchez-Campos, S. (2011). Emerging virus diseases transmitted by whiteflies. Annu Rev Phytopathol. **49**: 219–248.

Nicholson, R. L., and Hammerschmidt, R. (1992). Phenolic compounds and their role in disease resistance. Annu. Rev. Phytopathol. **30**: 369–389.

Qi, J., Song, C.P., Wang, B., Zhou, J., Kangasjärvi, J., Zhu, J.K. and Gong, Z. (2018). Reactive oxygen species signaling and stomatal movement in plant responses to drought stress and pathogen attack. J Integr Plant Biol. **60**: 805–826.

Rocha, C.S., Santos, A.A., Machado, J.P.B. and Fontes, E.P.B. (2008). The ribosomal protein L10/QM-like protein is a component of the NIK-mediated antiviral signaling. Virology. **380**: 165–169.

Sakamoto, T.; Deguchi, M.; Brustolini, O.J.B.; Santos, A.; Silva, F.F.; Fontes, E.P.B.(2012).The tomato RLK superfamily: Phylogeny and functional predictions about the role of the LRRII-RLK subfamily in antiviral defense. BMC Plant Biol., **12**: 229.

Santos, A.A., Carvalho, C.M., Florentino, L.H., Ramos, H.J.O., and Fontes, E.P.B. (2009).Conserved threonine residues within the A-loop of the receptor NIK differentially regulatethe kinase function required for antiviral signaling. PLoS ONE. **4**: e5781.

Sattler S. E. and Funnell-Harris D. L. (2013). Modifying lignin to improve bioenergy feedstocks: strengthening the barrier against pathogens? Front. Plant Sci. **4**: 70.

Scholthof, K.B.G., Adkins, S., Czosnek, H., et al. (2011). Top 10 plant viruses in molecular plant pathology. Mol Plant Pathol. **12**: 938–954.

Stotz, H.U., Mitrousia, G.K., De Wit, P.J.G.M. and Fitt, B.D.L. (2014). Effector-triggered defence against apoplastic fungal pathogens. Trends Plant Sci. **19**: 491-500.

Teixeira, R.M., Ferreira, M.A., Raimundo, G.A.S., and Fontes, E.P.B. (2021).Geminiviral triggers and suppressors of plant antiviral immunity. Microorganisms **9**.

Teixeira, R.M., Ferreira, M.A., Raimundo, G.A.S., Loriato, V.A.P., Reis, P.A.B., and Fontes, E.P.B. (2019). Virus perception at the cell surface: revisiting the roles of receptor-like kinases as viral pattern recognition receptors. Mol. Plant Pathol. **20**: 1196–1202.

Tian, D., Traw, M.B., Chen, J.Q., Kreitman, M. and Bergelson J. (2003). Fitness costs of R- gene-mediated resistance in Arabidopsis thaliana. Nature. **423**: 74–77.

Tian, H., Wang, X., Hongyan, G., Cheng, Y., Hou, C., Chen, Jin-Gui. and Wang, S.(2017). NTL8 regulates trichome formation in Arabidopsis by directly activating R3 MYB genes 9 TRY and TCL1. Plant Physiology. **174**: 2363-2375.

Torii, K.U. (2018). Transmembrane Receptors in Plants: Receptor Kinases and Their Ligands. Annual Plant Reviews online. **33**: 1–29.

Torres, M. A. (2010). ROS in biotic interactions. Physiol. Plant **138**: 414–429.

Tsuda, K., and Katagiri, F. (2010). Comparing signaling mechanisms engaged in pattern-triggered and effector-triggered immunity. Curr. Opin. Plant Biol. **13**: 459– 465.

Vogt, S.L., Nevesinjac, A.Z., Humphries, R.M., Donnenberg, M.S., Armstrong, G.D., and Raivio, T.L. (2010). The Cpx envelope stress response both facilitates and inhibits elaboration of the enteropathogenic Escherichia coli bundle-forming pilus. Mol. Microbiol.**76**: 1095-110.

Xie, Z., Lee, E., Lucas, J.R., Morohashi, K., Li, D., Murray, J.H., Sack, F.D. and Grotewold, E. (2010). Regulation of cell proliferation in the stomatal lineage by the Arabidopsis MYB FOUR LIPS via direct targeting of core cell cycle genes. The Plant cell.**22**:2306–2321.

Zangerl, A.R. and Berenbaum, M.R. (1997). Cost of chemically defending seeds: furanocoumarins and Pastinaca sativa. Amer Nat. **150**: 491–504.

Zangerl, A.R. and Berenbaum, M.R. (2003). Phenotype matching in wild parsnip and parsnipwebworms: causes and consequences. Evolution. **57**: 806–815.

Zavala, J.A. and Baldwin, I.T. (2004). Fitness benefits of trypsin proteinase inhibitor expression in Nicotiana attenuata are greater than their costs when plants are attacked. BMC Ecology. **4**: 11.

Zorzatto, C., Machado, J.P., Lopes, K.V., Nascimento, K.J., Pereira, W.A., Brustolini, O.J., Reis, P.A., Calil, I.P., et al. (2015). NIK1-mediated translation suppression functionsas a plant antiviral immunity mechanism. Nature. **520**: 679-82.

CHAPTER I

Geminiviral Triggers and Suppressors of Plant Antiviral Immunity

Publicado 8 Abril, 2021, na revista *Microorganisms*

Teixeira, R.M.; Ferreira, M.A.; Raimundo, G.A.S.; Fontes, E.P.B. Geminiviral Triggers and Suppressors of Plant Antiviral Immunity. Microorganisms 2021, 9, 775.

(doi: https://doi.org/10.3390/ microorganisms9040775)

microorganisms

MDPI

Review

Geminiviral Triggers and Suppressors of Plant Antiviral Immunity

Ruan M. Teixeira, Marco Aurélio Ferreira, Gabriel A. S. Raimundo and Elizabeth P. B. Fontes * Department of Biochemistry and Molecular Biology, BIOAGRO, National Institute of Science and Technology in Plant-Pest Interactions, Universidade Federal de Viçosa, Viçosa 36571.000, MG, Brazil; ruanmaloni@gmail.com (R.M.T.); marco.aurelioferreira@hotmail.com (M.A.F.); gabriel88saraiva@gmail.com (G.A.S.R.)

* Correspondence: bbfontes@ufv.br

check for updates

Citation: Teixeira,R.M.; Ferreira, M.A.; Raimundo, G.A.S.; Fontes, E.P.B. GeminiviralTriggers and Suppressors of Plant Antiviral Immunity. *Microorganisms* **2021**, *9*, 775. https://doi.org/10.3390/microorganisms9040775

Academic Editor: Jesús Navas Castillo
Received: 2 March 2021 Accepted: 26 March 2021
Published: 8 April 2021

Publisher's Note: MDPI stays neutral with regard to jurisdictional claims in published maps and institutional affiliations.

Abstract: Geminiviruses are circular single-stranded DN A plant viruses encapsidated into geminate virion particles, which infect many crops and vegetables and, hence, represent significant agricultural constraints worldwide. To maintain their broad-range host spectrum and establish productive infection, the geminiviruses must circumvent a potent plant antiviral immune system, which con- sists of a multilayered perception system represented by RNA interference sensors and effectors, pattern recognition receptors (PRR), and resistance (R) proteins. This recognition system leads to the activation of conserved defense responses that protect plants against different co-existing viral and nonviral pathogens in nature. Furthermore, a specific antiviral cell surface receptor signaling is activated at the onset of geminivirus infection to suppress global translation. This review highlighted these layers of virus perception and host defenses and the mechanisms developed by geminiviruses to overcome the plant antiviral immunity mechanisms.

Keywords: PAMP-triggered immunity; effector-triggered immunity; RNA silencing; viral suppressors; NIK1; PTI; ETI; geminiviruses

1. Introduction

Geminiviruses are circular single-stranded D N A viruses grouped into one of the largest and most successful families of plant viruses (*Geminiviridae* family) [1]. Collectively, the geminiviruses cause devasting diseases in a large variety of economically relevant crops and vegetables, resulting in the most diverse symptoms. The broad-range host spectrum of the viruses from the Geminiviridae family may be associated with the large capacity of geminiviruses to overcome the multilayered antiviral immune system of the plant cell, which is broadly divided into RNA interference (RNAi), pathogen associated molecular pattern (PAMP)-triggered immunity (PTI), and effector-triggered immunity (ETI) (see Abbreviations) [2]. Signaling from the cell surface, PTI is the first line of plant defense mediated by immune pattern recognition receptors (PRRs), which detect and interact with conserved molecular motifs from the pathogens, PAMPs [3]. As a second line of defense, ETI is mediated by intracellular immune receptors that specifically recognize, directly or indirectly, viral effectors delivered into the cytosol by the pathogens.

RNAi or RNA-silencing-derived antiviral immunity is a well-characterized plant antiviral immunity mechanism, which has been shown to operate against virtually all plant viruses [4,5]. Likewise, ETI, also referred to as resistance (R) gene-mediated immunity, has long been recognized as an efficient plant defense layer against viruses [6,7]. Studies with plant viruses pioneered in describing hallmarks in ETI responses, including the hypersensitive response (HR), salicylic acid accumulation, and systemic acquired resistance (SAR) [8–10]. In addition, several viral effectors (avirulence gene products) and their cognate R proteins have been characterized [2]. Emerging evidence has demonstrated that the classical PTI characterized in nonviral

pathogen–plant interactions also operates against plant viruses [11,12]. These multilayered immune defenses are activated and suppressed by viral components or effectors, functioning as virulence factors in susceptible genotypes and as avirulence (Avr) factors in resistant genotypes.

Like any other plant virus, geminiviruses both activate and suppress RNA-silencing- mediated antiviral immunity. Infected hosts accumulate geminivirus-derived small interfering RNA (siRNA) of 21–24 bp, and almost all geminivirus proteins have been shown to suppress critical steps in the RNA-silencing mechanism [13]. Evidence that viral PTI functions against geminiviruses includes the finding that PTI upstream receptors are virulence targets of geminivirus proteins, which can also suppress downstream PTI-like responses, fulfilling the concept that PTI must be inhibited for successful infection [14,15]. Likewise, some geminiviruses proteins have been shown to activate and suppress ETI-like responses [16]. As further evidence that plants deploy ETI to fight geminiviruses, the tomato Ty-1 locus, which confers resistance to tomato yellow leaf curl virus (TYLCV), encodes a nucleotide-binding leucine-rich repeat (NLR) domain-containing protein, a reminiscent structural configuration of typical ETI receptors [17]. This review focuses on RNA silencing and the antiviral innate immunity mechanisms that plants deploy to fight viruses and the strategy that geminiviruses evolved to overcome these defense barriers. Virtually all geminiviral proteins, which carry a primary function (movement, replication, encapsidation) required to complete the virus life cycle, evolved to accommodate virulence functions as well. Although not covered in this review, hormone signaling has been shown to be connected with anti-geminiviral immunity. For in-depth information on this topic, the reader is referred to a recent review in the molecular interplay between hormones and geminiviruses [18].

2. Structural and Functional Organization of the Geminivirus Genome

The *Geminiviridae* family encompasses circular single-stranded DN A viruses that are packed into icosahedral, geminate virion particles. The family is further divided into nine genera (*Begomovirus, Mastrevirus*, *Capulavirus*, *Curtovirus*, *Becurtovirus*, *Eragrovirus*, *Grablovirus*, *Topocuvirus*, and *Turncurtovirus*), according to the genome organization and phylogenetic relationship of the geminivirus species and types of the transmissible insect vectors [19].

The geminiviruses can be either monopartite with a single genomic configuration (DNA-A-like) or bipartite with two genomic components, designated DNA- A and DNA- B, with a coding capacity ranging from 4 to 8 viral proteins (Figure 1). Their genome is transcribed into bidirectional transcriptional units from the origin of replication (Ori). The functional structures of Ori include a conserved stem-loop structure and the non a nucleotide sequence TAGTATTAC that constitutes the site of replication initiation by the viral replication initiator protein (Rep), encoded by the complementary-sense strand and, hence, also designated C1 (AC1) [1]. The remaining complementary-sense strand-encoded viral proteins are designated C2 (AC2), which functions as a transcriptional activator protein (TrAP); C3 (AC3), or replication enhancer protein (REn); C4 (AC4), a pathogenicity determinant; and C5 (AC5), not identified in all geminivirus genomes. The virion strand encodes V1 (AV1); the coat protein (CP); V2 (AV2), which exhibits movement functions; and V3, not present in all geminivirus genomes.

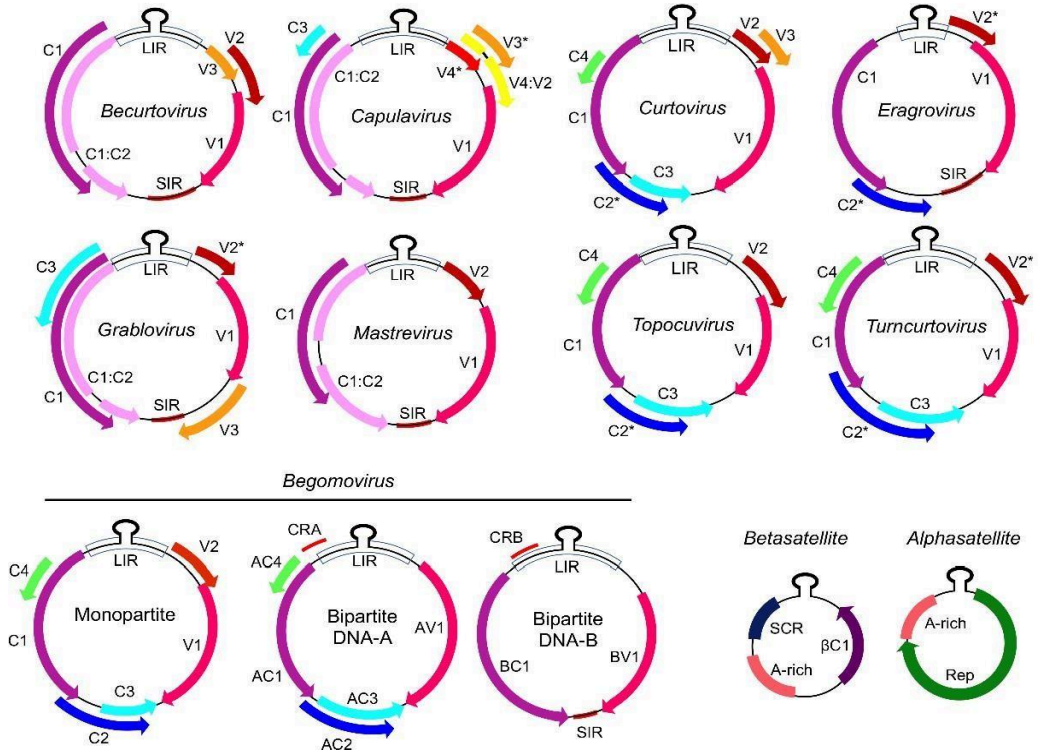

Figure 1. Genomic organization of geminiviruses (Geminiviridae family). The Geminiviridae family includes nine genera represented by monopartite or bipartite species. LIR denotes the long intergenic region; SIR, the short intergenic region; and CR, the common region. The open reading frame (ORF) C1 /AC1 encodes the replication initiator protein (Rep) and C3/AC3 encodes the replication enhancer protein (Ren), which are associated with replication. The ORF C2/AC2 encodes a transcriptional activator protein (TrAP) that controls the transcription of viral and host genes; C4 /AC4 is a virulence factor. The capsid protein (CP) is indicated in the monopartite and bipartite genomes, as V1 and AV1. In monopartite species, V2 represents the movement protein (MP). V3, present in some genomes, is an inhibitor of gene silencing. ORFs with asterisks (*) have not been functionally assayed. In bipartite begomoviruses, MP (BC1) is encoded by the DNA- B, which also encodes the nuclear shuttle protein, NSP (BV1), which facilitates the nucleocytoplasmic movement of viral DNA. Bipartite begomoviruses are often associated with ssDNA satellites, i.e., the alphasatellites, which encode a replication protein (Rep), and the betasatellites, which encode the virulence-related βC1 protein. A-rich is a conserved adenine rich region of the DNA satellites, and SCR is the satellite conserved region. Adapted from [1]

The B component of bipartite geminiviruses encodes BC1 and BV1. BV1 is a nuclear shuttling protein (NSP) that facilitates the intracellular transport of viral D N A from the nucleus to the cell periphery and assists BV1, the classic movement protein (MP), to move the viral DNA to the adjacent, uninfected cell via plasmodesmata [20]. Some geminiviruses are often associated with D N A satellites, designated beta- and alphasatellites, which affect geminiviral pathogenicity and symptom development [21,22] (Figure 1). The genus *Betasatellite* belongs to the family *Tolecusatellitidae*, whereas the *Alphasatellite* genus belongs to the *Alphasatellitidae* family. These circular ssDNA satellites are approximately 1–1.4 kb ssDNA; alphasatellites encode a replication-associated protein (Rep), whereas the betasatellites encode βC1 involved in symptom induction and suppression of transcriptional and post- transcriptional gene silencing.

3. RNA-Silencing-Mediated Antiviral Mechanisms

RNA silencing, also designated RNA interference (RNAi), is a primary antiviral defense mechanism of plant cells that is activated by double-stranded (ds) RNAs [4,23]. The dsRNA- induced gene-silencing mechanisms are divided into three phases: biogenesis, amplification, and effector phases. The type III RNases dicers (DCLs) carry out the siRNA biogenesis phase by recognizing and processing ds RNA derived from several sources, including viral dsRNA or micro (mi)RNA precursors. DCL2 and DLC4 generate short dsRNAs of 21 and 22 nucleotides (nt), whereas DCL3 processes ds RNA precursors into 24-nt siRNAs [24–28].

As a plant D N A virus, geminiviruses can generate dsRNA triggers (precursors) via different mechanisms, including overlapping transcripts from a divergent transcription of virus genes, structured (hairpin) transcripts, or dsRNA synthesized from viral m RNA by the host RNA-directed RNA polymerase (RdRP or RDR) (Figure 2). These dsRNA precursors are then cleaved by DCLs and converted into virus-derived small interfering RNAs (vsiRNAs) [29,30]. In the amplification phase, vsiRNAs are amplified by RdRP or RDR and are subsequently stabilized by HU A enhancer 1 (HEN1)-mediated 2′O-methylation, which protects the 3′-end of siRNAs from uridylation activity and subsequent degradation [31–33].

The effector phase initiates with the assembly of newly synthesized vsiRNAs with one member of the effector AGO (argonaute) family into RNA-induced silencing complexes (RISCs) or RNA- induced transcriptional silencing complexes (RITSs), which target complementary RNA or D N A for silencing (Figure 2) [34–36]. RISC acts at the post- transcriptional level and targets viral RNAs for degradation through cleavage (slicing) or translational arrest, leading to post-transcriptional gene silencing (PTGS). RITS is in- volved in transcriptional gene silencing (TGS) through D N A or histone methylation and heterochromatin formation.

In PTGS-mediated antiviral defense, DCL2 and DCL4 often process dsRNA precursors into 21- and 22-nt siRNAs that interact with AGO1 and AGO 2 [28,30,37]. PTGS predominantly involves RNA cleavage via the endonucleolytic activity of AGO1 [38]. Recent studies have identified AGO-mediated translational repression as an additional RNA-silencing mechanism against plant viruses [39–42]. Loss-of-function mutations have implicated AGO 1 and AGO10 in translational repression, whereas the AGO2-mediated translational suppression has been studied through an in vivo reporter assay [43–46]. The mechanism of AGO-mediated translational repression in plants is still poorly understood, but it seems to depend on the complementary site for siRNA or miRNA on mRNA. Targeting the 5′UTR enables AGO1-RISC to sterically hinder ribosomal recruitment [45], whereas siRNA targeting sites within the open reading frame (ORF) may impair ribosome elongation [45]. At the 3′ UTR on mRNA, AGO1-RISC may repress translational initiation by interfering with 48S initiation complex formation, resembling the mechanism observed in animal cells [45,47]. Plants also deploy siRNA-directed TGS as an antiviral defense against DNA viruses [48]. The TGS mechanism is often used by plant cells to control endogenous gene expression. In this case, the RNA polymerase (pol) IV transcript is converted into ds RNA by RNA pol IV-associated RDR2 (RNA-dependent RNA polymerase 2) [49]. Then, DCL3 cleaves dsRNA to produce 24-nt siRNA, which is transported to the cytoplasm for AGO 4 loading and RITS assembling. The AGO4:siRNA complex is redirected to the nucleus to target the complementary transcript of RNA polymerase V, synthesized in the opposite direction from the RNA pol IV transcript. Therefore, siRNA correctly positions AGO 4 that recruits the Novo D N A methyltransferase DRM2-containing RNA-directed D N A methylation (RdDM) complex to methylate D N A on the target locus [49–52]. The RNA-directed D N A methylation is often directed to promoter regions to interfere with gene expression at the transcriptional level.

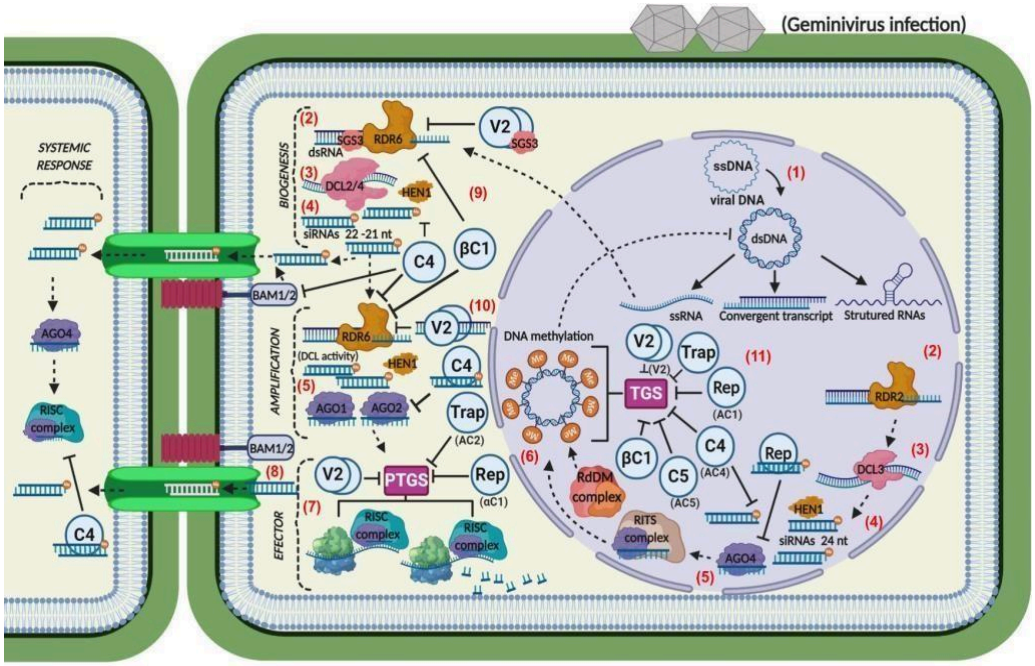

Figure 2. Geminivirus-induced RNA silencing and viral suppressors. Geminivirus particles are delivered into the cytoplasm, where they are uncoated and CP-bound viral ssDNA complexes are imported into the nucleus. (1) In the nucleus, the viral ssDNA is converted into dsDNA, the replicative form. (2) Then, viral ssRNAs are synthesized and are recognized by the RNA-silencing machinery, initiating the biogenesis phase by converting ssRNA to dsRNA via RDR2 (RNA-dependent RNA polymerase 2 in the nucleus) or RDR6 (in the cytoplasm) with the help of suppressor gene silencing 3 (SGS3), which stabilizes the substrates for (3) dicer (DCL)-mediated processing into 21-, 22-, or 24-nt siRNAs (virus-derived small interfering RNA; vsiRNA). (4) HUA Enhancer 1 (HEN1)-methylated siRNAs are then amplified by RDR1 or RDR6 enhancing siRNA-mediated viral immunity. (5) During the effector phase, Argonaute 4 (AGO4) and AGO1/2 (in the cytoplasm) interact with siRNAs to form RNA-induced transcriptional silencing complex (RITS) and RNA-induced silencing complex (RISC), respectively.(6) In the nucleus, RITS targets the viral transcribed genome and sequesters the RNA-dependent DN A methylation (RdDM) complex, which remodulates the chromatin for transcriptional gene silencing (TGS) of the viral genome. (7) In the cytoplasm, RISC mediates post-transcriptional gene silencing (PTGS) inhibiting the transcription of viral genes via degradation of viral mRNAs. (8) Viral siRNAs generated in the biogenesis and amplification phases are systemically spread via plasmodesma in a barely any meristem 1 (BAM1)- or BAM2-dependent process. For successful infection, geminiviral suppressors of RNA silencing or (VSRs) can act at all levels of TGS and PTGS to suppress siRNA- or RNA interference-mediated antiviral immunity. (9) AC4/C4, Rep, βC1, and V2 inhibit biogenesis of siRNA; (10) βC1, V2, AC2/C2, C4 suppress amplification of siRNA; and (11) βC1, Rep, AC2/C2, and V2 impair the effector phase. Furthermore, the geminivirus suppressors of RNA silencing, Rep, V2, AC4/C4, AC2/C2, and AC5, may interfere with downstream events of TGS. AC4 also interferes with siRNA systemic translocation by targeting BAM1/2. Some geminiviral suppressors interfere with R NA silencing by targeting siRNA (Rep and C4) and long non-coding RNAs (lncRNAs; V2). They also act by activating or inducing the expression of endogenous suppressors of RNA silencing. See Figure 1 for the designations of the viral proteins. The figure was created with BioRender.com.

4. Geminiviral Suppressors of PTGS and TGS

As an adaptive antiviral defense mechanism, RNA silencing is induced during infection, and virus-derived siRNAs accumulate at high levels. Likewise, geminivirus infection induces siRNA accumulation [24]. Cabbage leaf curl virus (CabLCV) infection in *Arabidopsis* and African cassava mosaic virus (ACMV) infection in *Nicotiana benthamiana* and cassava have been associated with the biogenesis of 21-, 22-, and 24-nt vsiRNAs derived from the coding and the intergenic regions of these geminiviruses [5,24,53,54].

In these previous studies, all 24-nt vsiRNAs and a large fraction of 22-nt vsiRNAs were generated by DCL3 and DCL2, respectively, demonstrating the assembly of several distinct silencing pathways in geminivirus–plant interactions [24]. In addition to siRNAs, long non-coding RNAs (lncRNAs) accumulate in plants infected by TYLCV [55]. These long RNAs can be derived from intergenic sequences and antisense sequences of natural tran- scripts and may mimic endogenous targets to compete with TYLCV-related siRNAs by a yet unknown mechanism.

Antiviral TGS is considered a primary defense pathway against geminiviruses. Accordingly, reverse genetics studies have demonstrated that loss-of-function mutants of TGS components increase hypersensitivity to geminivirus infection and interfere with host recovery [48,52]. DCL3 is essential to combat D N A viruses because antiviral immunity persists in *dcl2* and *dcl4* mutants but not in *dcl3* mutants. Loss of *DCL3* function enhances *Begomovirus* pathogenicity and abolishes 24-nt vsiRNAs biogenesis [24,52]. In TGS, gem- iniviral ss DNA is converted into the replicative form ds DNA, which is recognized by RNA polymerase IV, in the nuclei of infected cells [48]. The RNA pol IV-transcribed single- stranded RNA is converted to ds RNA by RDR2 and then processed by DCL3 into 24-nt vsiRNAs. AGO4 is loaded with 24-nt vsiRNAs, which target the complementary nascent transcript of the RNA pol IVb complex, recruiting the RdDM complex for viral DNA methylation. The Histone H3 lysine 9 (H3K9) methyltransferase (kyp2/suvh4) is also involved in chromatin modification of the viral genome, resulting in epigenetic modification of the viral genome [56].

Many plant viruses have evolved viral suppressors of RNA silencing (VSRs) as a virulence strategy [57–60]. The geminiviral VSRs are multifunctional proteins displaying host defense-suppressing activities and viral life cycle–supporting functions. They can interfere with both PTGS and TGS in all three steps of the processes (Figure 2). They also act downstream of TGS, directly or indirectly affecting DNA methylation [13]. Mechanistically, geminiviral VSRs either suppress the activity or repress the accumulation (expression) of RNA-silencing machinery components.

Rep, also designated AC1 (bipartite geminiviruses) and C1 (monopartite geminiviruses), has been shown to function as an efficient VSR at both PTGS and TGS (Figure 2). Tomato yellow leaf curl Sardinia virus (TYLCSV) Rep directly reduces methyltransferase *1* (*MET1*) and chromomethylase 3 (*CTM3*) expression in infected plants, interfering with the cycle of D N A methylation and TGS (Figure 2) [61]. Wheat dwarf virus (WDV) Rep suppresses PTGS by binding to 21-nt single-stranded and double-stranded vsiRNAs, thereby prevent- ing their association with the respective AGOs to impair RNA silencing of viral genes [62]. Likewise, TrAP (AC2 or C2) suppresses antiviral TGS and PTGS via different mechanisms depending on the cognate TrAP-encoding geminivirus genome. Among the effective mechanisms for suppressing RNA silencing, TrAP either directly interacts with silencing host factors or transactivates expression of host suppressors of RNA silencing; thereby, the TrAP silencing–suppressing function is often coupled to its transcriptional activity that targets and transactivates not only viral gene promoters but also host genes [63–66]. Both AC 2 and C2 have been shown to interact with and inhibit common host RNA-silencing factors, including adenosine kinases (ADKs), H3K9me2 histone methyltransferase, SU(VAR)3-9 homolog 4/kryptonite (SUVH4/KYP) involved in TGS [66–68], AGO 1 and RDR6, in- volved in PTGS [69], and calmodulin- like protein (rgs-CaM), an endogenous suppressor of PTGS [63,65]. Beet severe curly top virus (BSCTV) C2 also interacts with and stabilizes S-adenosyl-methionine decarboxylase 1 (SAMDC1); thereby, C2 interferes with the host defense mechanism of DNA methylation-mediated gene silencing by attenuating the 26S proteasome-mediated degradation of SAMDC 1 [70]. In addition to directly interacting with calmodulin-like protein 39 (rgsCaM), AC2 from tomato golden mosaic virus (TGMV) induces the expression of *rgsCaM*, [65]. which may target silencing suppressors of RNA viruses for degradation via the autophagy pathway [63]. Likewise, AC2 proteins from the mung- bean yellow mosaic virus-*Vigna* (MYMV) and ACMV have been shown to target promoters and regulate gene expression of endogenous silencing suppressors, including the Werner exonuclease-like 1 (*WEL1*) gene [65].

C4/AC4 is also part of the virus arsenal against antiviral RNA silencing by interacting and with 21-nt vsiRNAs to prevent the spread of vsiRNAs and, hence, suppresses RNA silencing systemic immunity [72,73]. TYLCV C4 strongly associates with the intracellular kinase domain of the plasmodesma-localized RLKs, barely any meristem 1 (BAM1) and BAM2, required for systemic

immunity [73]. C4 from cotton leaf curl Mul- tan virus (CLCuMuV) also interacts with and inhibits *S*-adenosyl methionine (SAM), the universal donor of methyl groups in methylation reactions [74]. Therefore, C4 decreases SAM and HEN1 activities indirectly and interferes with the viral genome's methylation and PTGS [74]. Additionally, C4 protein accessorizes Rep in the suppression of TGS via downregulation of MET1 and interaction with AGO 4 [61,75]. The AC5/C5 ORF, located downstream of AC3/C3 in the complementary sense of D NA overlapping a region of the CP sequence, has been recently described as a potent suppressor of RNA silencing [76]. Mungbean yellow mosaic India virus (MYMIV) AC5 affects ds RNA production by sup- pressing sense ssRNA-induced gene silencing and interferes with TGS by inhibiting the expression of a C H cytosine methyltransferase in *N. benthamiana* [76]. AV2 and V2 also suppress antiviral RNA silencing in the amplification phase and interfere with host methylation activities, downstream events of TGS [77–79]. TYLCV V2 interacts with and inhibits the suppressor of gene silencing 3 (SGS3), the cofactor of RDR6; thereby, affecting vsiRNA amplification [80]. V2 may also sequester the RDR6/SGS3 intermediate/substrate ds RNA with 5' overhang ends from SGS3 association, further interfering with vsiRNA amplification [77,80]. Likewise, V2 from the curtovirus beet curly top virus (BCTV) has been recently shown to suppress post-transcriptional gene silencing (PTGS) by impairing the RDR6/SGS3 pathway [77,78]. CLCu MV V2 interacts with long dsRNA to prevent DCL processing, whereas tomato yellow leaf curl China virus (TYLCCV) V2 interacts with siRNAs to prevent A G O incorporation [70,81]. V2 also suppresses TGS by interacting with histone deacetylase 6 (NbHDA6) and interfering with the recruitment of MET1 by HDA 6 resulting in decreased methylation of the viral genome and consequent increase in TYLCV pathogenicity [79]. Mulberry crinkle leaf virus (MCLV), a newly characterized geminivirus species, encodes a novel viral protein V3, which has been shown to suppress antiviral RNA silencing by a yet unknown mechanism [82]. Cab LCV BVI (NSP) induces asymmetric leaves 2 (AS2) expression that activates DCP2 decapping activity and, in turn, accelerates m RNA turnover rate and inhibits siRNA accumulation [83].

Geminiviruses are often associated with alpha- and betasatellites, which encode efficient suppressors of viral genome methylation in infected plants and PTGS [84,85]. The betasatellite genome-encoded βC1 protein functions as an efficient VSR via different mechanisms [22]. TYLCCNV βC1 has been shown to inhibit *S*-adenosyl-L-homocysteine hydrolase (SAHH) activity, a methyl cycle enzyme required for TGS, interfering with the host methylation–mediated virus defense pathway [85]. Furthermore, βC1 from different betasatellites affects vsiRNA amplification by inducing the calmodulin-like protein (CaM),a negative regulator of RDR6 expression [86,87]. This scenario demonstrates that geminiviruses are very efficient in suppressing all steps in RNA-silencing-mediated antiviral mechanisms.

5. Does PAMP-Triggered Immunity Operate against Geminiviruses? What about Effector-Triggered Immunity?

In plant–virus interactions, the host immune system often recognizes viral components or effectors to activate defenses [2]. The plant antiviral innate defense consists of a two- level perception system represented by the cell surface receptor, PRR, and the intracellular immune receptors, the resistance (R) proteins [6]. PRRs are represented by two classes of transmembrane receptors, the receptor-like kinases (RLKs) and receptor-like proteins (RLPs). These PRRs recognize PAMPs exclusively expressed by pathogens, or endogenous danger signals released by host plants during infection, designated damage-associated molecular patterns (DAMPs) [88]. Activation of RLKs and RLPs often requires a coreceptor to form an active immune complex [89]. Mechanistically, PAMPs/DAMPs function as ligands that induce dimerization/oligomerization of single-pass transmembrane receptor PRRs with RLK coreceptors to initiate signaling via phosphorylation-induced activation of the immune complexes [88].

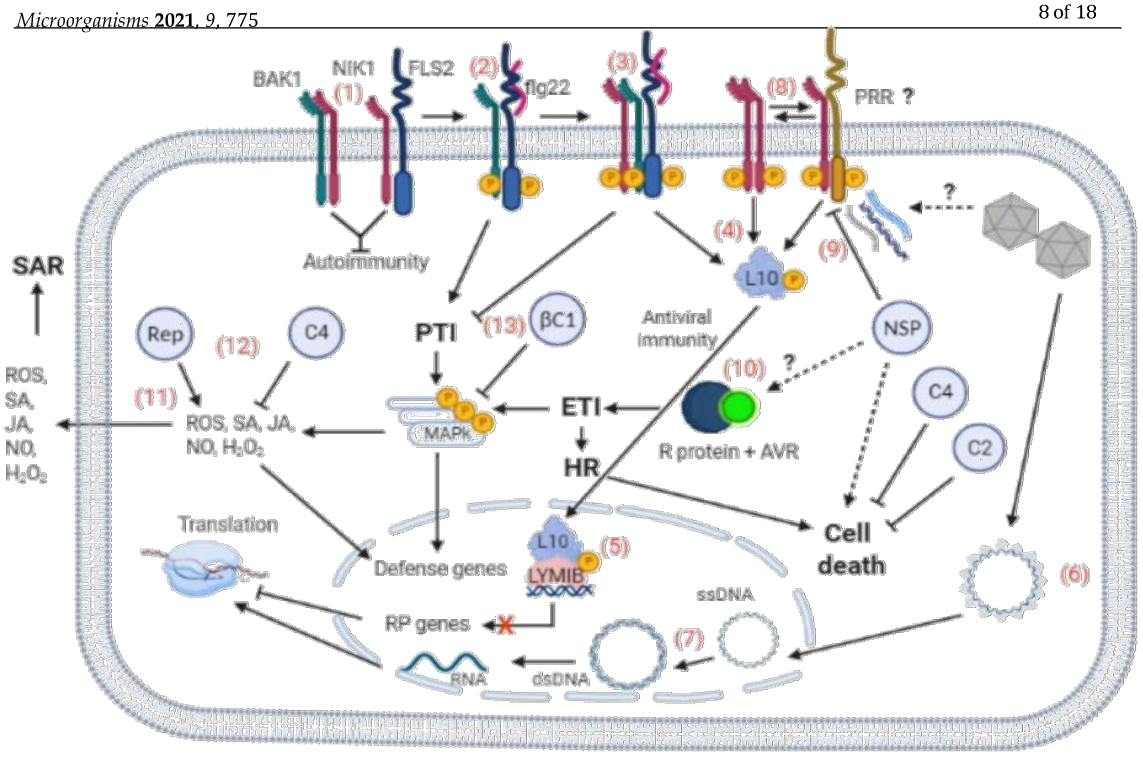

Figure 3. Antiviral innate immunity, interactions with viral suppressors and bacterial PTI (1). Under normal, resting conditions, NSP-interacting kinase 1 (NIK1) is bound to the flagellin receptor FLS2 (Flagellin-sensitive 2) and coreceptor BAK1 (Brassinosteroid insensitive 1-associated receptor kinase 1) to prevent autoimmunity. (2) Upon bacterial infection, the bacterial PAMP (pathogen-associated molecular pattern) flg22 is sensed by FLS2, inducing its oligomerization with BAK1, which results in phosphorylation-mediated activation of the immune complex to initiate PAMP-triggered immunity (PTI), activating the mitogen-activated protein kinase (MAPK) cascade and inducing defense genes. (3) Activated BAK1 also phosphorylates NIK1 at Thr-474, which in turn inhibits further PTI (4) and activates the NIK1-mediated antiviral signaling pathway, mediating ribosomal protein 10 (RPL10) phosphorylation. (5) Phosphorylated RPL10 is translocated to the nucleus, where it interacts with L10-interacting Myb domain-containing protein (LIMYB) to repress protein ribosomal (RB) genes and translational factors, suppressing global translation. (6) In infected cells, the geminivirus particles are disassembled in the cytoplasm and the CP-viral ssDNA complex is directed to the nucleus where (7) the viral ssDNA is converted into dsDNA for replication and transcription of the viral genome. (8) Begomoviruses-derived nucleic acids also function as viral PAMPs inducing NIK1 dimerization with itself or an unidentified viral PAMP recognition receptor (PRR) to transduce the antiviral signal that culminates in translational suppression. Then, viral m RNA is not efficiently translated impairing infection. (9) The begomovirus nuclear shuttling protein (NSP) counters the activation of this defense pathway by binding to the NIK1 kinase domain and, hence, prevents phosphorylation and transduction of the antiviral signal that otherwise would impair infection. (10) In resistant genotypes, NSP may also function as an avirulence (AVR) factor to activate effector-triggered immunity (ETI) via resistance (R) protein recognition, inducing hypersensitive response (HR) and cell death. (11) The PTI and ETI products (ROS, SA, JA, NO, H_2O_2) can induce defense genes and systemic acquired resistance (SAR). Geminivirus suppressors of innate immunity include (12) C4 that inhibits PTI by interacting and inhibiting FLS2 and along with Rep inhibits SA- and ROS-dependent signaling; C4 and C2 inhibit HR and cell death. (13) Furthermore, the betasatellite βC1 inhibits the MAP kinase cascade. The question marks indicate either events not well clarified or unknown. See Figure 1 for the designations of the viral proteins. The figure was created with BioRender.com.

Downstream events of PTI activation include ROS accumulation, followed by MAP kinase cascade activation, induction of PTI-associated defense genes, ethylene and salicylic acid synthesis, and callose deposition [90] (Figure 3). Although geminiviral PAMPs and their cognate PRRs have not been identified, several lines of evidence indicate that PTI is part of the host defense arsenal against geminivirus infection. First, the C4 protein from TYLCV has been shown to associate with a classical PRR, the bacterial flagellin receptor FLS2 (Flagellin- sensitive 2), and inhibits early PTI responses [14] (Figure 3). TYLCV C4 also interacts with NSP-interacting kinase 1 (NIK1), an antiviral immune leucine- rich repeat receptor-like kinase (LRR-RLK) that protects plants against begomoviruses [15]. NSP from CabLCV associates with the almost universal coreceptor of PRRs, the Brassinosteroid insensitive 1- associated kinase 1 (BAK1) [91]. NSP interaction with the BAK1 kinase domain may prevent phosphorylation and activation of the coreceptor in the same fashion as it does with the receptor-like kinase NIK1 [92]. Second, geminiviral proteins also activate and suppress downstream immune events of PTI activation (Figure 3). Rep from different geminiviruses induces PTI-associated marker genes and SA-dependent defenses [93,94]. However, when co-expressed with TYLCV C4 protein, Rep redirects C4 to the chloroplasts, where it acts as a PTI suppressor by reducing SA- and ROS-dependent defense signals [93]. The C4 immune-suppressing function co-opts a protein trafficking route directed by protein myristoylation/de-myristoylation process- ing [95]. Upon geminivirus infection, a fraction of the membrane-bound *N*-myristoylated C4 protein is de-myristoylated and translocated to the chloroplast. Inside the chloroplast, nonmyristoylated C4 interacts with the thylakoid membrane- bound plant calcium-sensing receptor (CAS) and hampers SA biosynthesis and mediated defenses [95]. Finally, the betasatellite βC1 protein from TYLCCV has been shown to interfere with PTI-induced MAPK activation and downstream responses by targeting mitogen-activated protein kinase 2 (MKK2) in *Arabidopsis thaliana* and *N. benthamiana* (Figure 3) [96–98].

The second level of microbe perception by the host plant is mediated by intracellular immune receptors (R proteins), which recognize pathogen avirulent effectors to activate ETI [3,93,99]. ETI represents a more specific and robust line of host defense, often associated with programmed cell death, HR that restricts the pathogen to the site of infection [100]. Most, but not all, antiviral R proteins harbor a nucleotide-binding leucine-rich repeat (NLR) domain, reminiscent of nonviral intracellular R proteins, which are further classified into coiled-coil (CC)- NLR or Toll/interleukin 1 receptor-like (TIR)-NLR proteins [2,6,101]. The natural Ty-2 resistance locus to TYLCV encodes an NB-LRR protein, named TYNBS1, which might mediate ETI-like resistance. However, the geminiviral effector that would interact specifically with TYNBS1 to activate ETI remains to be determined. Therefore, the underlying mechanism for TYNBS1 activation to mediate resistance is still elusive [17].

Compelling evidence that plants deploy ETI against geminiviruses results from infectivity assays demonstrating that geminiviruses induce and suppress HR and ETI-like responses. In *Arabidopsis*, CabLCV infection induces HR- and senescence-related genes without developing a visible cell death phenotype [102]. More specifically, TYLCV, cotton leaf curl Kokhran virus (CLCuKoV) and ACMV Rep, bean dwarf mosaic virus (BDMV) and bean golden yellow mosaic virus (BGYMV) NSP, and CLCuKoV V2 have been shown to induce HR (Figure 3) [81,103,104]. In contrast, the C2 proteins from the papaya leaf curl virus (PaLCuV) and CLCuKoV have been shown to inhibit V2-mediated HR, and C2 from tomato leaf curl New Delhi virus (ToLCNDV) suppresses NSP-mediated HR [105,106]. Likewise, TYLCV infection reduces cell death in tomato plants, which is induced by the inactivation of heat shock protein 90 (HSP90) and suppressor of the G2 allele of skp1 (SGT1), via an unknown TYLCV- mediated cell death suppression mechanism [107]. In contrast, the under- lying mechanism for the cell death- suppressing activity of C4 from tomato leaf curl Yunnan virus (TLCYnV) has been recently unraveled [16]. C4 interacts with hypersensitive induced reaction 1 (HIR1),promotes its degradation by impairing HIR1 self-oligomerization, and hence inhibits the HIR1-mediated HR, increasing virus pathogenicity. Although several lines of evidence indicate that both monopartite and bipartite begomoviruses induce and suppress HR, with few exceptions, the mechanisms underlying these viral activities are still far from understood.

6. Transmembrane Receptor-Mediated Antiviral Immunity via Translational Suppression

As obligate intracellular parasites, viruses interact extensively with the host cell functions to

complete their life cycle. Independent of the repertoire of viral genome–encoded proteins, all viruses are dependent on the host protein synthesis machinery to translate viral messenger RNAs (mRNAs) [108–110]. Therefore, many host cell-intrinsic immune defenses target translation factors to inhibit protein synthesis in the infected cells [108,110]. Among the translational control-mediated immune defenses, plant cells employ an LRR- RLK to sense viruses at the cell surface and activate a defense pathway that culminates in suppressing host and viral m RNA translation [12,111–113]. This translational control in antiviral immunity is mediated by the LRR-RLK NIK1, which was first identified as a virulence target of the begomovirus-encoded NSP [92,114]. NIK1 belongs to the subfamily II of LRR-RLK, which is further subdivided into phylogenetically related subclades, including a NIK antiviral subclade (NIK1-NIK3) and a somatic embryogenesis receptor kinase (SERK1-5) subclade of coreceptors in innate immunity [115]. In *Arabidopsis*, this subfamily of RLKs encompasses14 proteins that harbor four complete LRRs (with 24 residues) and a fifth incomplete LRR (with 16 residues) arranged in a single continuous block within the N-terminal extracellular domain, a single- pass transmembrane segment, and a highly conserved serine/threonine kinase domain at the C- terminal cytosolic side [116]. As a common property of the LRR-RLK subfamily II members, they often serve as coreceptors of multiple signaling receptors [89]. Accordingly, BAK1/SERK3, the best- characterized member of this subfamily II, acts as a coreceptor for the Brassinosteroid insensitive 1 (BRI- 1) receptor in developmental signaling and several different PRRs in innate immunity. In addition to structural conservation, NIK1 also shares other properties with members of the LRR-RLK subfamily II [117]. The phosphorylation of the threonine (Thr) residue position 474 constitutes a critical regulatory mechanism for NIK1 activation [113,118]. Likewise, the activation site of BAK1/SERK3, SERK4, and SERK1 lies in a conserved position with NIK1 Thr-474 within the activation loop of the kinases [117]. Like BAK1/SERK4, which is activated upon PAMP-induced oligomerization of PRRs, NIK1 has been recently shown to be activated by begomoviruses-derived nucleic acids that may act as viral PAMPs. NIK1 may serve as a coreceptor for a yet unknown viral PAMP-sensing PRR.

According to the current model for the NIK1-mediated antiviral signaling, at the onset of infection, *Begomovirus*-derived nucleic acids act as viral a PAMP to activate NIK1 via phosphorylation on Thr-474 (Figure 3) [12,118]. As a member of the LRR-RLK subfamily II, NIK1 may function as a coreceptor of a yet-to-be-identified immune receptor that may recognize the viral PAMPs for the assembly of the active immune complex. Alternatively, NIK1 may undergo viral PAMP-induced dimerization with itself or its paralog NIK2. This latter hypothesis is based on in vitro phosphorylation assays demonstrating that NIK1 undergoes dimerization and autophosphorylation [92]. Phosphorylation-induced activation of NIK1 mediates the phosphorylation of the downstream component ribosomal protein (RP) L10 on the Ser-104 residue, which in turn is redirected to the nucleus [119,120]. Activated NIK1 also undergoes sequential autophosphorylation at Thr-469 that antagonistically inhibits NIK1 activation providing a mechanism to fine-tune the extent of RPL10 phosphorylation [117,118]. In the nucleus, RPL10 interacts with the transcriptional repressor L10-interacting Myb domain-containing protein (LIMYB) to fully repress the expression of ribosomal protein genes and translational regulatory factors [113]. Prolonged repression of translational- machinery-related genes leads to the suppression of global host translation. Begomoviral mRNAs cannot escape this translational regulatory mechanism of plant cells; they are not translated efficiently, impairing infection. NSP from begomoviruses counters this activation mechanism by binding to the NIK1 kinase domain and preventing phosphorylation atThr-474, thereby enhancing *Begomovirus* pathogenicity [92,117]. In infected cells, RPL10 is trapped into the cytosol and is not translocated to the nucleus to mount the defense against begomoviruses. NIK1 overexpression titrates the viral suppressor NSP and restores the RPL10 nuclear localization upon NIK1 activation [118].

The NSP binding site on NIK1 was mapped to an 80-amino acid stretch within the activation loop, overlapping the essential Thr-474 for activation [92]. Therefore, NSP binding on the NIK1 kinase domain may cause stereochemical constraint on NIK1 phosphorylation at Thr-474, suggesting that NSP inhibition is upstream to NIK1 phosphorylation [120]. Consistent with this observation, the replacement of Thr-474 with the phosphor mimetic aspartate residue creates a constitutively activated NIK1 mutant, NIK1-T474D, which is barely inhibited by the viral suppressor NSP [117]. Furthermore, expression of the gain- of- function mutant NIK1-T474D in *Arabidopsis* enhances resistance to CabLCV,

and, in tomato plants, increases resistance to tomato yellow spot virus (ToYSV) and tomato severe rugose virus (ToSRV) [111,113]. This enhanced resistance phenotype has been associated with repression of translation-related regulatory genes, reduced loading of coat protein viral m RNA in actively translating polysomes, lower infection rate, and reduced viral DNA accumulation in systemic leaves [111]. However, a pitfall in this engineered defense strategy may be the side effects on development from impairing protein synthesis in trans- genic crops under field growth conditions. Expression of NIK1-T474D in *Arabidopsis* causes stunted growth, although, in tomato plants, the transgenic lines are phenotypically indistinguishable from the untransformed lines under greenhouse standard conditions [111,113]. This difference in developmental performance between these plant species may be due to their differential intrinsic capacity to withstand the deleterious effect of translational inhibition under environmentally controlled conditions, which may not be sustained under field conditions.

Recent studies have shown that NIK1 not only plays an essential role in the translational control of antiviral immunity but regulates bacterial PTI negatively [121]. NIK1 interacts with the bacterial PAMP flagellin receptor, FLS2, and its coreceptor BAK1 to prevent autoimmunity under normal, non-infected conditions (Figure 3). However, during *Pseudomonas* infection, the bacterial PAMP flagellin induces FLS2 and BAK1 oligomerization and transphosphorylation, forming an active immune complex to initiate PTI signaling. The active FLS2–BAK1 immune complex, in turn, phosphorylates NIK1 on Thr- 474, strengthening the NIK1 interaction with FLS2–BAK1 and concurrently activating the NIK1-mediated antiviral signaling. Significantly, bacterial flagellin (PAMP)- induced phosphorylation of NIK1 requires both FLS2 PRR and BAK1 coreceptor, indicating that NIK1 acts downstream of receptor signaling [121]. These results may implicate NIK1 as a coreceptor in receptor-mediated antiviral signaling that senses viral PAMPs via yet- unknown viral PRRs [12]. Furthermore, they demonstrate that a bacterial PAMP can induce NIK1 activation via the immune complex FLS2–BAK1, thereby allowing bacteria to activate antiviral immunity prior to virus infection. However, the finding that NIK1 suppresses antibacterial immunity further complicates the attempts to target NIK1-mediated antiviral signaling for engineered resistance against begomoviruses.

7. Conclusions

In RNA-silencing-mediated antiviral immunity, two mechanisms are fundamental to protect plants against invading nucleic acids from viruses, PTGS and TGS. PTGS is used as a defense mechanism against RNA and DN A viruses, whereas TGS targets virus DNA. PTGS acts at the post-transcriptional level by directing m RNA targets to degradation or translational suppression. In contrast, TGS represses transcription of target loci by con- trolling the chromatin methylation status and heterochromatin formation. Geminiviruses have evolved different suppressing strategies of host RNA-silencing-derived antiviral defenses. The geminiviral suppressors of RNA silencing can interfere with PTGS, TGS, and downstream events of TGS. They also act by activating or inducing the expression of endogenous suppressors. The immune-suppressing activities of geminiviruses may account for their broad host range and compromise the success of siRNA-based strategies for engineering host resistance.

The interactions of the plant's innate immune system with geminiviruses are far less understood. Nevertheless, growing evidence has demonstrated that the classical plant PTI limits geminivirus infection similarly to nonviral pathogens. Geminiviral proteins have been shown to target PTI components to both induce and suppress PTI-like responses. Furthermore, begomoviruses-derived nucleic acids act as viral PAMPs and activate the transmembrane receptor NIK1, which shares with PTI coreceptors conserved regulatory mechanisms for activation. However, geminiviral PAMPs and their cognate PRRs have yet to be identified, and hence, the mechanism of geminiviral PTI activation remains unknown. Likewise, plants may deploy ETI as part of the defense arsenal to combat geminiviruses. Accordingly, geminivirus infection induces ETI-like responses, including cell death, HR, ROS, SA accumulation in resistant genotypes, and at least one isolated resistant gene to TYLCV encodes an NLR protein, although the cognate geminiviral effector (Avr gene) is missing. The current studies designed to uncover geminiviral PTI- and ETI-suppressing functions are limited as they mostly target conserved features between the antiviral and anti-nonviral pathogen immunity. The discovery of

geminiviral PAMPs and their cognate PRRs, intracellular R proteins, and the matching geminiviral effectors will potentially shed light on the mechanism of antiviral PTI and ETI activation uncovering specific and conserved features and their specific roles in resistance against viruses.

Author Contributions: R.M.T., G.A.S.R. and M.A.F. wrote the first draft of the manuscript. E.P.B.F. conceived and supervised the review topics. All authors contributed to the article and approved the submitted version. All authors have read and agreed to the published version of the manuscript.

Funding: This work was partially funded by Coordenação de Aperfeiçoamento de Pessoal de Nível Superior (CAPES) finance code 001, Conselho Nacional de Desenvolvimento Cientifico e Tecnológico (CNPq), Fundação de Amparo à Pesquisa do Estado de Minas Gerais (FAPEMIG), and the National Institute of Science and Technology in Plant–Pest interactions. R.M.T. and G.A.S.R. are supported by FAPEMIG and CNPq graduate fellowships, respectively. M. A. is a recipient of a CNPq post-doctoral fellowship.

Conflicts of Interest: The authors declare no conflict of interest.

Abbreviations

ACMV	African cassava mosaic virus
ADKs	Adenosine kinases
A G O	Argonaute
AS2	Asymmetric leaves 2
Avr	Avirulence
BAK1	Brassinosteroid insensitive 1-associated receptor kinase
BAM1	1Barely any meristem 1
BCTV	Beet curly top virus
BDMV	Bean dwarf mosaic virus
BGYMV	Bean golden yellow mosaic virus
BRI-1	Brassinosteroid insensitive 1
BSCTV	Beet severe curly top virus
CabLCV	Cabbage leaf curl virus
CAS	Calcium-sensing receptor
CC- NLR	Coiled-coil nucleotide-binding leucine-rich repeat
CLCu KoV	Cotton leaf curl Kokhran virus
CLCu Mu	Cotton leaf curl Multan virus
VCP	Coat protein
CTM3	Chromomethylase 3
DAMPs	Damage-associated molecular patterns
DCLs	Dicers
dsDNA	Double-stranded DNA
DRM	DNA (cytosine-5)-methyltransferase 2
dsRNA	Double-stranded RNA
ETI	Effector-triggered immunity
FLS2	Flagellin-sensitive 2
H3K9	Histone H3 lysine 9
HEN1	Hua enhancer 1
HIR1	Hypersensitive induced reaction 1

HR	Hypersensitive response
HSP90	Heat shock protein 90
JA	Jasmonic acid
Kyp2/suvh4	suvh4/kryptonite2
LIR	Long intergenic region
LRR-RLK	Leucine-rich repeat receptor-like kinase
lncRNAs	Long non-coding RNAs
MAPK	Mitogen-activated protein kinase
MET1	Methyltransferase 1
miRNA	MicroRNA
MKK2	Mitogen-activated protein kinase 2
MP	Movement protein
mRNA	Messenger RNA
MYMIV	Mungbean yellow mosaic India
MYMV	Mungbean yellow mosaic virus-*Vigna*
NbHDA6	*Nicotiana benthamiana* histone deacetylase 6
NB-LRR	Nucleotide-binding site-leucine-rich repeat
NIK1	NSP-interacting kinase1
NLR	Nucleotide-binding leucine-rich repeat
NSP	Nuclear shuttling protein
nt	Nucleotides
ORF	Open reading frame
Ori	Origin of replication
PaLCuV	Papaya leaf curl virus
PAMP	Pathogen-associated molecular pattern
pol	Polymerase
PRR	Pattern recognition receptor
PTGS	Post-transcriptional gene silencing
PTI	PAMP-triggered immunity
R	Resistance
RdDM	RNA-directed D N A methylation
RdRP or RDR	RNA-dependent RNA polymerase
REn	Replication enhancer protein
Rep	Replication initiator protein
rgs-CaM	Regulator of G-protein signaling calmodulin-like
RISC	RNA-induced silencing complex
RITS	RNA-induced transcriptional silencing complex
RLK	Receptor-like kinase
RNAi	RNA interference
ROS	Reactive oxygen species
RP	Ribosomal protein
SA	Salicylic acid
SAHH	*S*-adenosyl-L-homocysteine hydrolase
SAM	*S*-adenosyl methionine
SAMDC1	*S*-adenosyl-methionine decarboxylase 1
SAR	Systemic acquiredresistance
SERK 1-5	Somatic embryogenesis receptor kinase 1–5
SGS3	Suppressor genesilencing 3
SGT1	Suppressor of the G2 allele of skp1
SIR	Short intergenicregion
siRNA	Small interfering RNA

ssDNA	Single-stranded DNA
ssRNA	Single-stranded RNA
TGMV	Tomato golden mosaic virus
TGS	Transcriptional gene silencing
Thr	Threonine
TIR-NLR	Toll/interleukin 1 receptor-like nucleotide-binding leucine-rich repeat
TLCYnV	Tomato leaf curl Yunnan virus
ToLCNDV	Tomato leaf curl New Delhi virus
ToSRV	Tomato severe rugose virus
ToYSV	Tomato yellow spot virus
TrAP	Transcriptional activator protein
TYLCCV	Tomato yellow leaf curl China virus
TYLCSV	Tomato yellow leaf curl Sardinia virus
TYLCV	Tomato yellow leaf curl virus
UTR	Untranslated region
vsiRNAs	Virus-derived short interfering RNAs
VSRs	Viral suppressors of RNA silencing
WDV	Wheat dwarf virus
WEL1	Werner exonuclease-like 1

References

1. Kumar, R.V. Plant antiviral immunity against Geminiviruses and viral counter-defense for survival. *Front. Microbiol.* **2019**, *10*, 1460. [CrossRef] [PubMed]
2. Calil, I.P.; Fontes, E.P.B. Plant immunity against viruses: Antiviral immune receptors in focus. 3. *Ann. Bot.* **2017**, *119*, 711–723. [CrossRef]
3. Jones, J.D.; Dangl, J.L. The plant immune system. *Nature* **2006**, *444*, 323–329. [CrossRef]
4. Li, F.; Wang, A. RNA-Targeted Antiviral Immunity: More Than Just RNA Silencing. *Trends Microbiol.* **2019**, *27*, 792–805. [CrossRef] [PubMed]
5. Pooggin, M. M. Small RNA-Omics for plant virus identification, virome reconstruction, and antiviral defense characterization. *Front. Microbiol.* **2018**, *9*, 2779. [CrossRef] [PubMed]
6. Gouveia, B.C.; Calil, I.P.; Machado, J.P.B.; Santos, A. A.; Fontes, E.P.B. Immune receptors and coreceptors in antiviral innate immunity in plants. *Front. Microbiol.* **2017**, *7*, 2139. [CrossRef] [PubMed]
7. Mandadi, K.K.; Scholthof, K.-B.G. Plant immune responses against viruses: How does a virus cause disease? Plant Cell 2013, 25, 1489–1505. [CrossRef] [PubMed]
8. Holmes, F.O. Local lesions in tobacco mosaic. *Bot. Gaz.* **1929**, *87*, 39–55. [CrossRef]
9. Holmes, F.O. Inheritance of resistance to tobacco-mosaic disease in tobacco. *Phytopathoogy* **1938**, *28*, 553–561.
10. Ross, A.F. Systemic acquired resistance induced by localized virus infections in plants. *Virology* **1961**, *14*,340–358. [CrossRef]
11. Amari, K.; Niehl, A. Nucleic acid-mediated PAMP-triggered immunity in plants. *Curr. Opin. Virol.* **2020**, *42*, 32–39. [CrossRef]
12. Teixeira, R.M.; Ferreira, M.A.; Raimundo, G.A.; Loriato, V.A.; Reis, P.A.; Fontes, E.P.B. Virus perception at the cell surface: Revisiting the roles of receptor-like kinases as viral pattern recognition receptors. *Mol. Plant Pathol.* **2019**, *20*, 1196–1202. [CrossRef] [PubMed]
13. Loriato, V.A.P.; Martins, L.G.C.; Euclydes, N.C.; Reis, P.A.B.; Duarte, C.E.M.; Fontes E.P.B. Engineering resistance against geminiviruses: A review of suppressed natural defenses and the use of RNAi and the CRISPR/Cas system. Plant Sci. 2020, 292, 110410. [CrossRef]
14. Gómez, B.G.; Zhang, D.; Díaz, R.T.; Wei, Y.; Macho, A.P.; Lozano-Durán, R. The C4 protein from *Tomato Yellow leaf curl virus* can broadly interact with plant receptor-like kinases. *Viruses* **2019**, *11*, 1009. [CrossRef]
15. Macho, A.P.; Lozano-Duran, R. Molecular dialogues between viruses and receptor-like kinases in plants. Mol. Plant Pathol. 2019, 20, 1191–1195. [CrossRef] [PubMed]

16. Mei, Y.; Ma, Z.; Wang, Y.; Zhou, X. Geminivirus C4 antagonizes the HIR1-mediated hypersensitive response by inhibiting the HIR1 self-interaction and promoting degradation of the protein. *New Phytol.* **2020**, *225*, 1311–1326. [CrossRef]

17. Yamaguchi, H.; Ohnishi, J.; Saito, A.; Ohyama, A.; Nunome, T.; Miyatake, K.; Fukuoka, H. An NB-LRR gene, TYNBS1, is responsible for resistance mediated by the Ty-2 Begomovirus resistance locus of tomato. *Theor. Appl. Genet.* 2018, 131, 1345– 1362. [CrossRef]

18. Ghosh, D.; Chakraborty, S. Molecular interplay between phytohormones and geminiviruses: A saga of a never-ending arms race. *J. Exp. Bot. 2021,* in *press*. [CrossRef]

19. Zerbini, F.M.; Briddon, R.W.; Idris, A.; Martin, D.P.; Moriones, E.; Navas-Castillo, J.; Rivera- Bustamante, R.; Roumagnac, P.; Varsani, A. ICTV Virus Taxonomy Profile: Geminiviridae. *J. Gen. Virol*. 2017, 98, 131–133. [CrossRef] [PubMed]

20. Martins, L.G.C.; Raimundo, G.A.S.; Ribeiro, N. G. A.; Silva, J.C.F.; Euclydes, N.C.; Loriato, V.A.P.; Duarte, C.E.M.; Fontes, E.P.B. A Begomovirus Nuclear Shuttle Protein-Interacting Immune Hub: Hijacking Host Transport Activities and Suppressing Incom- patible Functions. *Front. Plant Sci*. 2020, 11, 398. [CrossRef]

21. Briddon, R.W.; Martin, D.P.; Roumagnac, P.; Navas-Castillo, J.; Fiallo-Olivé, E.; Moriones, E.; Lett, J.- M.; Zerbini, F.M.; Varsani, A. Alphasatellitidae: A new family with two subfamilies for the classification of geminivirus- and nanovirus-associated alphasatellites. *Arch. Virol.* **2018**, *163*, 2587–2600. [CrossRef]

22. Yang, X.; Guo, W.; Li, F.; Sunter, G.; Zhou, X. Geminivirus-associated betasatellites: Exploiting chinks in the antiviral arsenal of plants. *Trends Plant Sci.* **2019**, *24*, 519–529. [CrossRef] [PubMed]

23. Ding, S.W.; Voinnet, O. Antiviral immunity directed by small RNAs. Cell 2007, 130, 413–426. [CrossRef]

24. Akbergenov, R.; Si-Ammour, A.; Blevins, T.; Amin, I.; Kutter, C.; Vanderschuren, H.; Zhang, P.; Gruissem, W.; Meins, F.; Hohn, T.; et al. Molecular characterization of geminivirus-derived small RNAs in different plant species. *Nucleic Acids Res.* **2006**, *34*, 462–471. [CrossRef]

25. Bouché, N.; Lauressergues, D.; Gasciolli, V.; Vaucheret, H. An antagonistic function for Arabidopsis DCL2 in development and a new function for DCL4 in generating viral siRNAs. *EMBO J.* **2006**, *25*, 3347–3356. [CrossRef] [PubMed]

26. Reinhart, B.J.; Weinstein, E.G.; Rhoades, M.W.; Bartel, B.; Bartel, D.P. MicroRNAs in plants. *Genes Dev.* **2002**, *16*, 1616–1626. [CrossRef]

27. Xie, Z.; Johansen, L.K.; Gustafson, A.M.; Kasschau, K.D.; Lellis, A.D.; Zilberman, D.; Jacobsen, S.E.; Carrington, J.C. Genetic and functional diversification of small R NA pathways in plants. *PLoS Biol.* **2004**, *2*, e104. [CrossRef]

28. Wang, X.-B.; Jovel, J.; Udomporn, P.; Wang, Y.; Wu, Q.; Li, W.-X.; Gasciolli, V.; Vaucheret, H.; Ding, S.-W. The 21-nucleotide, but not 22-nucleotide, viral secondary small interfering RNAs direct potent antiviral defense by two cooperative Argonautes in *Arabidopsis thaliana*. *Plant Cell* **2011**, *23*, 1625–1638. [CrossRef]

29. Baulcombe, D. RNA silencing in plants. *Nature* **2004**, *431*, 356–363. [CrossRef] [PubMed]

30. Blevins, T.; Rajeswaran, R.; Aregger, M.; Borah, B.K.; Schepetilnikov, M.; Baerlocher, L.; Farinelli, L.; Meins, F.; Hohn, T.; Pooggin, M. M. Massive production of small RNAs from a non-coding region of Cauliflower mosaic virus in plant defense and viral counter-defense. *Nucleic Acids Res.* **2011**, *39*, 5003–5014. [CrossRef]

31. Li, J.; Yang, Z.; Yu, B.; Liu, J.; Chen, X. Methylation protects miRNAs and siRNAs from a 3′-end uridylation activity in Arabidopsis. *Curr. Biol.* **2005**, *15*, 1501–1507. [CrossRef]

32. Yang, Z.Y.; Ebright, Y.W.; Yu, B.; Chen, X.M. HEN1 recognizes 21–24 nt small RNA duplexes and deposits a methyl group onto the 2′ OH of the 3′ terminal nucleotide. *Nucleic Acids Res.* **2006**, *34*, 667–675. [CrossRef]

33. Yu, B.; Yang, Z.; Li, J.; Minakhina, S.; Yang, M.; Padgett, R.W.; Steward, R.; Chen, X. Methylation as a crucial step in plant microRNA biogenesis. *Science* **2005**, *307*, 932–935. [CrossRef]

34. Bühler, M.; Verdel, A.; Moazed, D. Tethering RITS to a nascent transcript initiates RNAi- and heterochromatin-dependent gene silencing. *Cell* **2006**, *125*, 873–886. [CrossRef] [PubMed]

35. Song, J.J.; Smith, S.K.; Hannon, G.J.; Joshua-Tor, L. Crystal structure of Argonaute and its implications for RISC slicer activity. Science 2004, 305, 1434–1437. [CrossRef] [PubMed]

36. Verdel, A.; Jia, S.; Gerber, S.; Sugiyama, T.; Gygi, S.; Grewal, S.I.S.; Moazed, D. RNAi-mediated targeting of heterochromatin by the RITS complex. *Science* **2004**, *303*, 672–676. [CrossRef] [PubMed]

37. Deleris, A.; Gallego-Bartolome, J.; Bao, J.; Kasschau, K.D.; Carrington, J.C.; Voinnet, O. Hierarchical action and inhibition of plant dicer-like proteins in antiviral defense. *Science* **2006**, *313*, 68–71. [CrossRef]

38. Baumberger, N.; Baulcombe, D. C. *Arabidopsis* ARGONAUTE 1 is an RNA slicer that selectively recruits microRNAs and short interfering RNAs. *Proc. Natl. Acad. Sci. USA* **2005**, *102*, 11928–11933. [CrossRef]

[PubMed]

39. Bhattacharjee, S.; Zamora, A.; Azhar, M.T.; Sacco, M.A.; Lambert, L.H.; Moffett, P. Virus resistance induced by NB-LRR proteins involves Argonaute4-dependent translational control. *Plant J.* **2009**, *58*, 940–951. [CrossRef] Ghoshal, B.; Sanfaçon, H. Symptom recovery in virus-infected plants: Revisiting the role of RNA silencing mechanisms. *Virology* **2015**, *479–480*, 167–179. [CrossRef] [PubMed]

40. Karran, R.A.; Sanfaçon, H. Tomato ringspot virus coat protein binds to ARGONAUTE 1 and suppresses the translation repression of a reporter gene. *Mol. Plant Microbe Interact.* **2014**, *27*, 933– 943. [CrossRef] [PubMed]

41. Ma, X.; Nicole, M.C.; Meteignier, L.V.; Hong, N.; Wang, G.; Moffett, P. Different roles for RNA silencing and RNA processing components in virus recovery and virus-induced gene silencing in plants. *J. Exp. Bot.* **2015**, *66*, 919–932. [CrossRef]

42. Brodersen, P.; Sakvarelidze-Achard, L.; Bruun-Rasmussen, M.; Dunoyer, P.; Yamamoto, Y.Y.; Sieburth, L.; Voinnet, O. Widespread translational inhibition by plant miRNAs and siRNAs. *Science* **2008**, *320*, 1185–1190. [CrossRef]

43. Fátyol, K.; Ludman, M.; Burgyán, J. Functional dissection of a plant Argonaute. *Nucleic Acids Res.* **2016**, *44*, 1384–1397. [CrossRef]

44. Iwakawa, H.O.; Tomari, Y. Molecular insights into microRNA-mediated translational repression in plants. *Mol. Cell* **2013**, *52*, 591–601. [CrossRef]

45. Lanet, E.; Delannoy, E.; Sormani, R.; Floris, M.; Brodersen, P.; Crété, P.; Voinnet, O.; Robaglia, C. Biochemical evidence for translational repression by *Arabidopsis* microRNAs. *Plant Cell* **2009**, *21*, 1762–1768. [CrossRef]

46. Wilczynska, A.; Bushell, M. The complexity of miRNA-mediated repression. *Cell Death Differ.* **2015**, 22, 22–33. [CrossRef]

47. Raja, P.; Sanville, B.C.; Buchmann, R.C.; Bisaro, D.M. Viral genome methylation as an epigenetic defense against geminiviruses. *J. Virol.* **2008**, *82*, 8997–9007. [CrossRef]

48. Matzke, M.A.; Moshe, R.A. RNA-directed DNA methylation: An epigenetic pathway of increasing /complexity. Nat. Rev. Genet. 2014, 5, 394–408. [CrossRef]

49. El-Shami, M.; Pontier, D.; Lahmy, S.; Braun, L.; Picart, C.; Vega, D.; Hakimi, M.-A.; Jacobsen, S.E.; Cooke, R.; Lagrange, T. Reiterated WG/GW motifs form functionally and evolutionarily conserved ARGONAUTE-binding platforms in RNAi-related components. Genes Dev. 2007, 21, 2539–2544. [CrossRef] [PubMed]

50. Matzke, M.A.; Moshe, R.A. RNA-directed D N A methylation: An epigenetic pathway of increasing complexity.

51. *Nat. Rev. Genet.* **2014**, *5*, 394–408. [CrossRef]

52. El-Shami, M.; Pontier, D.; Lahmy, S.; Braun, L.; Picart, C.; Vega, D.; Hakimi, M.-A.; Jacobsen, S.E.; Cooke, R.; Lagrange, T. Reiterated WG/ GW motifs form functionally and evolutionarily conserved ARGONAUTE-binding platforms in RNAi-related components. *Genes Dev.* **2007**, *21*, 2539–2544. [CrossRef] [PubMed]

53. Fang, X.; Qi, Y. RNAi in plants: An Argonaute-Centered view. *Plant Cell* **2016**, *28*, 272–285. [CrossRef] [PubMed]

54. Raja, P.; Jackel, J.N.; Li, S.; Heard, I.M.; Bisaro, D. M. Arabidopsis double-stranded RNA binding protein DRB3 participates in methylation-mediated defense against geminiviruses. *J. Virol.* **2014**, *88*, 2611–2622. [CrossRef] [PubMed]

55. Rodríguez-Negrete, E.A.; Carrillo-Tripp, J.; Rivera-Bustamante, R.F. RNA silencing against geminivirus: Complementary action of posttranscriptional gene silencing and transcriptional gene silencing in host recovery. *J. Virol.* **2009**, *83*, 1332–1340. [CrossRef]

56. Aregger, M.; Borah, B.K.; Seguin, J.; Rajeswaran, R.; Gubaeva, E.G.; Zvereva, A.S.; Windels, D.; Vazquez, F.; Blevins, T.; Farinelli, L.; et al. Primary and secondary siRNAs in geminivirus-induced gene silencing. *PLoS Pathog.* **2012**, *8*, e1002941. [CrossRef]

57. Wang, J.; Yu, W.; Yang, Y.; Li, X.; Chen, T.; Liu, T.; Ma, N.; Yang, X.; Liu, R.; Zhang, B. Genome-wide analysis of tomato long non-coding RNAs and identification as endogenous target mimic for microRNA in response to TYLCV infection. *Sci. Rep.* **2015**, *5*, 16946. [CrossRef] [PubMed]

58. Sun, Y.W.; Tee, C.S.; Ma, Y.H.; Wang, G.; Yao, X.M.; Ye, J. Attenuation of histone methyltransferase KRYPTONITE- mediated transcriptional gene silencing by Geminivirus. *Sci. Rep.* **2015**, *5*, 16476. [CrossRef] [PubMed]

59. Csorba, T.; Kontra, L.; Burgyan, J. Viral silencing suppressors: Tools forged to fine-tune host-pathogen coexistence. *Virology* **2015**, *479*, 85–103. [CrossRef]

60. Ding, S.W. RNA-based antiviral immunity. *Nat. Rev. Immunol.* **2020**, *10*, 632–644. [CrossRef]

61. Incarbone, M.; Dunoyer, P. RNA silencing and its suppression: Novel insights from in planta analyses.*Trends Plant Sci.* **2013**, *18*, 382–392. [CrossRef]

62. Yang, Z.; Li, Y. Dissection of RNAi-based antiviral immunity in plants. *Curr. Opin. Virol.* **2018**, *32*, 88–99. [CrossRef]

63. Rodríguez-Negrete, E.; Lozano-Durán, R.; Piedra-Aguilera, A.; Cruzado, L.; Bejarano, E.R.; Castillo, A. G. Geminivirus Rep protein interferes with the plant D N A methylation machinery and suppresses transcriptional gene silencing. *New Phytol.* **2013**, *199*, 464–475. [CrossRef]

64. Wang, Y.; Dang, M.; Hou, H.; Mei, Y.; Qian, Y.; Zhou, X. Identification of an RNA silencing suppressor encoded by a mastrevirus. *J. Gen. Virol.* **2014**, *95*, 2082–2088. [CrossRef]

65. Castillo-González, C.; Liu, X.; Huang, C.; Zhao, C.; Ma, Z.; Hu, T.; Sun, F.; Zhou, Y.; Zhou, X.; Wang, X.-J.; et al. Geminivirus- encoded TrAP suppressor inhibits the histone methyltransferase SUVH 4 /KYP to counter host defense. *Elife* **2015**, *4*, e06671. [CrossRef] [PubMed]

66. Wang, H.; Hao, L.; Shung, C.Y.; Sunter, G.; Bisaro, D. M. Adenosine kinase is inactivated by geminivirus AL2 and L2 proteins. *Plant Cell* **2003**, *15*, 3020–3032. [CrossRef] [PubMed]

67. Kumar, V.; Mishra, S.K.; Rahman, J.; Taneja, J.; Sundaresan, G.; Mishra, N.S.; Mukherjee, S.K. Mungbean yellow mosaic Indian virus-encoded AC2 protein suppresses RNA silencing by inhibiting Arabidopsis RDR6 and AGO1 activities. *Virology* **2015**, *486*, 158–172. [CrossRef] [PubMed]

68. Zhang, Z.; Chen, H.; Huang, X.; Xia, R.; Zhao, Q.; Lai, J.; Teng, K.; Li, Y.; Liang, L.; Du, Q.; et al. BSCTV C2 attenuates the degradation of SAMDC1 to suppress D N A methylation-mediated gene silencing in *Arabidopsis*. *Plant Cell* **2011**, *23*, 273–288. [CrossRef]

69. Amin, I.; Patil, B.L.; Briddon, R.W.; Mansoor, S.; Fauquet, C. M. Comparison of phenotypes produced in response to transient expression of genes encoded by four distinct begomoviruses in *Nicotiana benthamiana* and their correlation with the levels of developmental miRNAs. *Virol. J.* **2011**, *8*, 238. [CrossRef] [PubMed]

70. Sunitha, S.; Shanmugapriya, G.; Balamani, V.; Veluthambi, K. *Mungbean yellow mosaic virus* (MYMV) *AC4* suppresses post- transcriptional gene silencing and an *AC4* hairpin RN A gene reduces MYMV D N A accumulation in transgenic tobacco. *Virus Genes* **2013**, *46*, 496–504. [CrossRef] [PubMed]

71. Rosas-Diaz, T.; Zhang, D.; Fan, P.; Wang, L.; Ding, X.; Jiang, Y.; Jimenez-Gongora, T.; Medina-Puche, L.; Zhao, X.; Feng, Z.; et al. A virus-targeted plant receptor-like kinase promotes cell-to-cell spread of RNAi. *Proc. Natl. Acad. Sci. USA* **2018**, *115*, 1388–1393. [CrossRef]

72. Ismayil, A.; Haxim, Y.; Wang, Y.; Li, H.; Qian, L.; Han, T.; Chen, T.; Jia, Q.; Liu, A.Y.; Zhu, S.; et al. *Cotton Leaf Curl Multan virus* C4 protein suppresses both transcriptional and post-transcriptional gene silencing by interacting with SAM synthetase. *PLoS Pathog.* **2018**, *14*, e1007282. [CrossRef] [PubMed]

73. Vinutha, T.; Kumar, G.; Garg, V.; Canto, T.; Palukaitis, P.; Ramesh, S.; Praveen, S. Tomato geminivirus encoded RNAi suppressor protein, AC4 interacts with host AGO4 and precludes viral D N A methylation. *Gene* **2018**, *678*, 184–195. [CrossRef]

74. Li, F.; Xu, X.; Huang, C.; Gu, Z.; Cao, L.; Hu, T.; Ding, M.; Li, Z.; Zhou, X. The AC5 protein encoded by *Mungbean yellow mosaic India virus* is a pathogenicity determinant that suppresses RNA silencing-based antiviral defenses. *New Phytol.* **2015**, *208*, 555–569. [CrossRef]

75. Luna, A.P.; Rodríguez-Negrete, E.A.; Morilla, G.; Wang, L.; Lozano-Durán, R.; Castillo, A.G.; Bejarano, E.R. V2 from a curtovirus is a suppressor of post-transcriptional gene silencing. *J. Gen. Virol.* **2017**, *98*, 2607– 2614. [CrossRef] [PubMed]

76. Luna, A.P.; Romero-Rodríguez, B.; Rosas-Díaz, T.; Cerero, L.; Rodríguez-Negrete, E.A.; Castillo, A.G.; Bejarano, E.R. Characterization of Curtovirus V2 protein, a functional homolog of begomovirus V2. *Front. Plant Sci.* **2020**, *11*, 835. [CrossRef] [PubMed]

77. Wang, B.; Yang, X.; Wang, Y.; Xie, Y.; Zhou, X. Tomato yellow leaf curl virus V2 interacts with host histone deacetylase 6 to suppress methylation-mediated transcriptional gene silencing in plants. *J. Virol.* **2018**, *92*, e0036-1. [CrossRef]

78. Glick, E.; Zrachya, A.; Levy, Y.; Mett, A.; Gidoni, D.; Belausov, E.; Citovsky, V.; Gafni, Y. Interaction with host SGS3 is required for suppression of RNA silencing by tomato yellow leaf curl virus V2 protein. *Proc. Natl. Acad. Sci. USA* **2008**, *105*, 157–161. [CrossRef]

79. Amin, I.; Hussain, K.; Akbergenov, R.; Yadav, J.S.; Qazi, J.; Mansoor, S.; Hohn, T.; Fauquet, C.M.; Briddon, R.W. Suppressors of RNA silencing encoded by the components of the cotton leaf curl begomovirus-beta satellite

complex. *Mol. Plant Microbe Interact.* **2011**, *24*, 973–983. [CrossRef] [PubMed]

80. Lu, Q.Y.; Yang, L.; Huang, J.; Zheng, L.; Sun, X. Identification and subcellular location of an RNA silencing suppressor encoded by mulberry crinkle leaf virus. Virology 2019, 526, 45–51. [CrossRef] [PubMed]

81. Yang, X.; Xie, Y.; Raja, P.; Li, S.; Wolf, J.N.; Shen, Q.; Bisaro, D.M.; Zhou, X. Geminivirus activates *ASYMMETRIC LEAVES 2* to accelerate cytoplasmic DCP2-mediated m RNA turnover and weakens RNA silencing in *Arabidopsis*. *PLoS Pathog.* **2015**, *11*, e1005196.

82. Saeed, M.; Briddon, R.; Dalakouras, A.; Krczal, G.; Wassenegger, M. Functional analysis of *Cotton Leaf Curl Kokhran Virus*/*Cotton Leaf Curl Multan* beta satellite RNA silencing suppressors. *Biology* **2015**, *4*, 697–714. [CrossRef] [PubMed]

83. Yang, X.; Xie, Y.; Raja, P.; Li, S.; Wolf, J.N.; Shen, Q.; Bisaro, D.M.; Zhou, X. Suppression of methylation-mediated transcriptional gene silencing by β C1 - SAHH protein interaction during geminivirus-beta satellite infection. *PLoS Pathog.* **2011**, *7*, e1002329. [CrossRef] [PubMed]

84. Kamal, H.; Minhas, F.-U.-A.A.; Tripathi, D.; Abbasi, W.A.; Hamza, M.; Mustafa, R.; Khan, M.Z.; Mansoor, S.; Pappu, H.R.; Amin, I. βC1, pathogenicity determinant encoded by Cotton leaf curl Multan beta satellite, interacts with calmodulin-like protein 11 (Gh-CML11) in *Gossypium hirsutum*. *PLoS ONE* **2019**, *14*, e0225876. [CrossRef]

85. Li, F.; Huang, C.; Li, Z.; Zhou, X. Suppression of RNA Silencing by a plant D N A virus satellite requires a host calmodulin-like protein to repress RDR6 expression. *PLoS Pathog.* **2014**, *10*, e1003921. [CrossRef] [PubMed]

86. Macho, A.P.; Zipfel, C. Targeting of plant pattern recognition receptor-triggered immunity by bacterial type-III secretion system effectors. *Curr. Opin. Microbiol.* **2015**, *23*, 14–22. [CrossRef]

87. Ma, X.; Xu, G.; He, P.; Chan, L. SERKing coreceptors for Receptors. *Trends Plant Sci.* **2016**, *21*, 1017– 1033. [CrossRef] [PubMed]

88. Bigeard, J.; Colcombet, J.; Hirt, H. Signaling mechanisms in pattern-triggered immunity (PTI).*Mol Plant* **2015**, *8*, 521–539. [CrossRef]

89. Sakamoto, T.; Deguchi, M.; Brustolini, O.J.; Santos, A.A.; Silva, F.F.; Fontes, E.P.B. The tomato RLK superfamily: Phylogeny and functional predictions about the role of the LRRII-RLK subfamily in antiviral defense. *BMC Plant Biol.* **2012**, *12*, 229. [CrossRef]

90. Fontes, E.P.B.; Santos, A.A.; Luz, D.F.; Waclawovsky, A.J.; Chory, J. The geminivirus NSP acts as a virulence factor to suppress an innate transmembrane receptor kinase-mediated defense signaling. *Genes Dev.* **2004**, *18*, 2545–2556. [CrossRef]

91. Aguilar, E.; Gomez, B.G.; Lozano-Duran, R. Recent advances on the plant manipulation by geminiviruses.

92. *Curr. Opin. Plant Biol.***2020**, *56*, 56–64. [CrossRef] [PubMed]

93. Wang, D.; Zhang, X.; Yao, X.; Zhang, P.; Fang, R.; Ye, J. A 7-amino-acid motif of Rep protein essential for virulence is critical for triggering host defense against Sri *Lankan cassava mosaic virus*. *Mol. Plant Microbe Interact.* **2020**, *33*, 78–86. [CrossRef]

94. Medina-Puche, L.; Tan, H.; Dogra, V.; Wu, M.; Rosas-Diaz, T.; Wang, L.; Ding, X.; Zhang, D.; Fu, X.; Kim, C.; et al. A Defense Pathway Linking Plasma Membrane and Chloroplasts and Co-opted by Pathogens. *Cell* **2020**, *182*, 1109–1124.e25. [CrossRef] [PubMed]

95. 97. Li, F.; Yang, X.; Bisaro, D.M.; Zhou, X. The βC1 Protein of Geminivirus-Betasatellite Complexes: ATarget and Repressor of Host Defenses. *Mol. Plant* **2018**, *11*, 1424–1426. [CrossRef]

96. Cui, X.; Tao, X.; Xie, Y.; Fauquet, C.M.; Zhou, X. A D N Aβ associated with *Tomato yellow leaf curl*China virus is required for symptom induction. *J. Virol.* **2004**, *78*, 13966–13974 [CrossRef]

97. Hu, T.; Huang, C.; He, Y.; Castillo-González, C.; Gui, X.; Wang, Y.; Zhang, X.; Zhou, X. βC1 protein encoded in geminivirus satellite concertedly targets MKK2 and MPK4 to counter host defense. *PLoS Pathog.* **2019**, *15*, e1007728. [CrossRef] [PubMed]

98. Decroocq, V.; Salvador, B.; Sicard, O.; Glasa, M.; Cosson, P.; Svanella-Dumas, L.; Revers, F.; García, J.A.; Candresse, T. The determinant of potyvirus ability to overcome the RTM resistance of *Arabidopsis thaliana* maps to the N-terminal region of the coat protein. *Mol. Plant Microbe Interact.* **2009**, *22*, 1302– 1311. [CrossRef] [PubMed]

99. Dalio, R.J.D.; Paschoal, D.; Arena, G.D.; Magalhães, D.M.; Oliveira, T.S.; Merfa, M.V.; Maximo, H.J.; Machado, M.Hypersensitive response: From NLR pathogen recognition to cell death response. *Ann. Appl. Biol.*

2020; in press. [CrossRef]

100. Ando, S.; Miyashita, S.; Takahashi, H. Plant defense systems against cucumber mosaic virus: Lessons learned from CMV— *Arabidopsis* interactions. *J. Gen. Plant Pathol.* **2019**, *85*, 174–181. [CrossRef]

101. Ascencio-Ibáñez, J.T.; Sozzani, R.; Lee, T.J.; Chu, T.M.; Wolfinger, R.D.; Cella, R.; Hanley-Bowdoin, L. Global analysis of *Arabidopsis* gene expression uncovers a complex array of changes impacting pathogen response and cell cycle during geminivirus infection. *Plant Physiol.* **2008**, *148*, 436–454. [CrossRef] [PubMed]

102. Garrido-Ramirez, E.R.; Sudarshana, M.R.; Lucas, W.J.; Gilbertson, R.L. Bean dwarf mosaic virus BV1 protein is a determinant of the hypersensitive response and avirulence in *Phaseolus vulgaris*. *Mol. Plant Microbe Interact.* **2000**, *13*, 1184–1194. [CrossRef] [PubMed]

103. Selth, L.A.; Randles, J.W.; Rezaian, M. A. Host responses to transient expression of individual genes encoded by Tomato leaf curl virus. *Mol. Plant Microbe Interact.* **2004**, *17*, 27–33. [CrossRef] [PubMed]

104. Hussain, M.; Mansoor, S.; Iram, S.; Zafar, Y.; Briddon, W. The hypersensitive response to Tomato leaf curl New Delhi virus nuclear shuttle protein is inhibited by transcriptional activator protein. *Mol. Plant Microbe Interact.* **2007**, *20*, 1581–1588. [CrossRef]

105. Mubin, M.; Amin, I.; Amrao, L.; Briddon, R.W.; Mansoor, S. The hypersensitive response induced

106. by the V2 protein of a monopartite begomovirus is countered by the C2 protein. *Mol. Plant Pathol.* **2010**, *1*

107. Moshe, A.; Gorovits, R.; Liu, Y.; Czosnek, H. Tomato plant cell death induced by inhibition oHSP90 is alleviated by tomato yellow leaf curl virus infection. *Mol. Plant Pathol.* **2016**, *17*, 247–260. [CrossRef]

108. Machado, J.P.B.; Calil, I.P.; Santos, A.A.; Fontes, E.P.B. Translational control in plant antiviral immunity.

109. Genet. *Mol. Biol.* **2017**, *40*, 292–304. [CrossRef] [PubMed]

110. Mohr, I.; Sonenber, N. Host Translation at the Nexus of Infection and Immunity. *Cell Host Microbe,* **2012**, *12*, 470–483. [CrossRef]

111. Stern-Ginossar, N.; Thompson, S.R.; Mathews, M.B.; Mohr, I. Translational Control in Virus-Infected Cells. *Cold Spring Harb. Perspect Biol.* **2019**, *11*, a03300. [CrossRef]

112. Brustolini, O.J.; Machado, J.P.B.; Condori-Apfata, J.A.; Coco, D.; Deguchi, M.; Loriato, V.A.; Pereira, W.A.; Alfenas-Zerbini, P.; Zerbini, F.M.; Inoue-Nagata, A.K.; et al. Sustained NIK-mediated antiviral signalling confers broad-spectrum tolerance to begomoviruses in cultivated plants. *Plant Biotechnol. J.* **2015**, *13*, 1300–1311. [CrossRef] [PubMed]

113. Machado, J.P.B.; Brustolini, O.J.B.; Mendes, G.C.; Santos, A.A.; Fontes, E.P.B. NIK1, a host factor specialized in antiviral defense or a novel general regulator of plant immunity? *Bioessays* **2015**, *37*, 1236–1242. [CrossRef]

114. Zorzatto, C.; Machado, J.P.B.; Lopes, K.V.G.; Nascimento, K.J.T.; Pereira, W.A.; Brustolini, O.J.B.; Reis, P.A.B.; Calil, I.P.; Deguchi, M.; Sachetto-Martins, G.; et al. NIK1-mediated translation suppression functions as a plant antiviral immunity mechanism. *Nature* **2015**, *520*, 679–682. [CrossRef]

115. Mariano, A. C.; Andrade, M.O.; Santos, A. A.; Carolino, S.M.; Oliveira, M.L.; Baracat-Pereira, M. C.; Brommonshenkel, S.H.; Fontes, E.P. Identification of a novel receptor-like protein kinase that interacts with a geminivirus nuclear shuttle protein. *Virology* **2004**, *318*, 24–31. [CrossRef] [PubMed]

116. Hosseini, S.; Schmidt, E.D.L.; Bakker, F.T. Leucine-rich repeat receptor-like kinase II phylogenetics reveals five main clades throughout the plant kingdom. *Plant J.* **2020**, *103*, 547–560. [CrossRef]

117. Zhang, X.S.; Choi, J.H.; Heinz, J.; Chetty, C.S. Domain-specific positive selection contributes to the evolution of Arabidopsis leucine rich repeat receptor-like kinase (LRR RLK) genes. *J. Mol. Evol.* **2006**, *63*, 612–621. [CrossRef]

118. Santos, A.A.; Lopes, K.V.G.; Apfata, J.A.C.; Fontes, E.P.B. NSP-interacting kinase, NIK: A transducer of plant defence signalling. *J. Exp. Bot.* **2010**, *61*, 3839–3845. [CrossRef]

119. Santos, A. A.; Carvalho, C.M.; Florentino, L.H.; Ramos, H.J.O.; Fontes, E.P.B. Conserved threonine residues within the A- loop of the receptor NIK differentially regulate the kinase function required for antiviral signaling. *PLoS ONE* **2009**, *4*, e5781. [CrossRef] [PubMed]

120. Carvalho, C.M.; Santos, A. A.; Pires, S.R.; Rocha, C.S.; Saraiva, D.I.; Machado, J.P.B.; Mattos, E.C.; Fietto, L.G.; Fontes, E.P.B. Regulated nuclear trafficking of rpL10A mediated by NIK1 represents a defense strategy of plant cells against viruses. *PLoS Pathog.* **2008**, *4*, e1000247. [CrossRef]

121. Rocha, C.S.; Santos, A. A.; Machado, J.P.B.; Fontes, E.P.B. The ribosomal protein L10/QM-like protein is a component of the NIK-mediated antiviral signaling. *Virology* **2008**, *380*, 165–169. [CrossRef]

CHAPTER II

Virus perception at the cell surface: revisiting the roles of receptor-like kinases as viral pattern recognition receptors

Publicado Em 16 De Maio De 2019, na revista *Molecular Plant Pathology*

Ruan Maloni Teixeira, Marco Aurélio Ferreira, Gabriel A. S. Raimundo, Virgílio A . P. Loriato, Pedro A. B. Reis And Elizabeth P. B. Fontes. *Molecular Plant Pathology* (2019.) 20(9), 1196–1202.

(Doi: 10.1111/Mpp.12816 1196)

Molecular Plant Pathology

MOLECULAR PLANT PATHOLOGY (2019) 20(9), 1196–1202 DOI: 10.1111/mpp.12816

Microreview

Virus perception at the cell surface: revisiting the roles of receptor-like kinases as viral pattern recognition receptors

RUAN M. TEIXEIRA[1,2], MARCO AURÉLIO FERREIRA[1,2], GABRIEL A. S. RAIMUNDO[1,3], VIRGÍLIO A. P. LORIATO[1,2], PEDRO A. B. REIS[1,2] AND ELIZABETH P. B. FONTES[1,2,*]

[1]National Institute of Science and Technology in Plant-Pest Interactions, Bioagro, Universidade Federal de Viçosa, Viçosa, Minas Gerais 36570-000, Brazil

[2]Departament of Biochemistry and Molecular Biology, Universidade Federal de Viçosa, Viçosa, Minas Gerais 36570-000, Brazil

[3]Agronomy Institute, Universidade Federal de Viçosa, Campus Florestal, Florestal, Minas Gerais 35690-000, Brazil

SUMMARY

Activation of antiviral innate immune responses depends on the recognition of viral components or viral effectors by host receptors. This virus recognition system can activate two layers of host defence, pathogen-associated molecular pattern (PAMP)-triggered immunity (PTI) and effector-triggered immunity (ETI). While ETI has long been recognized as an efficient plant defence against viruses, the concept of antiviral PTI has only recently been integrated into virus–host interaction models, such as the RNA silencing-based defences that are triggered by viral dsRNA PAMPs produced during infection. Emerging evidence in the literature has included the classical PTI in the antiviral innate immune arsenal of plant cells. Therefore, our understanding of PAMPs has expanded to include not only classical PAMPS, such as bacterial flagellin or fungal chitin, but also virus-derived nucleic acids that may also activate PAMP recognition receptors like the well-documented phenomenon observed for mammalian viruses. In this review, we discuss the notion that plant viruses can activate classical PTI, leading to both unique antiviral responses and conserved antipathogen responses. We also present evidence that virus-derived nucleic acid PAMPs may elicit the NUCLEAR SHUTTLE PROTEIN-INTERACTING KINASE 1 (NIK1)-mediated antiviral signalling pathway that transduces an antiviral signal to suppress global host translation.

Keywords: begomovirus, NIK1-mediated antiviral signalling, NSP-interacting kinase, PAMP-triggered immunity, pattern recognition receptor, PRR, receptor-like kinase, viral PAMPs.

INTRODUCTION

All plant cells are naturally and frequently exposed to microorganisms. To cope with invading pathogens, plant cells evolved a sophisticated immune system under constant pressure for dominance over the pathogens' virulence strategies, which in turn coevolved to escape the host recognition system (Jones and Dangl, 2006). The first layer of the plant immune system is represented by the pattern recognition receptors (PRRs) at the cell surface, which recognize either conserved signature molecules produced by the pathogens, designated pathogen-associated molecular patterns (PAMPs), or endogenous damage/danger signals associated with pathogen invasion, designated danger- or damage-associated molecular patterns (DAMPs) (Choi and Klessig, 2016; Ma *et al.*, 2016). The sensing of PAMPs by PRRs activates PAMP-triggered immunity (PTI), leading to a rapid, non-specific response to a broad range of pathogens (Ma *et al.*, 2016). To counterattack this first layer of defence, adapted pathogens deliver virulence effectors in the host cell cytoplasm, which prevent the activation of PTI and elicit effector-triggered susceptibility (ETS; Wang and Wang, 2018). In response, plant cells have evolved intracellular nucleotide-binding leucine-rich repeat (NLR) receptors, which recognize the virulence effectors in a highly specific manner to activate the second level of plant defence and are designated as effector-triggered immunity (ETI; Jones and Dangl, 2006).

In plant–virus interactions, a common theme that has emerged from recent studies is that plants may also employ classical PTI to fight virus infection similarly to non-viral pathogens (Iriti and Varoni, 2015; Korner *et al.*, 2013; Nicaise and Candresse, 2017; Niehl *et al.*, 2016). Activation of antiviral PRR pathways by viral PAMPs (VAMPs) has been extensively studied in mammals, and the mechanisms by which viral effectors manipulate PTI defences have been well characterized (Jensen and Thomsen, 2012; Yokota *et al.*, 2010). The mammalian Toll-like receptors (TLRs) are classic examples of antiviral PPRs with similar receptor configuration to plant leucine-rich repeats (LRR) receptor-like kinases (RLKs), which function as PRRs and

* *Correspondence*: Email: bbfontes@ufv.br

coreceptors in plant immunity (Botos *et al.*, 2011). Although these LRR-RLK receptors have collectively been shown to sense a variety of PAMPs, only viral infection-sensing LRR-RLKs are in the scope of this minireview.

PTI-based antiviral responses by receptor-like kinases

For non-viral pathogens, plant PTI and mammalian innate immune systems share similar activation mechanisms, including a similar structural configuration of PRRs and similar conserved PAMPs. However, plant antiviral PTI has been conceptually regarded as RNA silencing, in which viral dsRNAs are considered PAMPs, which activate Dicers as PRRs that can be suppressed by viral effectors (Calil and Fontes, 2017; Moon and Park, 2016). More recently, accumulated evidence has invoked the classic PTI initiated by transmembrane PRRs as part of the plant defence arsenal against viruses. Evidence for the classic PTI against plant viruses is based on experimental data of the betacarmovirus *Turnip crinkle virus* (TCV; Korner *et al.*, 2013; Yang *et al.*, 2010), the potyviruses *Soybean mosaic virus* (SMV; Liu *et al.*, 2011) and *Plum pox virus* (PPV; Nicaise and Candresse, 2017), the tobamoviruses *Tobaco mosaic virus* (TMV) and *Oilseed rape mosaic virus* (ORMV; Korner *et al.*, 2013), the alfamovirus *Alfalfa mosaic virus* (AMV) and the potexvirus *Potato virus X* (PVX; Iriti and Varoni, 2015), the caulimovirus *Cauliflower mosaic virus* (CaMV; Zvereva *et al.*, 2016), and the cucumovirus C*ucumber mosaic virus* (CMV; Kong *et al.*, 2018). Collectively, these studies provided several lines of evidence that the classical plant PTI limits virus infection similar to non-viral pathogens. First, preactivation of PTI with non-viral PAMPs confers resistance to virus infection, indicating that PTI-induced immune responses confer protection against viruses (Iriti and Varoni, 2015). Second, it has been conceptually accepted that pathogens have to suppress PTI in order to successfully colonize a host. Growing evidence has shown that viruses are not exceptions, and viral suppressors of PTI have been identified recently, including the PPV coat protein (CP; Nicaise and Candresse, 2017), CaMV P6 (Zvereva *et al.*, 2016) and the movement protein (MP) from CMV (Kong *et al.*, 2018). PPV CP also functions as an Avr factor recognized by the RTM resistance in *Arabidopsis* (Decroocq *et al.*, 2009). Therefore, PPV CP may link the suppression of PTI with activation of ETI, as predicted by the zigzag evolutionary model of plant innate immunity (Jones and Dangl, 2006; Fig. 1). Finally, reverse genetics and overexpression studies with characterized PTI components have demonstrated that plants efficiently use PTI to limit viral infection (Kørner *et al.*, 2013; Liu *et al.*, 2011; Nicaise and Candresse, 2017, Niehl, *et al.*, 2016; Yang *et al.*, 2010). An obvious caveat from these previous results is that no virus-derived PAMP detected by a plant PRR has been identified, and hence antiviral PRRs remain to be described. Recently, both virus-derived and synthesized double-stranded (ds) RNAs have been shown to activate plant PTI and to restrict virus infection in an RNA-silencing independent manner (Niehl, *et al.*, 2016; Fig. 1). This dsRNA-induced PTI in plants requires the function of the LRR-RLK coreceptor SOMATIC EMBRYOGENESIS RECEPTOR KINASE 1 (SERK1) linking virus perception to the membrane-anchored immune receptor signalling. The direct inactivation of plant PTI components has provided compelling evidence that transmembrane PRR-mediated PTI operates against viruses in plants. Frequently, the membrane-anchored immune RLKs and receptor-like proteins (RLPs) depend on ligand (PAMP/DAMP)-induced dimerization or oligomerization with coreceptors for activation (Ma *et al.*, 2016). The BRASSINOSTEROID INSENSITIVE1 (BRI1)-ASSOCIATED KINASE 1 (BAK1) functions as a coreceptor that interacts with multiple PAMP-interacting immune receptors (RLKs and RLPs) to assemble active PTI signalling complexes (Ma *et al.*, 2016). Like BAK1, other members of the subfamily II of LRR-RLKs, including SERK1, SERK4/BKK1 (BAK1-LIKE KINASE 1) and the NUCLEAR SHUTTLE PROTEIN-INTERACTING KINASE 1 (NIK1), function in antiviral immunity (Gouveia *et al.*, 2017). Accordingly, inactivation of the PTI regulator BAK1 or BKK1 enhances susceptibility to RNA virus infection, demonstrating that they are required to build an effective defence against RNA viruses in *Arabidopsis* (Kørner *et al.*, 2013; Yang *et al.*, 2010; Fig. 1). This assembled defence is more likely due to BAK1-dependent PTI because crude viral extracts from infected plants induced several PTI marker responses in a BAK1-dependent manner (Kørner *et al.*, 2013). Likewise, *serk1* knockout lines are more susceptible to virus infection (Niehl, *et al.*, 2016), and the *Arabidopsis* double mutant *bak1-5*/*bkk1* displays increased viral accumulation when inoculated with PPV (Nicaise and Candresse, 2017). Collectively, these results further substantiate the notion that plant PTI functions to combat virus infection similarly to non-viral pathogens. These recent data have also implicated plasma membrane-localized coreceptors of PRRs, such as BAK1, BKK1, and SERK1, in antiviral PTI, leaving an open question on how viruses, which are intracellular obligate parasites and are expected to deliver PAMPs intracellularly, are perceived extracellularly (Fig. 1).

NIK1-mediated antiviral immunity: from a PTI-like activation to a somewhat distinct response

NIK1 was first identified as a virulence target of the nuclear shuttle protein (NSP) from the bipartite begomoviruses, *Geminiviridae* family (Mariano *et al.*, 2004; Silva *et al.*, 2017). NSP mediates the nuclear export of begomoviral DNA to the cytoplasm, a process facilitated by the NSP-interacting GTPase (Carvalho *et al.*, 2008a, b). NIK1 belongs to the LRR-RLKs subfamily II, which includes the SERK clade, the NIK clade and a third clade of uncharacterized members (Zhang *et al.*, 2006). In phylogenetic

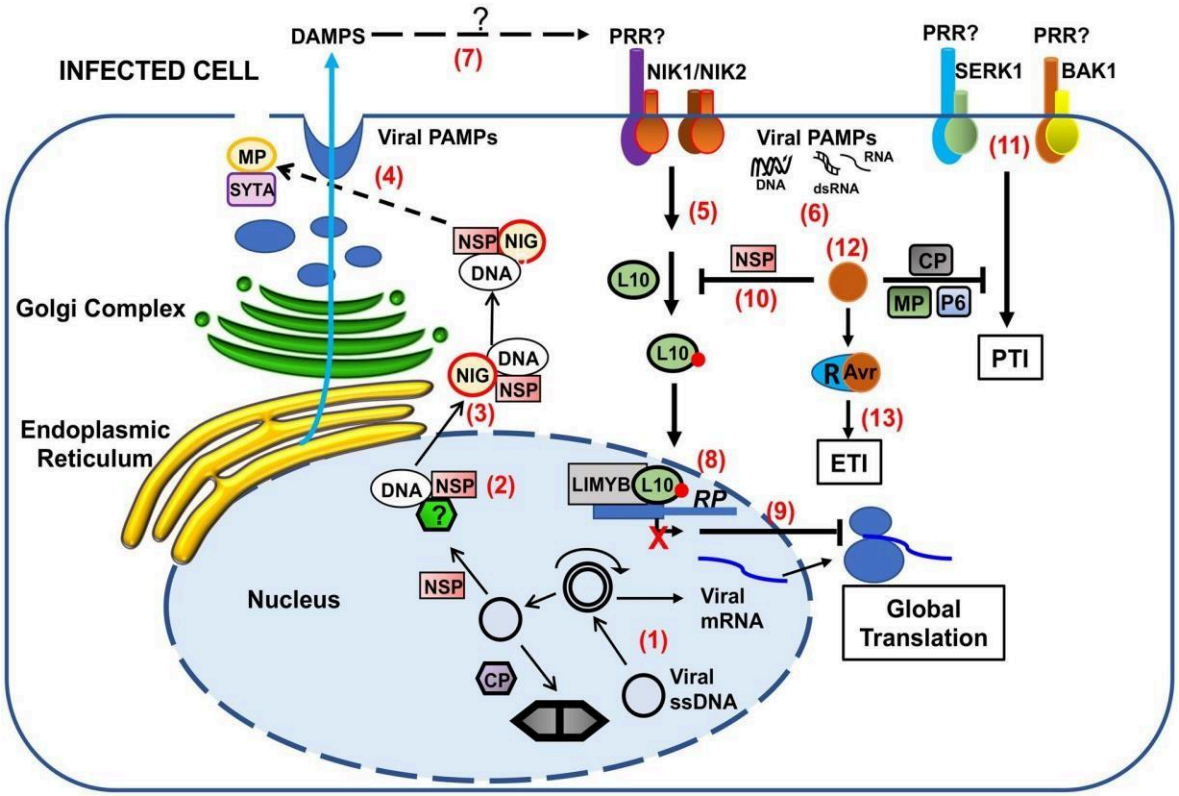

Fig. 1 Activation of the NIK1-mediated antiviral signalling and antiviral PTI. The viral single-stranded DNA from begomoviruses replicates via double-stranded DNA intermediates that are transcribed in the nucleus of infected plant cells (1). NSP binds to the nascent viral DNA and facilitates its movement to the cytoplasm via nuclear pores (2). At the cytosolic side, the NSP-interacting GTPase (NIG) helps the release of NSP-viral DNA complex from the nuclear pores into the cytoplasm (3) and then moves the viral DNA complex towards the cell periphery. MP associates with the endosomal synaptotagmin A (SYTA) and may interact directly with the NSP-viral DNA complex to move the viral DNA to plasmodesmata via an endocytic recyclizing pathway for the MP-assisted cell-to-cell spread (4). In incompatible interactions, plant cells may elicit the translational control branch of the NIK1-mediated antiviral signalling as an innate defence against DNA viruses (5). The mechanism of NIK1 transmembrane receptor activation is unknown, but we showed here that both RNA and DNA from infected plants activate the NIK1- mediated antiviral signalling (6). As plant viruses depend on the insect-vector-induced mechanical injury for entry into the plant cells, endogenous DAMPs induced during infection may also activate the antiviral innate immune system (7). Upon activation, NIK1/NIK2 mediates the phosphorylation of RPL10 and subsequent translocation to the nucleus, where it interacts with LIMYB to fully repress the expression of translational machinery-related genes [ribosome protein (RP) genes for instance] (8). Prolonged down-regulation of translation-related genes leads to global translation suppression, which also impairs viral mRNA (vmRNA) translation (9). In begomovirus–host compatible interactions, NSP binds to NIK1 and suppresses its activity, creating a favourable environment for virus infection (10). In the case of RNA and DNA viruses, replication and expression of viral genomes lead to the accumulation of non-self DNA or RNA motifs (virus-derived PAMPs, dsRNA, RNA and DNA), which may be recognized by PRRs that in turn heteromultimerize with co-receptors (BAK1 or SERK1) to trigger antiviral PTI (11), which may also be activated by endogenous DAMPs (7). In any case, in RNA or DNA viruses, a successful infection implicates in the accumulation of viral effectors (e.g. CP from PPV and NSP from begomoviruses) to suppress PTI, leading to disease (12). In resistant genotypes, however, the resistance (R) proteins specifically recognize, directly or indirectly, the viral effectors, called avirulence (Avr) factors, activating ETI and conferring resistance (13). Adapted from Gouveia *et al.*, 2017.

analysis, NIK1 and NIK2 cluster together and separately from NIK3 (Sakamoto *et al.*, 2012). Although NIK1 is structurally related to SERKs and is also implicated in plant immunity, the mechanism by which NIK1 propagates an antiviral signal, and the resulting immune responses are entirely different from the BAK1/SERK3-dependent PTI response against pathogens (Machado *et al.*, 2015). The mechanism of NIK1-mediated defence is underscored by repression of translational machinery genes and suppression of global translation, as a new paradigm for plant antiviral immunity (Machado *et al.*, 2017; Zorzatto *et al.*, 2015).

As Ser/Thr kinase receptors, NIK1 is activated by autophosphorylation (Santos *et al.*, 2010). Several lines of evidence indicate that phosphorylation at the essential Thr-474 residue within the A-loop constitutes a critical regulatory mechanism for NIK1 activation. NIK1 undergoes autophosphorylation *in vitro* at conserved threonine residues, positions Thr-468, Thr-469 and Thr-474 within the activation loop, and mediates substrate phosphorylation *in vivo* (Santos *et al.*, 2009). While phosphorylation at Thr-469 negatively regulates NIK1 kinase activity, phosphorylation at positions Thr-468 and Thr-474 enhances and

promotes kinase activation, respectively. Within the conserved activation loop of the members of the LRR-RLK subfamily II, Thr-468 and Thr-474 align to the same positions as the conserved BAK1 residues Thr-449 and Thr-455, and SERK1 residues Thr-462 and Thr-468, which are intramolecular targets for BAK1 and SERK1 kinase activation (Shah *et al.*, 2001; Wang *et al.*, 2005; Yun *et al.*, 2009). Furthermore, replacement of NIK1 Thr-474 with alanine impairs autophosphorylation and substrate phosphorylation activity *in vitro* (Santos *et al.*, 2009). Consistently, the ectopic expression of loss-of-function Thr-474 mutants, such as T474A or the double mutant G4743V/T474A, did not reverse the enhanced susceptibility phenotype of NIK1 knockout lines, demonstrating that Thr-474 autophosphorylation is required to transduce a defence response against begomoviruses (Santos *et al.*, 2009). Finally, the replacement of Thr-474 with the phosphomimetic amino acid aspartate promotes constitutive activation of the NIK1-mediated antiviral signalling (Santos *et al.*, 2009). Ectopic expression of T474D in *Arabidopsis* and tomato transgenic lines promotes RPL10 phosphorylation, causes repression of ribosomal protein genes, suppresses global translation, decreases viral mRNA association with actively translating polysome fractions and confers resistance to begomoviruses, as readouts of NIK1-mediated antiviral signalling elicitation (Brustolini *et al.*, 2015; Zorzatto *et al.*, 2015).

The current mechanistic model for the activation of NIK1-mediated signalling holds that in response to virus infection, NIK1 undergoes homodimerization with itself or heterodimerization with an unknown receptor, promoting transphosphorylation at the essential threonine residue position 474 within the activation loop of the kinase (Fig. 1). Upon activation, NIK1-mediated signalling mediates the phosphorylation of RIBOSOMAL PROTEIN L10 (RPL10), which in turn is redirected to the nucleus, where it interacts with L10-INTERACTING MYB DOMAIN-CONTAINING PROTEIN (LIMYB) to fully down-regulate the expression of translational machinery-related genes (Carvalho *et al.*, 2008c; Rocha *et al.*, 2008; Santos *et al.*, 2009; Zorzatto *et al.*, 2015). Therefore, the down-regulation of the translation-related genes is transcriptionally regulated through NIK1-mediated formation of transcription-repressing complexes by an association of phosphorylated RPL10 and LIMYB. The prolonged down-regulation of the translational machinery leads to suppression of global translation. Plant DNA viruses cannot escape this translation regulatory mechanism of plant cells, and hence the viral mRNA is not efficiently translated, compromising the infection (Zorzatto *et al.*, 2015). Counteracting this activation mechanism, the begomovirus NSP binds to the kinase domain of NIK1 and prevents activation of the signalling pathway (Fontes *et al.*, 2004). Therefore, in compatible interactions, begomoviruses increase their pathogenicity to susceptible hosts by suppressing the activity of NIK1 kinase via interaction of the viral suppressor NSP, a reminiscent feature of PTI inactivation by pathogen suppressors.

Although the NIK1-mediated antiviral responses are quite distinct from the PTI-mediated antiviral defences, some similarities can be observed regarding the mechanism of activation and suppression of NIK1 and PRRs. First, NIK1 is presumably activated by ligand-dependent complex formation that promotes phosphorylation and activation of the kinase domain. Phosphorylation of the functional analogues NIK1 Thr-474, SERK1 Thr-468 and BAK1 Thr-455 is essential for receptor/coreceptor signalling, which may underscore a similar mechanism for activation (Santos *et al.*, 2009; Shah *et al.*, 2001; Wang *et al.*, 2005; Yun *et al.*, 2009). Second, this activation of NIK1 is induced by virus infection, which may provide virus-derived PAMPs for NIK1-mediated virus perception (Zorzatto *et al.*, 2015). Finally, NIK1 is suppressed by the viral effector NSP, which also functions as an Avr factor for ETI activation in resistant *Phaseolus vulgaris* genotypes (Garrido-Ramirez *et al.*, 2000), linking a primary mechanism of antiviral immunity at the cell surface with ETI (Fig. 1). According to the zigzag evolutionary model of the two-branch innate immune system, the activation of ETI in plant–virus interactions (NSP in resistant bean genotypes) is conceptually associated with PTI inhibition (NIK1 signalling) by a viral effector (NSP).

A comparison of the transcriptome induced by ectopic expression of T474D and by begomovirus infection [*Cabbage leaf curl virus* (CaLCuV)/*Arabidopsis* and *Tomato yellow spot virus* (ToYCV)/Tomato] indicates that virus infection both activates and suppresses NIK1-mediated antiviral signalling (Brustolini *et al.*, 2015; Zorzatto *et al.*, 2015). While the inhibition of the NIK1-mediated antiviral signalling is due to the suppressive activity of the viral NSP, the mechanism by which the virus activates this antiviral response and the molecular bases for such elicitation are unknown. Here, we extended these studies by analysing whether begomovirus-derived nucleic acids could act as PAMPs to activate NIK1. *Arabidopsis* wild-type ecotype Columbia (Col-0) plants at the seven-leaf stage were inoculated by biolistic delivery with infectious clones of CaLCuV DNA-A, and DNA-B and the accumulation of viral DNA was monitored by PCR (Florentino *et al.*, 2006). Then, we used total RNA or total DNA isolated from infected plants subtracted from mock-inoculated plants as sources for begomovirus-derived nucleic acids. Leaf discs treated with RNA or DNA from virus-infected plants were from the ecotype Columbia (Col-0), the loss-of-function mutants *nik1-1* (Fontes *et al.*, 2004), *nik2-1* (Fontes *et al.*, 2004) and the double mutant *nik-11nik2-1* (Fig. 2A). *Arabidopsis* lines in which NIK1 was replaced by T474D (Zorzatto *et al.*, 2015) were also included as a positive control for NIK1 activation. The activation of the antiviral signal transduction was assayed by monitoring the down-regulation of the ribosomal protein (RB) genes *RPL13* and *RPS25*, which have been shown to function as NIK1 activation-associated marker genes (Brustolini *et al.*, 2015; Zorzatto *et al.*, 2015). Accordingly, ectopic expression of constitutively activated T474D in *nik1* null alleles caused the down-regulation

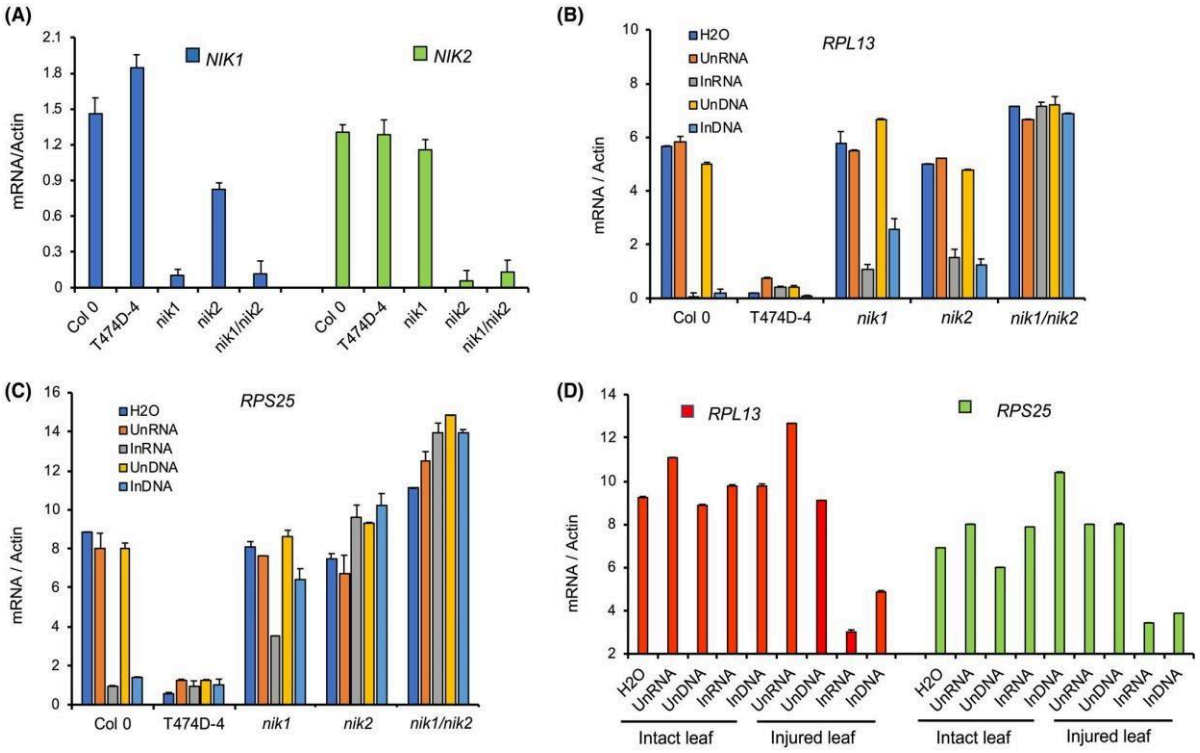

Fig. 2 RNA and DNA prepared from begomovirus-infected leaves activate the NIK1-mediated antiviral signalling. (A) Single and double knockout lines of *NIK1* and *NIK2*. The expression of NIK1 or NIK2 in the leaves of Col-0, *nik1-1*, *nik2-1* and *nik1-1nk2-1* lines was monitored by quantitative RT-PCR. Mean ± 95% confidence intervals (*n* = 3) based on bootstrap resampling replicates of three independent experiments. (B) and (C) Begomovirus infection-derived DNA and RNA down-regulate RP genes, *RPL13* and *RPS25*, in a NIK1- and/or NIK2-ependent manner. RP gene expression was monitored by qRT-PCR of RNA from Col-0, *nik1-1*, *nik2-1* and *nik1-1nk2-1* lines treated with RNA or DNA from mock-inoculated leaves (UnRNA and UnDNA) or CaLCuV-infected leaves (InRNA and InDNA). Mean ± 95% confidence intervals (*n* = 3) based on bootstrap resampling replicates of three independent experiments. (D) Begomovirus infection-derived RNA and DNA require mechanical injury in leaves to activate the NIK1/2-mediated antiviral signalling. Intact, unwounded leaves and injured leaves were treated with RNA or DNA from CaLCuV-infected leaves. After 3 h of treatment, *RP* gene expression was monitored by qRT–PCR.

of both RP genes compared to the wild-type, Col-0 line (Fig. 2B,C; Zorzatto *et al.*, 2015). In contrast, inactivation of both NIK1 and NIK2 in the double mutant *nik1-1nik2-1* released repression and caused up-regulation of the RB genes, indicating that NIK1 and NIK2 are functionally paralogs for the NIK-mediated repression of RB genes. These T474D- and *nik1nik2*-mediated phenotypes recapitulate those resulting from overexpression and inactivation of the downstream transcriptional repressor LIMYB, respectively (Zorzatto *et al.*, 2015). Both DNA and RNA from infected plants (InDNA and InRNA) promoted down-regulation of RP genes in Col-0, as opposed to RNA and DNA from mock-inoculated, uninfected plants (UnDNA and UnRNA, Fig. 2B,C). Inactivation of *NIK1* or *NIK2* caused a lower nucleic acid-mediated repression of the RP genes compared with the level of repression in Col-0. The down-regulation of *RPL13* and *RPL25* was totally blocked in the double mutant *nik1nik2*. These results confirmed that NIK1 and NIK2 are functionally redundant and that the elicitation of NIK1-mediated response by begomovirus-derived DNA and RNA is dependent on NIK1 and/or NIK2. We also showed that virus-derived RNA and DNA did not elicit NIK-mediated antiviral signalling in unwounded leaves but instead were only effective if intact leaves were rubbed with abrasives before the treatment, which might have mechanically provided intracellular access for viral PAMPs (Fig. 2D).

Our findings suggest that begomovirus-derived RNA and DNA function as viral PAMPs, which elicit the NIK-mediated antiviral signalling in a NIK1- and/or NIK2-dependent manner. However, the nature and origin of the viral PAMPs, how viruses are sensed by NIKs extracellularly, and whether NIK1 and NIK2 function as coreceptors or genuine PRRs remain to be determined.

Mechanistic hypotheses for the perception of viral PAMPs by RLKs at the cell surface

Because viruses are obligate intracellular parasites, viral PAMPs are expected to be produced intracellularly and there is no evi- dence that virus-derived nucleic acids can reach the apoplast to

be sensed directly by the LRR extracellular domain of NIKs and SERKs or associated PRRs. It is possible that plasma membrane anchored receptors sense viral PAMPs through their intracellular domain, thus antiviral PTI would be activated by viral PAMP-induced receptor–coreceptor dimerization via the kinase domain. The intracellular mammalian protein kinase RNA-activated (PKR) undergoes dsRNA ligand-mediated dimerization and activation upon direct association of viral dsRNA produced during infection with its kinase domain (Balachandran *et al.*, 2000).

Alternatively, the microsomal recycling pathway may provide the opportunistic colocalization for NIKs, SERKs and PRRs with viral PAMPs. The movement proteins (MPs) of plant viruses use the endocytic recycling pathway to move viral RNA– and viral DNA–protein complexes to the plasmodesmata for the MP-assisted cell-to-cell spread of the virus (Lewis and Lazarowitz, 2010). Plant PRRs have also been shown to be internalized via endosomes (Mbengue *et al.*, 2016). Therefore, the specific perception of a virus by PRRs would rely on the opportunistic subcellular colocalization of internalized PRRs and the MP-associated viral genome in host cells. Consistent with both alternatives, virus-derived nucleic acids did not activate the NIK1-mediated antiviral signalling in intact, unwounded leaves but instead required the leaves to be mechanically injured, which may have provided the intracellular access for viral PAMPs. Complementary experiments by expressing truncated, extracellular LRR-less NIKs and/or SERKs, which remain associated with the plasma membrane, may facilitate addressing this issue.

Although this endocytic recycling pathway is an attractive hypothesis for virus perception by plant PRRs, similar to mammalian endosomal TLRs, it may not be possible to synchronize PTI activation as a primary, early response to pathogen attack, with the later event of virus movement to adjacent cells. Therefore, only with the identification of the origin and nature of virus-derived PAMPs and the characterization of nucleic acid-sensing PRRs will it be possible to address these possibilities for virus perception by plasma membrane-anchored RLKs.

CONCLUSION

Recent studies with SERK-like coreceptors and known PRRs, which function in plant innate immunity, have demonstrated that the classical PTI is part of the antiviral defence arsenal of plant cells. Several components of classic PTI, including the co-receptor SERKs, BAK1 and SERK1, and the MAPK4 negative regulator, in addition to common immune responses, co-exist as part of antiviral PTI. As for viral PAMPs, dsRNAs isolated from virus-infected plants have been demonstrated to induce typical PTI responses dependent on the coreceptor SERK1. Likewise, begomovirus-derived nucleic acids were shown here to induce the NIK1-mediated antiviral signalling in a NIK1- and NIK2-dependent manner and were included as a piece of new complementary evidence for this review. However, the nature and origin of the nucleic acid PAMPs have not been deciphered, and the nucleic acid sensors have yet to be identified. Furthermore, as viruses are intracellular obligate parasites and may not have access to the apoplast, it remains to be determined how PRRs would sense viruses and viral PAMPS extracellularly. The identification of the origin and nature of virus-derived nucleic acid PAMPs and the discovery of the cognate PRRs will shed light on the mechanism of antiviral PTI activation and its role in resistance against viruses.

ACKNOWLEDGEMENTS

We are grateful to the Brazilian funding agencies CAPES, CNPq and FAPEMIG for supporting this study.

CONFLICT OF INTEREST

The authors declare no conflict of interest.

REFERENCES

Balachandran, S., Roberts, P.C., Brown, L.E., Truong, H., Pattnaik, A.K., Archer, D.R. and Barber, G.N. (2000) Essential role for the dsRNA-dependent protein kinase PKR in innate immunity to viral infection. *Immunity*, **13**, 129–141.

Botos, I., Segal, D.M. and Davies, D.R. (2011) The structural biology of Toll-like receptors. *Structure*, **19**, 447–459.

Brustolini, O.J.B., Machado, J.P.B., Condori-Apfata, J.A., Coco, D., Deguchi, M., Loriato, V.A., Pereira, W.A., Alfenas-Zerbini, P., Zerbini, F.M., Inoue-Nagata, A.K., Santos, A.A., Chory, J., Silva, F.F. and Fontes, E.P.B. (2015) Sustained NIK-mediated antiviral signalling confers broad-spectrum tolerance to begomoviruses in cultivated plants. *Plant Biotechnol. J.* **13**, 1300–1311.

Calil, I.P. and Fontes, E.P.B. (2017) Plant immunity against viruses: antiviral immune receptors in focus. *Ann. Bot.* **118**, 200–213.

Carvalho, C.M., Fontenelle, M.R., Florentino, L.H., Santos, A.A., Zerbini, F.M. and Fontes, E.P.B. (2008a) A novel nucleocytoplasmic traffic GTPase identified as a functional target of the bipartite geminivirus nuclear shuttle protein. *Plant J.* **5**, 869–880.

Carvalho, C.M., Machado, J.P., Zerbini, F.M. and Fontes, E.P. (2008b) NSP-interacting GTPase: a cytosolic protein as cofactor for nuclear shuttle proteins. *Plant Signal. Behav.* **3**, 752–754.

Carvalho, C.M., Santos, A.A., Pires, S.R., Rocha, C.S., Saraiva, D.I., Machado, J.P.B., Mattos, E.C., Fietto, L.G. and Fontes, E.P.B. (2008c) Regulated nuclear trafficking of rpL10A mediated by NIK1 represents a defense strategy of plant cells against virus. *PLoS Pathog.* **4**, e1000247.

Choi, H.W. and Klessig, D.F. (2016) DAMPs, MAMPs, and NAMPs in plant innate immunity. *BMC Plant Biol.* **16**, 232.

Decroocq, V., Salvador, B., Sicard, O., Glasa, M., Cosson, P., Svanella-Dumas, L., Revers, F., García, J.A. and Candresse, T. (2009) The determinant of potyvirus ability to overcome the RTM resistance of *Arabidopsis thaliana* maps to the N-terminal region of the coat protein. *Mol. Plant Microbe Interact.* **22**, 1302–1311.

Florentino, L.H., Santos, A.A., Fontenelle, M.R., Pinheiro, G.L., Zerbini, F.M., Baracat-Pereira, M.C. and Fontes, E.P.B. (2006) A PERK-like

receptor kinase interacts with the geminivirus nuclear shuttle protein and potentiates viral infection. *J. Virol.* **80**, 6648–6656.

Fontes, E.P.B., Santos, A.A., Luz, D.F., Waclawovsky, A.J. and Chory, J. (2004) The geminivirus nuclear shuttle protein is a virulence factor that suppresses transmembrane receptor kinase activity. *Genes Dev.* **18**, 2545–2556.

Garrido-Ramirez, E.R., Sudarshana, M.R., Lucas, W.J. and Gilbertson, R.L. (2000) Bean dwarf mosaic virus BV1 protein is a determinant of the hypersensitive response and avirulence in phaseolus vulgaris. *Mol. Plant Microbe Interact.* **13**, 1184–1194.

Gouveia, B.C., Calil, I.P., Machado, J.P.B., Santos, A.A. and Fontes, E.P.B. (2017) Immune receptors and co-receptors in antiviral innate immunity in plants. *Front. Microbiol.* **7**, 2139.

Iriti, M. and Varoni, E.M. (2015) Chitosan-induced antiviral activity and innate immunity in plants. *Environ. Sci. Pollut. Res. Int.* **22**, 2935-2944.

Jensen, S. and Thomsen, A.R. (2012) Sensing of RNA viruses: a review of innate immune receptors involved in recognizing RNA virus invasion. *J. Virol.* **86**, 2900–2910.

Jones, J.D. and Dangl, J.L. (2006) The plant immune system. *Nature*, **444**, 323–329.

Kong, J., Wei, M., Li, G., Lei, R., Qiu, Y., Wang, C., Li, Z.-H. and Zhu, S. (2018) The cucumber mosaic virus movement protein suppresses PAMP-triggered immune responses in Arabidopsis and tobacco. *Biochem. Biophys. Res. Comm.* **498**, 395–401.

Korner, C.J., Klauser, D., Niehl, A., Dominguez-Ferreras, A., Chinchilla, D., Boller, T., Heinlein, M. and Hann, D.R. (2013) The immunity regulator BAK1 contributes to resistance against diverse RNA viruses. *Mol. Plant Microbe Interact.* **26**, 1271–1280.

Lewis, J.D. and Lazarowitz, S.G. (2010) *Arabidopsis* synaptotagmin SYTA regulates endocytosis and virus movement protein cell-to-cell transport. *Proc. Natl. Acad. Sci. USA*, **107**, 2491–2496.

Liu, J.Z., Horstman, H.D., Braun, E., Graham, M.A., Zhang, C., Navarre, D., Qiu, W.L., Lee, Y., Nettleton, D., Hill, J.H. and Whitham, S.A. (2011) Soybean homologs of MPK4 negatively regulate defense responses and positively regulate growth and development. *Plant Physiol.* **157**, 1363–1378.

Ma, X., Xu, G., He, P. and Shan, L. (2016) SERKing coreceptors for Receptors. *Trends Plant Sci.* **21**, 1017–1033.

Machado, J.P.B., Brustolini, O.J.B., Mendes, G.C., Santos, A.A. and Fontes, E.P.B. (2015) NIK1, a host factor specialized in antiviral defense or a novel general regulator of plant immunity? *BioEssays*, **37**, 1236–1242.

Machado, J.P.B., Calil, I.P., Santos, A.A. and Fontes, E.P.B. (2017) Translational control in plant antiviral immunity. *Genet. Mol. Biol.* **40**, 292-304.

Mariano,A.C.,Andrade,M.O.,Santos,A.A.,Carolino,S.M.B.,Oliveira,M.L., Baracat-Pereira, M.C., Brommonshenkel, S.H. andFontes, E.P.B. (2004) Identification of a novel receptor-like protein kinase that interacts with a geminivirus nuclear shuttle protein. *Virology*, **318**, 24–31.

Mbengue, M., Bourdais, G., Gervasi, F., Beck, M., Zhou, J., Spallek, T., Bartels, S., Boller, T., Ueda, T., Kuhn, H. and Robatzek, S. (2016) Clathrin-dependent endocytosis is required for immunity mediated by pattern recognition receptor kinases. *Proc. Natl. Acad. Sci. USA*, **113**, 11034–11039.

Moon, J.Y. and Park, J.M. (2016) Cross-talk in viral defense signaling in plants. *Front. Microbiol.* **7**, 2068.

Nicaise, V. and Candresse, T. (2017) Plum pox virus capsid protein suppresses plant pathogen-associated molecular pattern (PAMP)-triggered immunity. *Mol. Plant Pathol.* **18**, 878–886.

Niehl, A., Wyrsch, I., Boller, T. and Heinlein, M. (2016) Double-stranded RNAs induce a pattern-triggered immune signaling pathway in plants. *New Phytol.* **211**, 1008–1019.

Rocha, C.S., Santos, A.A., Machado, J.P.B. and Fontes, E.P.B. (2008) The ribosomal protein L10/QM-like protein is a component of the NIK-mediated antiviral signaling. *Virology*, **380**, 165–169.

Sakamoto, T., Deguchi, M., Brustolini, O.J.B., Santos, A.A., Silva, F.F. and Fontes, E.P.B. (2012) The tomato RLK superfamily: phylogeny and functional predictions about the role of the LRRII-RLK subfamily in antiviral defense. *BMC Plant Biol.* **12**, 229.

Santos, A.A., Carvalho, C.M., Florentino, L.H., Ramos, H.J.O. and Fontes, E.P. (2009) Conserved threonine residues within the A-loop of the receptor NIK differentially regulate the kinase function required for antiviral signaling. *PLoS ONE*, **4**, e5781.

Santos, A.A., Lopes, K.V.G., Apfata, J.A.C. and Fontes, E.P.B. (2010) NSP-interacting kinase, NIK: a transducer of plant defence signalling. *J. Exp. Bot.* **61**, 3839–3845.

Shah, K., Vervoort, J. and de Vries, S.C. (2001) Role of threonines in the *Arabidopsis thaliana* somatic embryogenesis receptor kinase 1 activation loop in phosphorylation. *J. Biol. Chem.* **276**, 41263–41269.

Silva, J.C.F., Carvalho, T.F.M., Basso, M.F., Deguchi, M., Pereira, W.A.,Sobrinho, R.R., Vidigal, P.M.P., Brustolini, O.J.B., Silva, F.F.,Dal-Bianco, M., Fontes, R.L.F., Santos, A.A., Zerbini, F.M., Cerqueira, F.R. and Fontes, E.P.B. (2017) Geminivirus data warehouse: a database enriched with machine learning approaches. *BMC Bioinformatics*, **18**, 240.

Wang, Y. and Wang, Y. (2018) Trick or treat: microbial pathogens evolved apoplastic effectors modulating plant susceptibility to infection. *Mol. Plant-Microbe Interact.* **3**, 6–12.

Wang, X., Goshe, M.B., Soderblom, E.J., Phinney, B.S., Kuchar, J.A., Li, J., Asami, T., Yoshida, S., Huber, S.C. and Clouse, S.D. (2005) Identification and functional analysis of in vivo phosphorylation sites of the Arabidopsis BRASSINOSTEROID-INSENSITIVE1 receptor kinase. *Plant Cell*, **17**, 1685–1703.

Yang, H., Gou, X., He, K., Xi, D., Du, J., Lin, H. and Li, J. (2010) BAK1 and BKK1 in *Arabidopsis thaliana* confer reduced susceptibility to *Turnip crinkle virus*. *Eur. J. Plant Pathol.* **127**, 149–156.

Yokota, S.I., Okabayashi, T. and Fujii, N. (2010) The battle between virus and host: modulation of Toll-like receptor signaling pathways by virus infection. *Mediators Inflamm.* **2010**, 184323.

Yun, H.S., Bae, Y.H., Lee, Y.J., Chang, S.C., Kim, S.K., Li, J. and Nam, K.H. (2009) Analysis of phosphorylation of the BAK1/BRI1 complex in Arabidopsis reveals amino acid residues critical for receptor formation and activation of BR signaling. *Mol. Cells*, **27**, 183–190.

Zhang, X.S., Choi, J.H., Heinz, J. and Chetty, C.S. (2006) Domain-specific positive selection contributes to the evolution of Arabidopsis leucine-rich repeat receptor-like kinase (LRR RLK) genes. *J. Mol. Evol.* **63**, 612–621.

Zorzatto, C., Machado, J.P.B., Lopes, K.V.G., Nascimento, K.J.T., Pereira, W.A., Brustolini, O.J.B., Reis, P.A.B., Calil, I.P., Deguchi, M., Sachetto-Martins, G., Gouveia, B.C., Loriato, V.A.P., Silva, M.A.C., Silva, F.F., Santos, A.A., Chory, J. and Fontes, E.P.B. (2015) NIK1-mediated translation suppression functions as a plant antiviral immunity mechanism. *Nature*, **520**, 679-682.

Zvereva, A.S., Golyaev, V., Turco, S., Gubaeva, E.G., Rajeswaran, R., Schepetilnikov, M.V., Srour, O., Ryabova, L.A., Bolle, T. and Pooggin, M.M. (2016) Viral protein suppresses oxidative burst and salicylic acid-dependent autophagy and facilitates bacterial growth on virus-infected plants. *New Phytol.* **211**, 1020e1034.

CHAPTER III

A molecular link between photosynthesis and translation under biotic and abiotic stresses

A molecular link between photosynthesis and translation under biotic and abiotic stresses

Abstract

Photosynthesis and translation are targets of metabolic control and development in plants; yet, how stress signals coordinately regulate these opposing energy-producing and consuming processes remains enigmatic. Here, we described a growth control circuit that ties the photosynthetic functionto translational control in response to biotic and abiotic signals. We showed first that the downstream component of the NIK1/RPL10 antiviral signaling module, LIMYB, which represses translational machinery-related gene expression and translation, also suppresses photosynthetic apparatus-related genes leading to inhibition of the photosynthetic function. The repressing transcriptional activity of LIMYB was the primary determinant for the decrease in electron transport rate, exchange gas parameters, quantum efficiency, and water-use efficiency in the LIMYB-overexpressing lines. The decreased photosynthetic activity was linked to the NIK1 antiviral signaling and stunted growth. Activation of antiviral NIK1 by viral or bacterial PAMPs, or expressing a constitutively activated NIK1 mutant, T474D, inhibited the photosynthetic function in control lines but not in *lymyb* knockout lines. We also showed that heat and osmotic stress activate the NIK1/RPL10/LIMYB signaling circuit. The coordinated repression of photosynthesis and translation via the stress-activated NIK1/RPL10/LIMYB signaling module may adjust the plant growth pattern in response to the changing environment.

Introduction

Plants are constantly subjected to environmental changes that affect growth, including changes in temperature, water supply, and attacks by pathogens and insects. Nevertheless, the environmental changes-mediated growth control is highly complex, and the underlying mechanistic knowledge is still very fragmented and rudimentary to fully assemble the molecular puzzle that regulates plant growth under stress conditions. In plants, translation andphotosynthesis are recognized as cell growth-promoting processes profoundly affected by stressconditions (Reinbothe et al., 2010; Muhammad et al., 2021). In addition, activation of defense responses to pathogens often provokes stunted growth (Song et al., 2021a). However, the molecular mechanisms linking abiotic and biotic stress signals to photosynthesis and translationcoordinate regulation are barely understood.

The energy for plant growth is obtained from ATP produced via respiration and photosynthesis. Photosynthesis directly provides substrates for the ATP-generating mitochondrial reactions in addition to C skeletons for allocation in protein synthesis. Any stress condition that interferes with energy and carbon balance in the photosynthetic cell is expected to affect translation(Song et al., 2021). Accordingly, the photosynthesis rate has been recently shown to correlate with carbon allocation to translation, polysome abundance in addition to translational regulatory processes, including phosphorylation of ribosomal proteins and translation initiation factors (Tcherkez et al., 2020). While the impact of photosynthesis on translation has been established at some level, the molecular mechanisms underlying the coordinate regulation and linkage of these processes are still poorly understood.

As the most energy-consuming cellular process, translation is often tightly regulated under stress conditions. The most well-characterized mechanism for translational control in plant cells relies on the conserved TOR signaling pathway as a master regulator of cell growth (Burkart and Brandizzi, 2021). In both mammalian and plant cells, TOR signaling senses nutrient availability, energy status, hormones, and stress signals, and thereby regulates ribosome biogenesis, translation in addition to transcription of a set of translation machinery-related genes (Reinbothe et al., 2010).As a nutrient-sensing pathway, the TOR kinase is activated in response to the availability of sugar produced by photosynthesis and light (Song et al., 2021b). In addition to regulating translation, TOR signaling enhances photomorphogenesis and regulates leaf and chloroplast development.

Another translational control mechanism associated with plant immunity is the

NUCLEAR SHUTTLE PROTEIN (NSP)-INTERACTING KINASE 1 (NIK1)-mediated antiviral signaling(reviewed in Machado et al., 2015; 2019; Fontes et al., 2021; Teixeira et al., 2021; Ferreira et al., 2021). NIK1 is a leucine-rich repeat receptor-like kinase (LRR-RLK) first identified as a virulence target of begomoviral NSP (Fontes et al., 2004: Mariano et al., 2004). In response to viral infection, or viral PAMPs (begomovirus-derived nucleic acids), NIK1 undergoes oligomerization with itself or a yet-to-be-identified viral pattern recognition receptor (PRR), resulting in phosphorylation on a crucial threonine residue at position 474 (Santos et al., 2009; Teixeira et al., 2019). Activated NIK1 mediates the phosphorylation of the ribosomal protein L10, redirecting RPL10 to the nucleus (Carvalho et al., 2008). Inside the nucleus, phosphorylated RPL10 interacts with the transcriptional repressor L10-Interacting Myb domain-containing protein, LIMYB, to fully repress translational machinery-related genes, including ribosomal protein genes and translational initiation and elongation factors (Zorzatto et al., 2015). Prolonged activation of NIK1 leads to suppression of global translation (Zorzatto et al., 2015). Begomovirus cannot escape this translational regulatory mechanism of plant cells; the viral mRNAs are not efficiently translated, compromising infection (Brustolini et al., 2015: Zorzattoet al., 2015). Viral NSP binds to the kinase domain of NIK1 to counter activate this antiviral defense (Fontes et al., 2004; Santos et al., 2009). Therefore, the NIK1-mediated antiviral signaling is evolutionarily overcome by the viral suppressor NSP. Nevertheless, NIK1 antiviral signaling also cross-communicates with antibacterial immunity imposing relevant implications. First, NIK1 interacts with the pattern recognition receptor (PRR) FLS2 and its coreceptor BAK1 to modulate the formation of the PAMP (flagellin)-induced FLS2-BAK1 immune complex; thereby controlling the extent of PTI activation that otherwise would affect growth (Li et al., 2019). Second, the activated immune complex FLS2-BAK1 phosphorylates NIK1 to initiate the transduction of an antiviral signal that culminates with global translation suppression. Therefore, bacterial infection may induce NIK1-dependent resistance to a subsequent virus infection. The bacterial PAMP-induced activation of NIK1-mediated host translational suppression may also contribute to the immune response-induced stunted growth.

Recent data from network-centric analyses of the LRR- based cell surface interaction network (CSILRR) indicate that NIK1 may be one of the most influential LRR-RLKs as information spreader (Ahmed et al., 2018; Smakowska-Luzan et al., 2018; Li et al., 2019). Therefore, NIK1 may oligomerize with different stimulus-sensing receptors to control translation under adverse conditions. We tested this hypothesis using two different approaches. We first uncovered the transcriptional landscape resulting from NIK1 activation

by performing a ChIP-seq on LIMYB-GFP seedlings to examine whether NIK1 activation would be associated with cellular processes other than translation. Then we monitored the NIK1 activation by different stimuli expected to induce shared responses. We described a growth controlling NIK1/RPL10/LIMYB signaling module that ties the photosynthetic function to translational control in response to biotic and abiotic signals.

Results

LIMYB represses the promoter activity and expression of photosynthetic apparatus-related genes resulting in photosynthesis inhibition

As a downstream component of the NIK1 antiviral signaling, LIMYB represses the expression of translational machinery-related genes, which accounts for the NIK1-mediated translational control mechanism. To assess further the LIMYB regulon, we performed an RNA sequencing (RNA-seq) transcriptome analysis and chromatin immunoprecipitation sequencing (ChIP-seq) experiment on LIMYB-GFP-overexpressing seedlings (Figure S1). We narrowed down the direct LIMYB-target genes by overlapping the RNA-seq with the ChIP-seq results. RNA-seq was performed with Col- 0, LIMYB32-L1, and LIMYB32-L3 RNA (Figure S2). TheLIMYB-induced transcriptome was represented by 2351differentially expressed (DE) genes (>2- fold change up or down, $P < 0.01$, resulting from both transgenic lines), from which 1105annotated genes were upregulated and 1246genes downregulated in LIMYB-overexpressing lines(Figure S2). The top (ranked by false discovery rate [≤0.05]) significantly enriched GO term was structural constituents of ribosomes, which was consistent with the translation- repressing role of LIMYB (Figure S3; Zorzatto et al., 2015). The ChIP-seq analysis identified peaks mapped to the Arabidopsis genome resulting in a total of 6248 transcripts represented. Overlap of these transcripts with the RNA-seq results indicated that 204 annotated genes were upregulated and bound by LIMYB, whereas 156 were down-regulated and bound by LIMYB (Figure S4). These sets of overlapping genes were defined as the core LIMYB up regulon and down regulon and the enriched down- and upregulated categories are described in Tables S1 and S2. These regulons contained known directly LIMYB- regulated genes, including the ribosomal protein genes *RPL18E, RPL28E, RPS13*A, *RPS25*, *RPL13*, *RPL4/l1* (Zorzatto et al., 2015) and a large proportion of newly identified LIMYB targets. Consistent with a role in translational control, translation-related GO terms, including structural constituent of ribosomes and translation, were significantly enriched in the core of LIMYB down regulon (Figure S4; Table S1). Several translational regulatory genes (translational initiation and elongation factors), in addition to ribosomal

protein genes, were LIMYB-dependent based on the RNA-seq and ChIP-seq results (Table S3). *De novo* discovery of enriched motifs within the LIMYB binding peaks identified the MYB-related binding sites C[A/C/T]AA[A/C/G]C (E-value 3.0E-350) and AAGAA[A/G][A/C] (E-value 3.8-252) and a conserved element [A/G]TATAT[A/G] (E-value 1.0-0.97) as top- scoring motifs (Figure 1A). To examine whether these motifs were functional cis-regulatory elements for LIMYB binding, we mapped the ChIP- seq peaks and RNA-seq hits to the locus of three RP genes and three translational regulatory factors (Figure 1B). The ChIP-seq peaks were mapped to all three motifs on the promoter region of these LIMYB target genes, and the corresponding transcripts were downregulated in the LIMYB- overexpressing lines, as shown by the RNA-seq hits and confirmed by RT-qPCR (Supplemental Figure S5). Consistent with these results, a truncated version of the RPL18 promoter lacking the LIMYB binding sites was no longer downregulated by LIMYB in a transactivation assay in Arabidopsis protoplasts (Figure 1C). The accumulation of LIMYB transgene in the protoplast is shown in Supplemental Figure S6. These complementary experiments implicated the core LIMYB down regulon as direct target genes of LYMYB.

Another significantly enriched GO term in the down-regulated core was represented by photosynthesis-related genes, including photosystem II assembly, light reaction, and photosynthetic electron transport (Supplemental Figure S7; Table S4). The enrichment of photosynthesis-related genes in the LIMYB down regulon raised the hypothesis that LIMYB could coordinately repress translation and photosynthesis to balance carbon demand and allocation under biotic signals. Consistent with this hypothesis, responses to starvation-related GO terms were significantly enriched in the upregulated regulon (Table S2). This hypothesis was further tested by several different approaches. We first selected the *PHOTOSYSTEM II OXYGEN-EVOLVING COMPLEX* (*PHSIIOEC*) gene and *FERREDOXIN* (*FD1*) from the electron transport chain in photosystem I and confirmed that LIMYB overexpression represses the expression of the selected photosynthesis-related genes by RT-qPCR (Figure 1D). Then, we created firefly *LUCIFERASE* (fLUC) reporter constructs with 2-kb LIMYB sites-containing promoter region of the *PHSIIOEC* gene for transactivation assays with LIMYB in Arabidopsis protoplast (Figure 1C). Transient expression of LIMYB represses the PR promotor activity but not the UBQ promoter activity, which was not differentially expressed or bound to LIMYB (Figure 1C). Finally, we showed that LIMYB overexpression represses the electron transport rate (ETR), which was associated with a decreased photosynthetic rate (*A*), transpiration rate (*E*), stomatal conductance (*gs*), internal CO2 concentration (ci; Figure 1E, 1F, Figure S8A, and S8B) and

stunted growth either in short or long-day light regimes (Supplemental Figure S9A). Germination, root length and leaf number were lower in the LIMYB-overexpressing lines than wild-type (Supplemental Figure S9B, S9C, S9F). We next examined whether the decreased photosynthesis in LIMYB-overexpressing lines was primarily associated with the LIMYB transcriptional repressing activity or LIMYB- mediated suppression of global translation, which would have affected the expression of the photosynthetic genes. We have previously shown that the translational suppression by NIK1 is a late response with a 30% reduction of translation not until 8 h after NIK1 activation in Arabidopsis seedlings (Zorzatto et al., 2015). Here, we showed that LIMYB represses the promoter activity of *RPL18* marker gene and promotes a coordinated decrease in mRNA and protein (luciferase activity) level safter 3 h of the activated NIK1-T474D expression or viral PAMP-mediated NIK1 activation (Figure 1H; Supplemental Figure S10). In contrast, LIMYB does not control either UBQ promoter activity or luciferase mRNA accumulation that is kept to normal levels throughout the experiment but promotes a decrease in luciferase activity 8 h after NIK1 activation as a late response of translational control (Figure 1I; Supplemental Figure S10). Interestingly, luciferase mRNA and activity under the control of the LIMYB target promoter, RPL18, were coordinately decreased as an early transcriptional response to NIK1 activation, and luciferase activity did not decline further during the translational suppression phase. These results indicate that the LIMYB transcriptional repressing activity is the primary determinant for LIMYB-mediated control of photosynthesis.

Activation of NIK1 antiviral signaling by biotic signals culminates in the repression of photosynthesis-related genes.

As a downstream component of the NIK1-mediated antiviral signaling, we investigated whether the LIMYB-mediated control of photosynthesis was linked to NIK1 activation. We first determined whether activation of NIK1 by viral PAMPs would lead to the repression of photosynthetic apparatus-related genes. Treatment of NIK1-HA seedlings with RNA and DNA from begomovirus-infected, but not from mock-inoculated, Arabidopsis Col-0 lines induced rapid NIK1 phosphorylation (Figure 2A) and resulted in *PHSIIOEC* repression (Figure 2B). The extent of viral PAMP-mediated repression of *PHSIIOEC* was lower in the *nik1* and *nik2* single mutants and abolished in the *nik1nik2* double mutant. *PHSIIOEC* expression is much lower in transgenic lines expressing a constitutively activated NIK1 mutant, NIK1-T474D, than in Col- 0, indicating that NIK1 transduction controls the expression of the photosynthesis-related gene (Figure 2C).

LIMYB coordinates translation and photosynthesis via the NIK1 antiviral immunity

Consistent with the NIK1 activation-mediated repression of photosynthesis-related genes,T474D expression represses ETR in independently transformed lines compared to the control line, a phenotype associated with decreased A, gs, E, and Ci (Figure 3A, 3B, 3C, 3D). II and WUE were also lower in T47D-expressing lines (Figure 3E, 3F, 3H). Consistent with the results, T474 lines had a drastic, negative effect on growth, associated with lower germination,root length, leaf number (Supplemental Figure S11). In contrast, loss-of-NIK1 function enhanced ETR, increasing the gas exchange parameters, a more accentuated phenotype in the nik1nik2 double mutant line. These results link NIK1 activation to the LIMYB-mediated repression of photosynthesis-related genes, similar to the previously described control of translational machinery-related genes mediated by the NIK1/RPL10/LIMYB signaling module.

The NIK1/RPL10/LIMYB signaling module coordinately represses translation and photosynthesis under abiotic stress conditions

As a member of the subfamily II of LRR-RLKs containing predominantly coreceptors of stimulus-sensing transmembrane receptors, NIK1 may be a signal relay unit from different sensing receptors(Ma et al., 2016; Hosseini et al., 2020). Accordingly, NIK1 has been shown to interact with several receptor-like kinases and may be one of the most influential information spreaders from the cell surface (Smakowska-Luzan et al., 2018; Li et al., 2019). In addition, we have previously shown that NIK1 is phosphorylated by the bacterial PAMP-induced FLS2- BAK1 immune complex activating the NIK1/RPL10/LIMYB signaling module for translation control. In contrast we showed here that viral PAMPs do not require FLS2/BAK1 for NIK1 activation, consistent with the argument that NIK1 may serve as a coreceptor from different receptors (Figure 2D). In this experiment, to detect the NIK1 antiviral signaling activation, we monitored the phosphorylation of the downstream component RPL10 by probing immunoprecipitated RPL10 with anti- phosphoserine antibody. As a positive control, we used T474D expression that induces RPL10 phosphorylation without PAMPs. While the bacterial PAMP flg22 required the receptor FLS2 and coreceptor BAK1 to induce the NIK1-mediated phosphorylation of the downstream component RPL10 (Figure 2D), viral PAMP induced RPL10 phosphorylation in Col-0 but also in *fls2* and *bak1* knockout lines. Collectively, these results indicated that viral PAMP might require a yet-to-be-identified viral PAMP-sensing receptor for NIK1 phosphorylation and activation.

As NIK1 may interact with different stimulus-sensing receptors, we investigated whether the NIK1/RPL10/LIMYB signaling module would function as a molecular link for the coordinate suppression of photosynthesis and translation under abiotic stress conditions. To test this hypothesis, we subjected Arabidopsis Col-0, *nik1*, *nik2*, and *nik1nik2* lines to different stress conditions and monitored the readouts for NIK1 signal transduction activation. These include NIK1 phosphorylation as an early response, followed by L10 phosphorylation and repression of translational machinery- and photosynthesis-related genes. NIK1 and RPL10 phosphorylation was monitored by probing the immunoprecipitated protein with anti-phospho amino acid antibody. As an early response, heat promoted endogenous NIK1 phosphorylation 10 min after treatment in Col-0 and *nik2* lines, but not in *nik1* and *nik1/nik2* mutants, confirming they were true NIK1 knockouts (Figure 4A). As expected, T474D was constitutively phosphorylated. NIK1-HA aldo undergoes phosphorylation under heat treatment, indicating that the fusion protein was functional(Figure 4B). We also monitored the effectiveness of the heat treatment by measuring HSP70 induction (Figure 4C). Heat treatment also promotes phosphorylation of the downstream component RPL10-GFP as early as 30 min after treatment (Figure 4D), followed by repression of photosynthesis-related marker genes *PHSIIOEC* and *FD1* in Col-0, but not in *nik1/nik2* knockouts(Figure 4E). Likewise, heat treatment promoted the repression of ribosomal protein genes and translation initiation factor genes in control lines but not in *nik1nik2* double mutant (Figures 4F, 4G). Collectively, these data indicate that heat treatment activates the NIK1-mediated antiviral signaling probably to coordinate translation andphotosynthesis during stress conditions.

We also monitored the activation of the NIK1 signal transduction by osmotic stress, which inhibits growth (Figure 5). The effectiveness of the osmotic stress treatment was confirmed bythe induction of the drought-responsive marker gene *RAB18* 3h and 24 h after treatment in all genotypes (Figure 5A). The osmotic stress inducer PEG promotes NIK1-HA phosphorylation (Figure 5B), leading to RPL10-GFP phosphorylation (Figure 5C), followed by repression of NIK1activation-associated marker genes in Col-0, *nik1*, and *nik2*, but not in the *nik1/nik2* double mutant (Figure 5D, 5E, 5F). Therefore, the NIK1/RPL10/LIMYB regulatory circuit is activated by different biotic and abiotic signals and may represent a molecular link controllingtranslation and photosynthesis under stress conditions.

Discussion

All organisms must perceive and respond to changing growth conditions and environmental stimuli. Under acute adverse conditions, including heat shock, osmotic stress, and pathogen attack, the induced changes in energy-consuming cellular processes must be coordinated with the rate of energy-producing metabolic processes to prevent excessive stress built up and ensure cell survival. In-plant cells, photosynthesis, a chemical energy-producing process, must be coordinated with translation, the most energy-consuming process, under stressconditions but direct links between these major cellular processes have not been thoroughly investigated. Here, we showed that, in plant cells, stress signals are perceived at the cell surfaceand transduced via the NIK1/RPL10/LIMYB signaling module to regulate translation and photosynthesis coordinately. Both biotic signals, viral and bacterial PAMPs, and abiotic signals, high temperature and osmotic signals, induce phosphorylation and activation of the NIK1 transmembrane receptor-like kinase that relay the stress signals to cytosolic RPL10 and then tothe nuclear transcriptional repressor LIMYB, culminating in repression of ribosome protein genes, translation regulatory genes as well as photosynthetic apparatus genes. This stress- induced LIMYB-mediated repression of the translational machinery- and photosynthesis- related genes leads to a coordinated suppression of photosynthesis and translation, probably to balance carbon fixation and allocation, that otherwise would lead to excessive oxidative stress. Therefore, the stress-induced repression of photosynthesis and translation coordinated by the NIK1/RPL10/LIMYB signaling module contributes to growth control in response to changingenvironment.

In contrast to TOR signaling that rapidly activates translation via phosphorylation of regulatory factors, the NIK1 signaling coordinates stress-induced suppression of translation and photosynthesis via de transcriptional repressing activity of LIMYB on photosynthesis- and translation-related genes. Therefore NIK1-mediated regulation of photosynthesis and translation represents a late response to biotic and abiotic signals, as it depends on the half-life of the target genes. Consistent with a late kinetics response, the NIK1-mediated repression of translation has been shown to suppress global translation after 8h of NIK1 activation, and photosynthesis repression may not be different (Zorzatto et al., 2015). Upon NIK1 activation, LIMYB predominantly targets genes encoding components of the photosynthetic electron transport chain, photosystem II and I. Accordingly, NIK1/RPL10/LIMYB module activation leads to a concomitant decrease in ETR, gas exchange parameters (A, gs, E and Ci), the fluorescence quantum efficiency, and WUE.

These results indicate that photosynthesis activity decreases in LIMYB-overexpressing lines and T474 lines may be caused by the LIMYB-mediated decrease in the abundance of Photosystem II, I, and electron transport chain components, rather than by defects in C fixation or damages of the photosynthetic apparatus. Adjustments in the photosystem stoichiometry have been shown to affect the quantum efficiency of photosynthesis (Chow et al., 1990).

We show that multiple abiotic and biotic signals activate the NIK1/RPL10/LIMYB signaling circuit, which regulates coordinately translation and photosynthesis in plant cells. NIK1 has also been shown to interact with different LRR-RLK forming a hub with high centrality. We propose that NIK1 transduces different abiotic and biotic signals by relaying information from different stress-sensing receptors (Figure 6). Consistent with this interpretation, the bacterial PAMP flg22, but not viral PAMPs, requires the immune complex FLS2-BAK1 for mediating NIK1 phosphorylation and activation. Very likely a yet-to-be- determined viral pattern recognition receptor may sense viral PAMPs to mediate NIK1 activation in response to viral infection. As an influential LRR-RLK spreader of information (Ahmed et al., 2018; Smakowska-Luzan et al., 2018;Li et al., 2019), we propose that NIK1 represents a central signaling hub that integrates signals from multiple stress-sensing receptorsto control growth under stress conditions.

Materials and Methods

Plant material and growth conditions

The *Arabidopsis thaliana* ecotype Columbia-0 (Col-0) was used as control lines. The knockout lines *nik1-1* (SALK_060808), *nik2-1* (SALK_044363), *fls2* (Salk_141277), *bak1-4* (Salk_116202) and *limyb-32* (SALK_032054) were obtained from the Arabidopsis Biological Resource Center and have been previously characterized (Fontes et al., 2004; Li et al., 2015; Zorzatto et al., 2015).The double mutant *nik1-1/nik2*, the transgenic line RPL10-1, harboring the construct 35S: YFP- GR-RPL10 in the Col-0 genetic background, two independently nik1- 1 transformed lines, T474D- 4, T474D-6, expressing the NIK1-T474D-GFP mutant transgene, the NIK1-HA transgenic line, harboring 35S:NIK1-HA in Col-0 and the *limyb*/T474D-2 line expressing 35S:T474D-GFP in the *limyb-32* mutant background have been generated previously (Zorzatto et al., 2015; Li et al., 2019). Plants were grown in soil (Metro Mix 366) in a growth chamber at 23 °C, 45% humidity, and 75 $\mu E/m^2/s^1$ light with a 10-h-light/14-h-dark photoperiod. Four-week-old plants were used for treatments with viral nucleic acid elicitors, heat stress, and protoplast isolation. For

osmotic stress experiments, seedlings were germinated for up to 12 days on half-strength Murashige and Skoog ($MS^1/_2$) plates containing 1% (w/v) sucrose and 0.8% (w/v) agar, grown under the same conditions.

Plasmid construct for transient expression in protoplast

The generation of pK7F-NIK1T474D (pUFV 632), which expresses a T474D mutant fused in frame with the N-terminal of GFP under the control of CaMV 35S promoter, has been previously described (Santos et al., 2009). The clones pK7F-L10 (pUFV1862) and pYFP-L10 (pUFV 2365) have been previously described. They contain RPL10A ORF fused in frame to GFP after its last codon or YFP before its first codon under the control of the 35S promoter (Santos et al., 2009). The recombinant plasmid pYFP-LIMYB (pUFV1886), containing LIMYB ORF fused in-frame to the C-terminus of YFP under the control of the 35S promoter and inserted into the binary vector 35S-YFP-casseteA-Nos-pCAMBIA1300, has been previously described (Zorzatto et al., 2015). The recombinant plasmid AT5G05800NS- pK7FWG2 (pUVF 1395), containing LIMYB ORF fused-in frame to the N-terminal of GFP under control of the 35S promoter has been described before (Zorzatto et al., 2015).

Plasmid constructs for promoter transactivation assay in protoplast

The clone prAt1g29970-Lucif-term-2X35S RLucifpH7M34GW (pUVF2231), previously described (Zorzatto et al., 2015), contains the firefly luciferase cDNA under the control of the rpL18A promoter, as well as the Renilla luciferase cDNA under the control of a 2 x 35S promoter. Likewise, the clones containing the firefly luciferase cDNA under the control of the RPL28e, RPS13A, and ubiquitin promoters for luciferase transactivation assays were previously obtained (Zorzatto et al., 2015). The At2G28605 (PHSIIOEC or PsbP-OEC) promoter (-2000 PB) was obtained from *Arabidopsis* DNA by PCR using the gene-specific primers (Table 1), and cloned into pDONR-P4-P1R vector, generating pUFV 4015 clone. The clone LUCF-term-pDON221 (pUFV 2132) harbors the firefly luciferase cDNA in the entry vector pDON221, whereas the clone2×35S-RLUCF-pDONR-P2R-P3 (pUFV 2131) contains *Renilla* luciferase cDNA under the control of a 2× 35S promoter. The At2G28605 promoter (- 2000 PB) was inserted into the destination vector pH7m34GW (pUFV 1918), along with 2×35S-RLUCF-pDONR-P2R-P3 (pUFV 2131) and LUCF-term-pDON221 (pUFV 2132), by triple recombination using the gateway system (Promega, Gateway™ LR Clonase™ Enzyme mix, cat # 11791019). The resulting clone

proPHSIIOEC:Lucif-term-2X35S:RLucif pH7M34GW (pUFV 3427) contains the firefly luciferase cDNA under the control of the PHSIIOEC promoter (2000 5' flanking sequences), as well as the *Renilla* luciferase cDNA under the control of a 2× 35S promoter. The same procedure was used to clone the firefly luciferase cDNA under the control of the FD1 promoter (-2000 PB), yielding the clone proFD1:Lucif-term-2X35S:RLucif pH7M34GW (pUFV 3431), and the promoter truncatedversions of proRPL18Ae (positions -400 and -1000 bp), proRPL28e (positions -810 PB, -500 PB and -240 PB) and proRPS13A (positions -1045 and -740 PB). The resulting clones of truncated promoters were: proL18(3):Lucif-term-2X35S:RLucif pH7M34GW (-325 pb) (pUFV 3435); All promoter-specific primers used for amplifying promoter and truncated sequences are listed in Table 1.

Plant transformation

The *limyb-32* lines were transformed with pYFP-LIMYB using the floral dip method, generating *LIMYB-32-L1, LIMYB-32-L3,* and *LIMYB-32-L4* lines. Primary transformants wereselected using30 µgmL^{-1} hygromycin, and transgene stable insertion was monitored by PCR with gene-specific primers (Table 1). The transgene expression level was determined byimmunoblotting and real- time qPCR with gene-specific primers (Table 1). *The actin* gene wasused as an internal control to quantify gene expression by RT-qPCR.

Whole-genome chromatin immunoprecipitation sequencing (ChIP-Seq) and data analysis

Seedlings (600 mg) harboring a YFP-LIMYB transgene were crosslinked using 1% formaldehyde in PBS solution (Sigma-Aldrich, cat. # F8775) under vacuum for 1-3 min, as previously described (Yamaguchi et al., 2014). After nuclei isolation, chromatin was sonicated up to 100–800 bp fragments. *LIMYB-GFP targets from LIMYB-32-L1 LIMYB-32-L3, and LIMYB-32-L4* isolated nuclei were immunoprecipitated using rabbit polyclonal anti-GFP - IgG antibody (Thermo Fisher Scientific, MA, USA, cat. # A11122) and captured with protein-A agarose beads (Invitrogen^{TM}, Cat # 15918014). After elution, reverse crosslinking, and DNA purification, ChIPed-DNA was used to generate sequencing libraries through Illumina TruSeq kit (Illumina, cat # IP-202-1012, IP-202-1014) according to the manufacturer's protocols. Libraries were sequenced using an Illumina HiSeq 4000. The quality of the reads was evaluated through the statistical metrics implemented in the FastQC data quality analysis tool (Andrews, 2017); low-quality sequencing reads were filtered using the printSEQ software package (Schmieder & Edwards, 2011). ChIP-Seq raw reads were

aligned to TAIR10 genome sequence using Bowtie 2 (Langmead et al., 2009). ChIP-seq peaks were calculated with the software ChIPpeakAnno (Zhu et al., 2010; Zhu L., 2013), and MACS2 (Zhanget al., 2008) was used to analyze the ChIP-seq data. Putative target genes and peak distribution of the ChIP-seq data were figured out using the ChIPpeakAnno software (Zhu *etal*.,2010; Zhu L., 2013). Motif discovery was performed by MEME-ChIP version 4.9.0 (Machanick and Bailey, 2011). Motifs were grouped by applying hierarchical clustering using motif distances, calculated by Pearson correlated coefficients as the metric for base comparison and Smith-Waterman Ungapped alignment method (Song et al., 2016). The binding intensity was measured from log2 (normalized counts of reads/peaks) and evaluated at E-value cut-off of 1e-05 for sequence identification. ChIP-seq data have been deposited in the Gene ExpressionOmnibus under accession number GSE197332.

RNA-sequencing (RNA-seq) method and data analysis

For RNA-seq experiments, we used three biological replicates of a pool of 12-day-old Col-0, *LIMYB-32-L1,* and *LIMYB-32-L3* seedlings and examined differences between Col-0 and LIMYB lines using the Deseq2 differential gene expression method (Robinson and Oshlack, 2010;Anders and Huber, 2010). RNA sequencing was obtained using the Illumina Hi-seq 2500 platform. Libraries for RNA-seq were prepared with the kit TrueSeq-RNA Sample Prep Kit Illumina (Illumina, cat # 20020595). The paired-end 100-bp protocol was used with the following quality filter parameters: 5 bases trimmed at the 3′ and 5′ ends of the reads and a minimum average Phredscore of 30. Reads quality was evaluated by FastQC (Andrews, 2017). Illumina adapters were removed using Trimmomatic software (Bolger et al., 2014), and low- quality sequencing reads were filtered and trimmed using prinSEQ software package. (Schmieder& Edwards, 2011). Read mapping was performed using the Bowtie 2 program (Langmead et al., 2009). The global analysis of differential gene expression (DGE) was performed using the edger package (Robinson et al., 2010) and DEseq2 (Anders & Huber, 2010). Differential expression was determined using the p- value adjusted by the "False discover rate" (FDR). Log_2.Fold Change p-value < 0.01 e log2-fold-change >1.0 for up- regulated genes and log2-fold-change <1.0for down-regulated gene, were used as the cutoff point. Differentially expressed (DE) genes were stored using SQL tables in the PostgreSQL relational database (http://200.235.143.46/LiMyb/ or https://inctipp.bioagro.ufv.br/maloni/), which listed corresponding log2 FC (fold change) and p values corrected by false discovery rate (q value) for all DE genes. The classification of gene ontology (GO) and analysis of enrichment of pathways were performed using the

packages GoStats (Falcon & Gentleman, 2007) and PathView (Luo & Brouwer, 2013), both present in the R/Bioconductor GOstats repository. The significant p-value for enrichment was $P < 0.01$.

Activation of the NIK1 pathway by begomovirus-derived nucleic acids

Leaf discs from transgenic lines previously injured with an abrasive were excised by a cork borer and incubated overnight in 12-well plates containing 500 µL ultra-pure water. Then the water was immediately replaced with 500 µL TE buffer supplemented with 250 ng/µL of viral nucleic acids (DNA or total RNA prepared from begomovirus-infected plants) or ultra- pure water. NIK1 activation was monitored by phosphorylation at 10 to 60 min after treatment. Phosphorylation of RPL10 was examined at 30 min to 3 h post-treatment, whereas the transcript accumulation of target genes was measured at a minimum of 3 h after treatment.

Protoplast preparation from *A. thaliana* leaves

Expanded leaves from 3–4-week-old plants were cut in 0.5–1-mm pieces and digested with 5–10 ml enzyme solution (20 mM MES pH 5.7; 1.5% cellulase R10; 0.4% macerozyme R10; 0.4 M mannitol and 20 mM KCl) (reference). The leaf strips were vacuum-infiltrated for 30min in the dark using a desiccator. Then, the digestion was conducted without shaking, in the dark for at least 3 h at room temperature. The integrity of the protoplasts was examined under a light microscope. The protoplasts were filtered to remove undigested leaf tissues and recovered by centrifugation. The protoplasts were transformed using the protocol of DNA-PEG–calcium transfection, in which 10 µl DNA (10–20 µg of plasmid DNA) were mixed with 2×10^4 protoplasts along with 5% PEG solution (Polyethylene glycol 4000, sigma, Cat # 25322-68-3) at room temperature for up to 15 min and then incubated for recovery during 12 h (Yoo and Sheen, 2007).

Heterologous Expression of 6xHis-NBSNIK1 and Production of Anti-NIK1 Antibodies

The 6xHis-NBSNIK1 construction was previously cloned in pDEST17 via LR-mediated recombination (Gateway Invitrogen Life Technologies, Inc). An aliquot of plasmid DNA was used for E. coli strain C41(DE3) transformation. For the heterologous expression, a pre- inoculum was diluted 1:100 in 100 mL of LB medium and the culture was incubated at 37°C, under agitation at 225 rpm until reaching optical density (OD600nm) between 0.6 and 0.8. The recombinant protein synthesis was induced by 0,8 mM isopropyl-β-d-thiogalactopyranoside for 4h at 37 °C. Cells were harvested, washed, and suspended in

lysis buffer: 50 mM Tris pH 8.0, 50 mM NaCl, 5 mM EDTA, to which 100 µg/ml lysozyme, 0.1% Triton X-100 and 1 mM PMSF were added at the time of use. Cell pellets were suspended in 1/10 of the original volume of the culture and incubated at 30 °C for 5 minutes. Lysis was obtained by ultrasonication in 6 cycles of 10 seconds on/10 seconds off, amplitude 20%, keeping the tube on ice throughout the procedure. Finally, cell debris was removed by ultracentrifugation at 4 °C for 20 min at 14000 g. The His- tagged fusions were affinity purified using Ni-NTA agarose (Quiagen®), according to the manufacturer's recommendations and resolved by SDS-PAGE.

For antibody production, two male BALB/c mice (4- to 8-week-old) were used. The animals were kindly provided by Professor Dr Leandro Licursi, obtained from the Central Animal Laboratory of the Center of Biosciences and Health of the Federal University of Viçosa (Brazil) (CEUA/UFV – process number: 45/2013). The mice were maintained and handled in the experimental vivarium of the Immunology and Virology sector of the General Biology Department – DBG/UFV, where they remained in 12 h light/dark photoperiod cycle and received water and food ad libitum. Immunization was performed intraperitoneally with 200 µL of solution prepared from 3 to 4 protein bands, cut directly from the polyacrylamide gel and ground with a tissue homogenizer in PBS buffer added with 50 µg of saponin. The treatment consisted of 3 doses with intervals of 15 days between each dose. Four weeks after immunization, the mice were euthanized. Euthanasia was performed using the cervical dislocation technique. The blood obtained from the animals was kept at room temperature for 45 minutes, the time necessary for clotting. Then the material was centrifuged at 4000 g for 10minutes, and the serum obtained was transferred to a new tube. The hyperimmune serum was then heated in a thermoblock at 56 °C for 30 minutes to inactivate the complement proteins and titrated by dot blot to determine the minimum antibody concentration that still allowed the visualization of a positive reaction with substrate.

Phosphorylation assay

Protoplasts of *nik1-1, nik2-1, fls2, bak1-4* and *nik1-1/nik2-1* mutant lines were prepared aspreviously described (reference) and transformed with RPL10-GFP. After 16-h incubation for transient transgene expression, the protoplasts were treated with nucleic acids prepared from mock-inoculated and begomovirus-infected plants for 3 h. RPL10-GFP was immunoprecipitated with α-GFP antibodies and protein-A agarose beads, fractionated by SDS- PAGE and immunoblotted with an α-phosphoserine antibody (α-phosphoserine

peroxidase, Sigma-Aldrich, Cat # SAB5200087, 1:5000) and an α-GFP antibody (α -GFP, life technologies,cat # A11122, 1:5000; goat anti-mouse IgG-HRP, Santa Cruz, Cat # sc-2005, 1:10,000). Likewise, transgenic lines expressing RPL10-GFP and NIK1-HA were treated for 3h with nuclei acids prepared from uninfected and begomovirus-infected plants or 100 mM flg22. Then,RPL10-GFP and NIK1-HA were immunoprecipitated from leaf discs from treated and non- treated plants with α-GFP antibody or α-HA antibodies (α-HA, Thermo Fisher, Cat # 71-5500, 1:50) and protein-A agarose beads (InvitrogenTM, Cat # 15918014), fractionated by SDS- PAGE and immunoblotted with an α-phosphoserine antibody (α-phosphoserine peroxidase, Sigma-Aldrich, Cat # SAB5200087, 1:5000); and α-phosphothreonine antibody (α- phosphothreonine, Thermo Fisher, Cat # 71-8200, 1:250) and goat anti-rabbit IgG secondary antibody (Thermo Fisher, Cat # 65-6120,1:10.000). The same protocol examined the heat and osmotic-induced phosphorylation of NIK1- HA and RPL10 in 22-day-old transgenic lines.

RNA isolation and RT-qPCR analysis

For RNA isolation, either 12-day-old seedlings grown on half-strength MS plates or leaf discs of 22-day-old plants were transferred to 1 mL H_2O in a 12-well plate to recover overnightand then treated uninfected and begomovirus-infected nucleic acid preparation for 15 min to 3h, or 10% PEG 8000 for 3h and 24h. RNA was extracted using TRIzol reagent (Invitrogen™,cat # 15596018, USA) and quantified with a NanoSpec spectrophotometer. TotalRNA was treated with DNase I, RNase-free (Thermo Scientific™, cat # EN052) for 30 min at 37 °C and then reverse transcribed with M-MLV Reverse Transcriptase (Invitrogen™, cat # 28025013). Real-time PCR was performed using iTaq Universal SYBR Green Supermix (Bio-Rad, cat # 1725121, USA) and a 7500 Fast Real-Time PCR System (Applied Biosystems™, cat# 4351106, USA). The expression of each gene was normalized to the expression of Actin or UBQ10. The primers used to analyze specific transcripts for RT-qPCR are listed in Table 1.

Promoter transactivation assay in protoplasts and *Nicotiana benthamiana* leaves.

The protoplasts were isolated from the genotypes Col-0 and *limyb-32*, co-transformed with the combinations: pK7F-NIK1T474D; pK7F-NIK1T474D + AT5G05800NS-pK7FWG2 + proL18(2):Lucif-term-2X35S:RLucifpH7M34GW; AT5G05800NS-pK7FWG2 + proL18(2):Lucif-term-2X35S:RLucifpH7M34GW; proPHSIIOEC:Lucif-term-2X35S:RLucif pH7M34GW+AT5G05800NS-pK7FWG2; pK7F-NIK1T474D +

proUBQ:Lucif-term 2X35S:RLucifpH7M34GW; pK7F-NIK1T474D + AT5G05800NS-pK7FWG2 + proUBQ:Lucif- term-2X35S:RLucifpH7M34GW. *N. benthamiana* leaves were agro-infiltrated with *A. tumefaciens* GV3101 strains carrying the following combinations in absence and presence of LIMYB cDNA and the vector AT5G05800NS-pK7FWG2:proPHSIIOEC:Lucif- term- 2X35S:RLucif pH7M34GW: proFD1:Lucif-term-2X35S:RLucif pH7M34GW (-2000 bp); proL18Ae(2):Lucif-term-2×35S:RLucif pH7M34GW (- 2000 bp); proL18(3):Lucif-term- 2X35S:RLucif pH7M34GW (-325 bp) Forty-eight hours after infiltration, 200 mg of leaf tissue were harvested for total protein extraction. Luciferase activity was assayed with Dual-Luciferase® Reporter Assay System (Promega, cat # E1910) according to the manufacturer's instructions.

Photosynthetic and photochemistry analysis of LIMYB e T474D overexpressing lines

Gas exchange and chlorophyll fluorescence measurements were carried out in expanded leaves from 30-days-old LIMYB and T474D lines, grown in a chamber at 23°C. Gas exchange rates were determined in the morning, applying different photon rates m-2s-1 for photosynthetic efficiency analysis, using an infrared gas concentration determination system (IRGA, LCpro- SD - ®ADC Bioscientific, Hoddesdon, England). The net assimilation of carbon (A, µmol CO_2 m -2 s-1), stomatal conductance (gs, mol H_2O m-2s -1), the internal concentration of CO_2 (Ci, µmol CO_2 mol -1), transpiration rate (E, mmol m-2 s-1) and water-use efficiency (WUE, A/E µmol m-2 s- 1/mmol H2O m-2 s-1), under CO 2 concentrations controlled by the use of a gas cylinder attached to the equipment. Photochemical parameters of PSII and the energy transmission of the light- capturing complex (Lchb) were determined with the aid of amodulated light fluorometer (MINI-PAM, Walz, Effeltrich, Germany). Minimum (Fo) and maximum (Fm) fluorescences of dark-adapted leaves were also determined in the morning to analyze FSII Effective quantum yield (ΦYII) and electron transport rate (ETR = ΦFSII x RFA x 0,5 x 0,84) (Genty, Briantais e Baker,1989). ETR rate was determined via modulated light pulse, the response curve of chlorophyll-a fluorescence parameters (ETR, ΦFSII, ΦNO, and qL) in responses to eight increasing light levels based on Fo and Fm values (minimum value up to the saturating pulse).

Heat stress

The heat stress treatment was performed as described (Chao et al., 2017; Wang et al., 2020), with some modifications. 28 days-old plants were subjected to 38°C for 0 to 3h. NIK1 phosphorylation was monitored 0, 10, 15, 20, 30 and 60 min post-treatment. As for RPL10 phosphorylation and transcript accumulation of target genes, the intervals of 0, 1h, and 3h after treatment were taken. After the specified period of the treatment, the leaves were immediatelyfrozen in liquid nitrogen for protein and/or total RNA extraction.

Osmotic stress

Osmotic stress was induced in Arabidopsis seedling as described (Costa et al., 2008), with some modifications. 12-days-old *Arabidopsis thaliana* seedlings were germinated on Murashige and Skoog (MS) medium containing 1% sucrose (pH 5.7) in a petri dish and then placed in 12-well plates containing 90% liquid MS medium (1/4 strength) and 10% polyethylene glycol (PEG, MW8000, SIGMA, cat # 25322-68-3) (p/v) for 3 and 24 h. The control was performed only with water. After the treatment, plants were used for the in vivo phosphorylation assays and analysis of transcript accumulation.

Measurement of growth and developmental parameters

Development and growth experiments were performed in genotypes Col-0, T474D-4, T474D-6, *nik1-1, nik2-1, nik1-1/nik2-1*, LIMYB-32-1, LIMYB-32-3, and *limyb-32*, as previously described (Chirinos-Arias and Spaminato, 2020), with some modifications. Germination was evaluated fromseed protrusion in plates in medium MS$^1/_2$. Primary root growth was measured daily for 8 days onseeds grown in vertically positioned plates. Vegetative growth was studied in soil-grown plants, subjected to short diurnal periods, photoperiod 8h-light/16h-dark, or long periods of 10h-light/14h- dark; thus, the digital tool Image J (http://rsb.info.nih.gov/ij/) was used to analyze rosette area and total leaf number. Total chlorophylls were measured spectrophotometrically as previously described (Petrillo et al. 2014; Song et al., 2016). The transition from the vegetative to the adult phase was examined from number of primary and lateral inflorescences. Characteristics associated with the mean number of siliques also analyzed. The number of siliques was determined in primary and lateral shoots.

Statistical analysis

Student's t-test was used for statistical analysis, performed in Excel 2019 software. The analyses were executed with three-independent experiments, and the data were expressed as means ± sd. A significant difference was considered p-value ≤ 0.05. The photosynthetic parameters analysis used 3° order polynomial regression on adjusted radiation curves and Student's t-test as comparisons between curvature points.

References

Ahmed, H., Howton, T.C., Sun, Y., Weinberger, N., Belkhadir, Y., and Mukhtar, M.S. (2018). Network biology discovers pathogen contact points in host protein-protein interactomes. Nat.Commun. **9**: 1–13.

Anders, S. and Huber, W. (2010). Differential expression analysis for sequence count data. Genome Biol. **11**: 1–12.

Andrews, S. (2010). FastQC: A quality control tool for high throughput sequence data. Ref. Source Assoc. Bioinformatics. **23**: 257–258.

Bolger, A.M., Lohse, M., and Usadel, B. (2014). Trimmomatic: A flexible trimmer for Illuminasequence data. Bioinformatics **30**: 2114–2120.

Brustolini, O.J.B. et al. (2015). Sustained NIK-mediated antiviral signalling confers broad-spectrum tolerance to begomoviruses in cultivated plants. Plant Biotechnol. J. **13**: 1300– 1311.

Burkart, G.M. and Brandizzi, F. (2021). A Tour of TOR Complex Signaling in Plants. Trends Biocheimcal Sci. **46**: 417–428.

Carvalho, C.M., Santos, A.A., Pires, S.R., Rocha, C.S., Saraiva, D.I., Machado, J.P.B., Mattos, E.C., Fietto, L.G., and Fontes, E.P.B. (2008). Regulated nuclear trafficking of rpL10A mediated by NIK1 represents a defense strategy of plant cells against virus. PLoSPathog. **4**: e1000247.

Chao, L.M., Liu, Y.Q., Chen, D.Y., Xue, X.Y., Mao, Y.B., and Chen, X.Y. (2017). Arabidopsis Transcription Factors SPL1 and SPL12 Confer Plant Thermotolerance at Reproductive Stage. Mol. Plant **10**: 735–748**.**

Chirinos-Arias, M.C. and Spampinato, C.P. (2020). Growth and development ofAtMSH7 mutants in Arabidopsis thaliana. Plant Physiol. Biochem. **146**: 329–336.

Chow, W., Anderson, J. and Melis, A. (1990). The Photosystem Stoichiometry in Thylakoids of Some Australian Shade-adapted Plant Species. Funct. Plant Biol. **17**: 665.

Costa, M.D.L., Reis, P.A.B., Valente, M.A.S., Irsigler, A.S.T., Carvalho, C.M., Loureiro, M.E., Aragão, F.J.L., Boston, R.S., Fietto, L.G., and Fontes, E.P.B. (2008). A new branch of endoplasmic reticulum stress signaling and the osmotic signal converge on plant- specific asparagine-rich proteins to promote cell death. J. Biol. Chem. 283: 20209–20219**.**

Falcon, S. and Gentleman, R. (2007). Using GOstats to test gene lists for GO term association. Bioinformatics **23**: 257–258.

Ferreira, M.A., Teixeira, R.M., and Fontes, E.P.B. (2021). Geminivirus–host interactions: Action and reaction in receptor-mediated antiviral immunity. Viruses **13**.

Fontes, E.P.B., Santos, A.A., Luz, D.F., Waclawovsky, A.J., and Chory, J. (2004) 71 geminivirus nuclear shuttle protein is a virulence factor that suppresses transmembrane receptor kinase activity. Genes Dev. **18**: 2545–2556.

Fontes, E.P.B., Teixeira, R.M., and Lozano-Durán, R. (2021). Plant virus-interactions: unraveling novel defense mechanisms under immune-suppressing pressure. Curr. Opin.

Biotechnol. **70**: 108–114.

Hosseini, S., Schmidt, E.D.L., and Bakker, F.T. (2020). Leucine-rich repeat receptor-like kinaseII phylogenetics reveals five main clades throughout the plant kingdom. Plant J. **103**: 547– 560.**Langmead, B., Trapnell, C., Pop, M., and Salzberg, S.L.** (2009). Ultrafast and memory- efficient alignment of short DNA sequences to the human genome. Genome Biol. **10**.

Li, B. et al. (2019). The receptor-like kinase NIK1 targets FLS2/BAK1 immune complex and inverselymodulates antiviral and antibacterial immunity. Nat. Commun. **10**: 1–14.

Li, B., Jiang, S., Yu, X., Cheng, C., Chen, S., Cheng, Y., Yuan, J.S., Jiang, D., He, P., and Shan, L. (2015). Phosphorylation of trihelix transcriptional repressor ASR3 by MAP KINASE4 negatively regulates arabidopsis immunity. Plant Cell **27**: 839–856.

Luo, W. and Brouwer, C. (2013). Pathview: An R/Bioconductor package for pathway-based data integration and visualization. Bioinformatics **29**: 1830–1831.

Ma, X., Xu, G., He, P., and Shan, L. (2016). SERKing Coreceptors for Receptors. Trends PlantSci. **21**: 1017–1033.

Machado, J.P.B., Brustolini, O.J.B., Mendes, G.C., Santos, A.A., and Fontes, E.P.B. (2015). NIK1, a host factor specialized in antiviral defense or a novel general regulator ofplant immunity? BioEssays **37**: 1236–1242.

Machado, J.P.B., Calil, I.P., Santos, A.A., and Fontes, E.P.B. (2017). Translational controlin plant antiviral immunity. Genet. Mol. Biol. **40**: 292–304.

Machanick, P. and Bailey, T.L. (2011). MEME-ChIP: Motif analysis of large DNA datasets. Bioinformatics **27**: 1696–1697.

Mariano, A.C., Andrade, M.O., Santos, A.A., Carolino, S.M.B., Oliveira, M.L., Baracat- Pereira, M.C., Brommonshenkel, S.H., and Fontes, E.P.B. (2004). Identification of a novel receptor-like protein kinase that interacts with a geminivirus nuclear shuttle protein. Virology.**318**: 24–31.

Muhammad, I., Shalmani, A., Ali, M., Yang, Q.H., Ahmad, H., and Li, F.B. (2021). Mechanisms Regulating the Dynamics of Photosynthesis Under Abiotic Stresses. Front. Plant Sci. **11**: 1–25.

Petrillo, E., Herz, M. a G., Fuchs, A., Reifer, D., Fuller, J., Yanovsky, M.J., Simpson, C., Brown, J.W.S., Barta, A., Kalyna, M., and Kornblihtt, A.R. (2014). Regulates NuclearAlternative Splicing. Science (80-.). **344**: 427–430.

Reinbothe, C., Pollmann, S., and Reinbothe, S. (2010). Singlet oxygen signaling links photosynthesis to translation and plant growth. Trends Plant Sci. **15**: 499–506.

Robinson, M.D. and Oshlack, A. (2010). A scaling normalization method for differential expression analysis of RNA-seq data. Genome Biol. **11**: 1–9.

Santos, A.A., Carvalho, C.M., Florentino, L.H., Ramos, H.J.O., and Fontes, E.P.B. (2009). Conserved threonine residues within the A-loop of the receptor NIK differentially regulatethe kinase function required for antiviral signaling. PLoS ONE. **4**: e5781.

Schmieder, R. and Edwards, R. (2011). Quality control and preprocessing of

metagenomic datasets. Bioinformatics **27**: 863–864.

Smakowska-Luzan, E. et al. (2018). An extracellular network of Arabidopsis leucine-rich repeatreceptor kinases. Nature **553**: 342–346.

Song, L., Huang, S.S.C., Wise, A., Castanoz, R., Nery, J.R., Chen, H., Watanabe, M., Thomas, J., Bar-Joseph, Z., and Ecker, J.R. (2016). A transcription factor hierarchy defines an environmental stress response network. Science (80-.). **354**.

Song, Y., Alyafei, M.S., Masmoudi, K., Jaleel, A., and Ren, M. (2021a). Contributions of torsignaling on photosynthesis. Int. J. Mol. Sci. **22**: 1–10.

Song, Y., Feng, L., Alyafei, M.A.M., Jaleel, A., and Ren, M. (2021b). Function of Chloroplasts in Plant Stress Responses. Int. J. Mol. Sci. **22**: 1–17.

Tcherkez, G., Carroll, A., Abadie, C., Mainguet, S., Davanture, M., and Zivy, M. (2020). Protein synthesis increases with photosynthesis via the stimulation of translation initiation.Plant Sci. **291**: 110352.

Teixeira, R.M., Ferreira, M.A., Raimundo, G.A.S., and Fontes, E.P.B. (2021). Geminiviraltriggers and suppressors of plant antiviral immunity. Microorganisms **9**.

Teixeira, R.M., Ferreira, M.A., Raimundo, G.A.S., Loriato, V.A.P., Reis, P.A.B., and Fontes, E.P.B. (2019). Virus perception at the cell surface: revisiting the roles of receptor-like kinases as viral pattern recognition receptors. Mol. Plant Pathol. **20**: 1196–1202.

Wang, L., Ma, K.B., Lu, Z.G., Ren, S.X., Jiang, H.R., Cui, J.W., Chen, G., Teng, N.J.,Lam, H.M., and Jin, B. (2020). Differential physiological, transcriptomic and metabolomic responses of Arabidopsis leaves under prolonged warming and heat shock. BMC Plant Biol.**20**: 1–15.

Yamaguchi, N., Winter, C.M., Wu, M.-F., Kwon, C.S., William, D.A., and Wagner, D. (2014).PROTOCOL: Chromatin Immunoprecipitation from Arabidopsis Tissues. Arab. B.**12**: e0170.

Yoo, S.D., Cho, Y.H., and Sheen, J. (2007). Arabidopsis mesophyll protoplasts: A versatile cell system for transient gene expression analysis. Nat. Protoc. **2**: 1565–1572.

Zhang, Y., Liu, T., Meyer, C.A., Eeckhoute, J., Johnson, D.S., Bernstein, B.E., Nussbaum, C., Myers, R.M., Brown, M., Li, W., and Shirley, X.S. (2008). Model-based analysis of **ChIP- Seq (MACS).** Genome Biol. **9**.

Zhu, L.J. (2013). Integrative analysis of ChIP-chip and ChIP-seq dataset. Methods Mol. Biol. **1087**: 105–124.

Zhu, L.J., Gazin, C., Lawson, N.D., Pagès, H., Lin, S.M., Lapointe, D.S., and Green, M.R.(2010). ChIPpeakAnno: A Bioconductor package to annotate ChIP-seq and ChIP-chip data. BMC Bioinformatics **11**.

Zorzatto, C. et al. (2015). NIK1-mediated translation suppression functions as a plant antiviral immunity mechanism. Nature **520**: 679–682.

Figure and legends

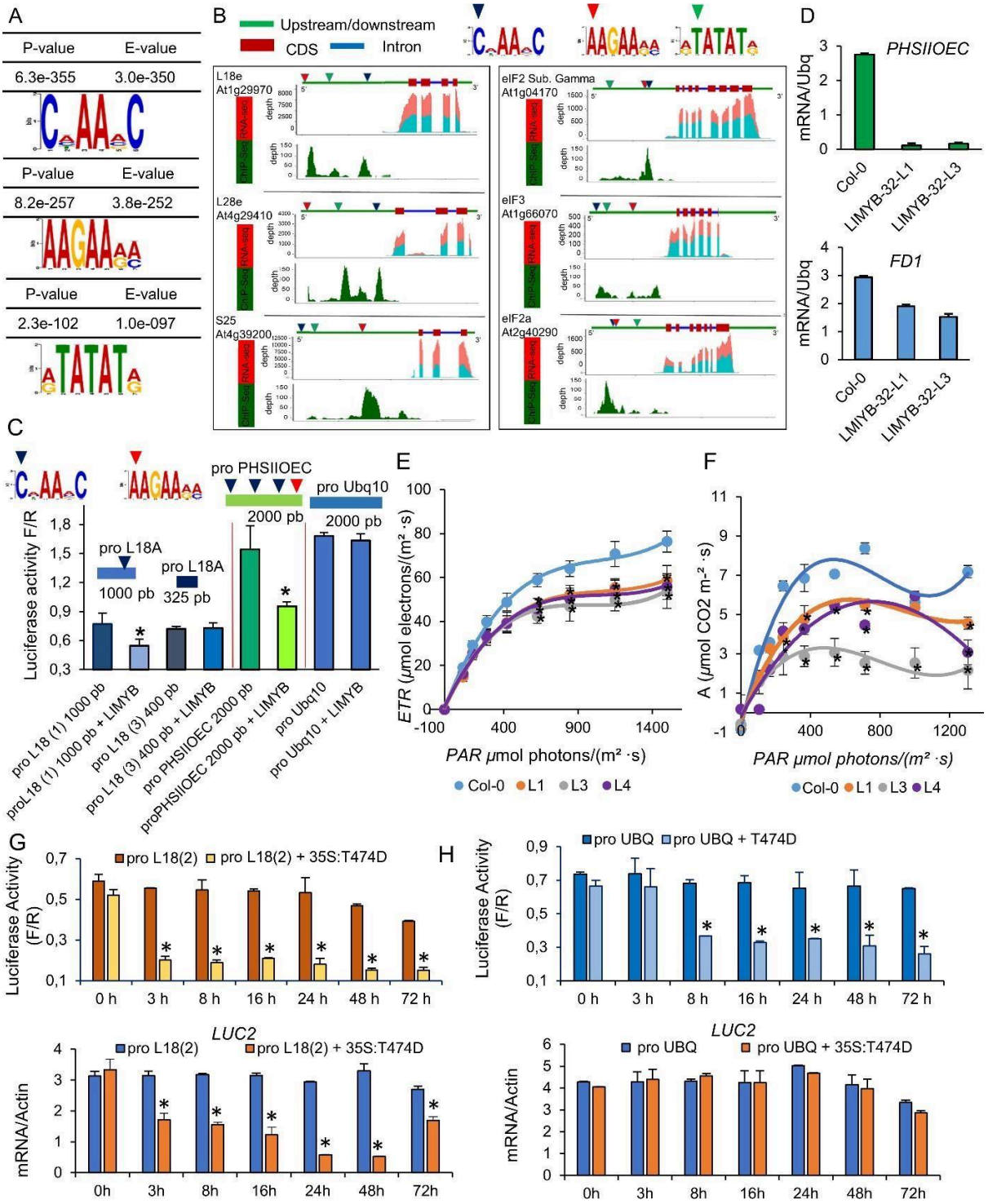

Figure 1. LIMYB represses the expression of photosynthetic apparatus-related genes and inhibits photosynthesis. **(A)** Top enriched motifs in the promoter region of LIMYB-regulated genes. **(B)** LIMYB DNA-binding motifs are strongly enriched in the promoter region of LIMYB down- regulated genes. In the schematic representation of the loci indicated in the Figure, upstream promoter sequences are green and coding regions red. ChIP-seq peaks map to the promoter region of the indicated LIMYB-repressed genes, whereas the RNA-seq hits lay inthe coding region. The relative expression of the indicated gene in Col-0 and LIMYB- overexpressing lines is shown by the abundance of RNA-

sequencing hits in blue (LIMYB) andred (Col-0). **(C)** LIMYB DNA- binding motifs function as cis-regulatory elements, and LIMYB represses the PSIIOEC promoter. *N. benthamiana* leaves were agroinfiltrated with plasmids carrying the promoter length (as indicated in the Figure) fused to luciferase and the 35S:LIMYB construct. After 48 h, luciferase activity was measured from total protein extracts of transformed leaves. An unrelated Ubiquitin promoter (UBQ) was used as a negative control. Results are mean values ±SD (n=6). Asterisks indicate significant differences from the control line (t-test, p<0,05). **(D)** *PHSII-OEC* (Photosystem II oxygen-evolving complex) and *FD1* (Ferredoxin) genes are repressed by LIMYB. The transcript levels of the indicated genes were quantified by RT-qPCR in *LIMYB*-overexpressing(LIMYB-32-1 and LIMYB-32-L3) lines and the wild-type (Col-0) line. Asterisks indicate significant differences from the control line (t- test, p<0,05). **(E)** Electron transport rate (ETR) in *LIMYB*-overexpressing lines LIMYB-32-L1, L3, and L4. PAR denotes Photosynthetically ActiveRadiation. **(F)** CO_2 assimilation rate (A) is inhibited in *LIMYB*-overexpressing lines. **(G)** The constitutively activated NIK1 mutant, T474, represses the activity of the RPL18 promoter. Arabidopsis protoplasts were transformed with the proL18: luciferase construct alone or combined with the 35S:T474 construct. Luciferase activity and transcript levels were determined at different time points. **(H)** T474 does not affect the activity of the UBQ unrelated promoter. Arabidopsis protoplasts were transformed with the proUBQ:luciferase construct alone or with the 35S:T474 construct. Luciferase activity and transcript levels were determined at different time points. For Gand H, the results are mean values ±SD (n=6). Asterisks indicate significant differences from the Control line (t-test, $p < 0.05$)

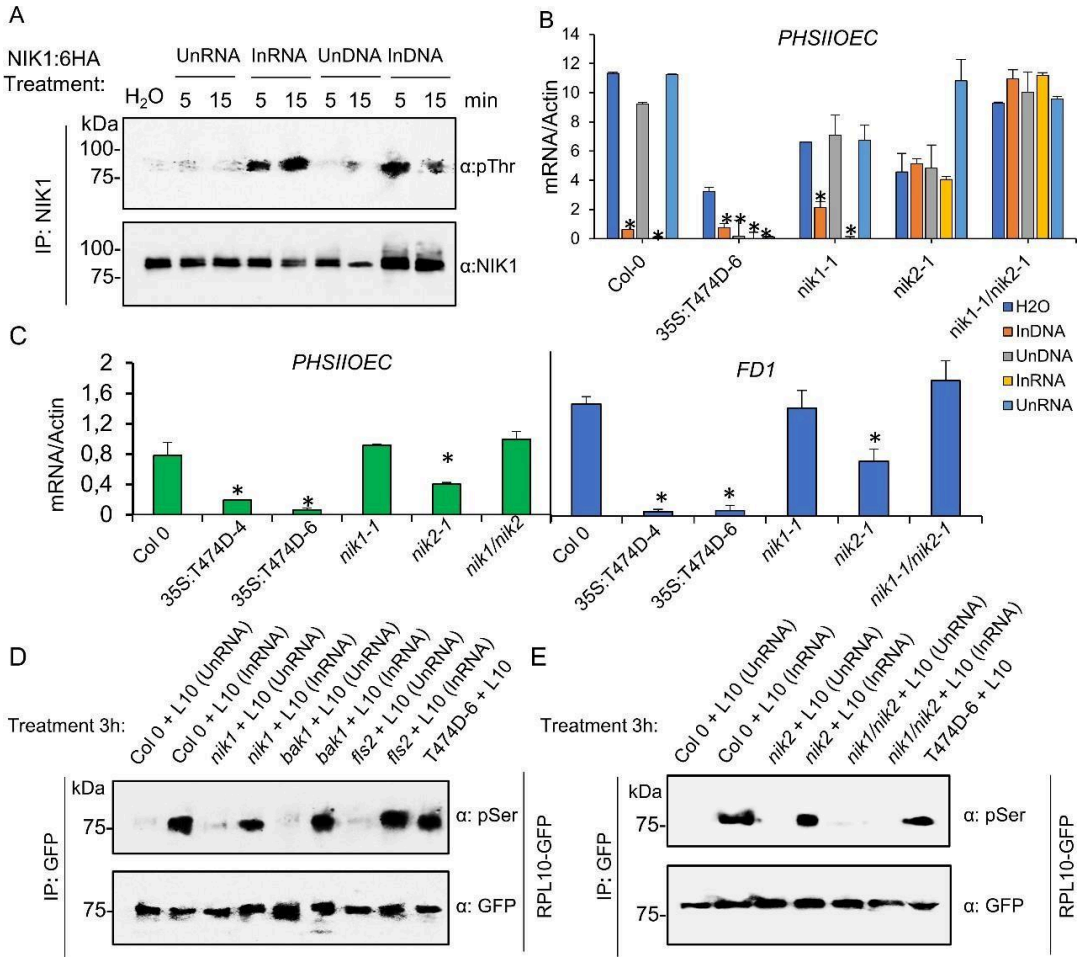

Figure 2. NIK1 activation by biotic signals represses the expression of photosynthetic apparatus-related genes. **(A)** NIK1 is rapidly phosphorylated by begomovirus-derived nuclei acids. Arabidopsis seedlings expressing NIK1-HA were treated with RNA or DNA prepared from mock-inoculated (UnRNA and UnDNA) or begomovirus-infected (InRNA and InDNA) plants for the time indicated in the Figure. NIK1 was immunoprecipitated with an α-NIK1 antibody and probed with an α-phosphoThreonine antibody. **(B)** Viral PAMPs require NIK1 and/or NIK2 to repress the expression of the *PHSII-OEC* gene. Leaf discs of the indicated genotypes were treated with InRNA and InDNA, and the PSII-OEC transcript levels were quantified by RT-qPCR. 35S:T474D-6 is a transgenic line that expresses the T474D NIK1 mutant. The bars represent a 95% confidence interval based on three replicates from independent experiments. Asterisks denote statistically significant differences to the control line. **(C)** Constitutive activation of NIK1 in T474D- expressing (T474D-4 and T474D-6) lines down-regulates *PHSII-OEC* and *Fd1*. Total RNA from the indicated genotypes and the transcript levels of the indicated genes were quantified by RT-qPCR. The bars represent a 95% confidence interval based on three replicates from independent experiments. Asterisks denote statistically significant differences to the control line. **(D)** Viral PAMPs not require FLS2 and BAK1, **(E)** but NIK1/NIK2 to mediate RPL10 phosphorylation. Arabidopsis protoplasts prepared from the indicated genotypes were transformed with35S:RPL10-GFP. After 12 h for RPL10-GFP expression, the protoplasts were treated with RNA prepared from mock-inoculated (UnRNA) or begomovirus-infected (InRNA) plants. Immunoprecipitated RPL10-GFP by an α- GFP antibody was probed with an α-phosphoserine antibody. T474D-6 line was used as a positive control.

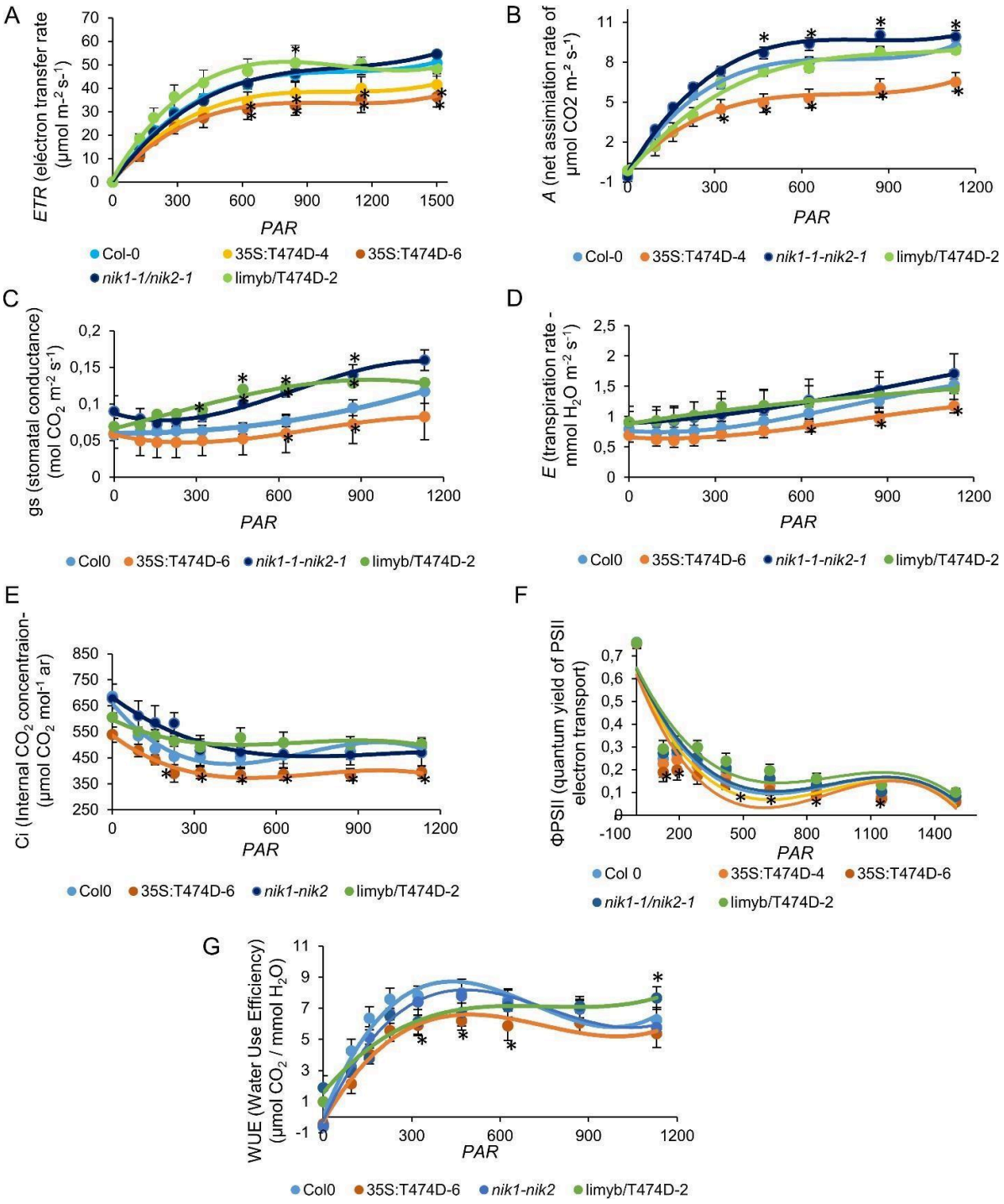

Figure 3. The LIMYB-mediated inhibition of photosynthesis depends on NIK1 activation. Leafgas exchange parameters, including net CO_2 assimilation rate (A), stomatal conductance (gs), transpiration rate (E), the internal concentration of CO_2 (Ci), water-use efficiency (WUE) and photochemical processes, including electron transport rate (ETR), quantum efficiency, and were measured in expanded leaves from 30-days-old plants from the indicated genotypes. Asterisks indicate significant differences from the control line (t-test, $p<0.05$)

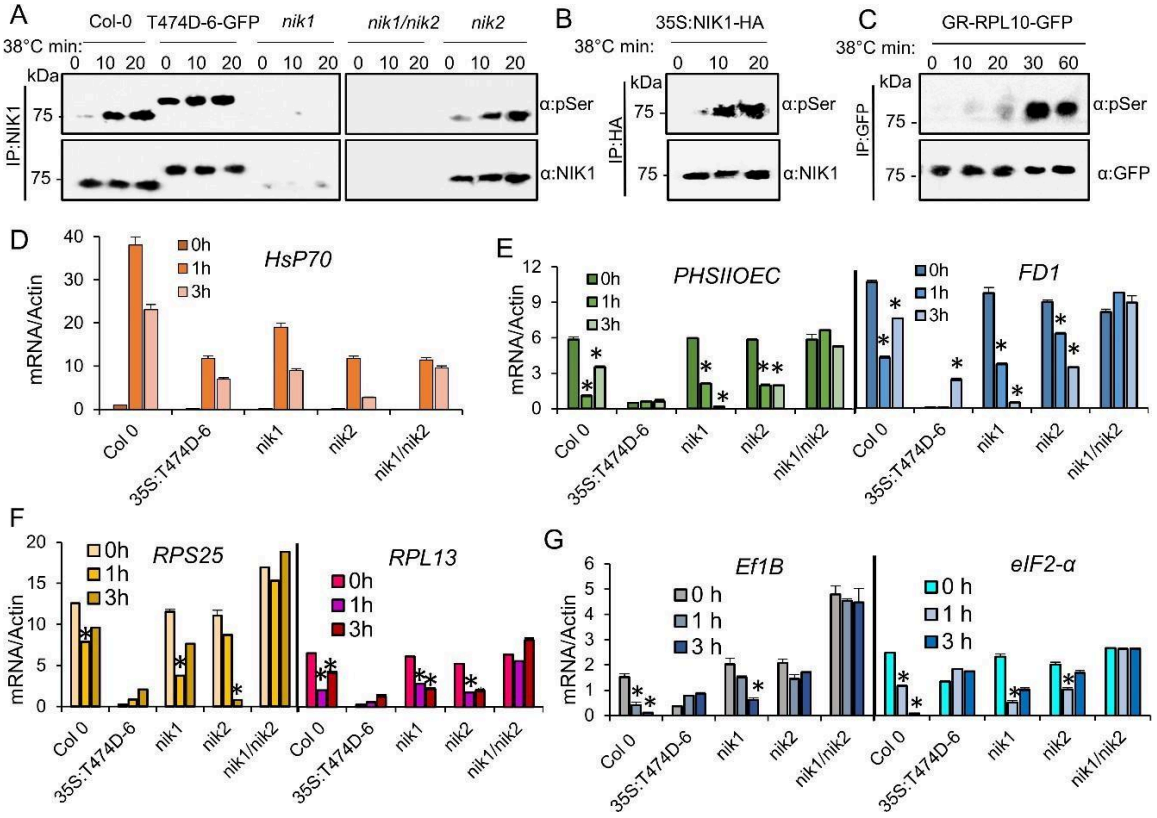

Figure 4. High temperature activates NIK1 antiviral signaling. **(A)** Rapid NIK1 phosphorylation in response to heat stress. Twenty-eight days-old plants were subjected to 38°Cfor 0 to 3h. Protein extracts were prepared at different intervals after the heat treatment. NIK1 was immunoprecipitated with an α-NIK antibody and probed with an α-phosphoserine antibody to monitor phosphorylation (top panel) and with α-NIK antibody to visualize the immunoprecipitatedNIK1 (bottom panel). A T474D-expressing line was used as a positive control. **(B)** NIK1-HA is correctly phosphorylated in response to heat. NIK1-HA expressing lines were subjected to the heat stress as in A. Phosphorylation was monitored as in A except that NIK1-HA was immunoprecipitated with α-HA antibody and probed with an α-pSer antibody (top panel) and an α-NIK1 antibody (bottom panel). **(C)** Heat stress mediates RPL10 phosphorylation 30 min after the treatment. RPL10-GFP-overexpressing lines were subjected to the heat treatment, and phosphorylation of RPL10-GFP was monitored by probing immunoprecipitated RPL10 with an α- pSer antibody (top panel). The immunoprecipitated RPL10-GFP was also probed with an α-GFP antibody (bottom panel). **(D)** The heat stress was effective for all genotypes examined. The induction of the heat-associated marker gene, HSP70,was examined by RT-qPCR after 1h and 3hof the treatment. **(E)** Heat stress represses the photosynthetic apparatus genes PSII-OEC and FD1in a nik1nik2 dependent manner. Plants of each genotype were subjected to heat treatment for 1h and 3h, and the expression of the indicated genes was analyzed by RT-qPCR. Data are shown as the mean ± SE (n=3). Asterisks indicate statistically significant differences to the untreated sample(test t, P<0.05). **(F)** High temperature suppresses ribosomal protein gene expression. RT-qPCR analysis of RB expression levels after heat stress. Data are shown as the mean ± SE (n=3). Asterisks indicate statistically significant differences to the untreated sample (test t, P<0.05). **(G)** Heat stress represses the expression of translational regulation-associated genes. The expression of translation initiation and elongation factor-encoding genes, *Ef1β* and *eIF2-α,* was examined by RT-qPCR, 1h, and 3h post-treatment. Data are shown as the mean ± SE (*n=3*). Asterisks indicate statistically significant differences to the untreated sample (test t, $p < 0.05$).

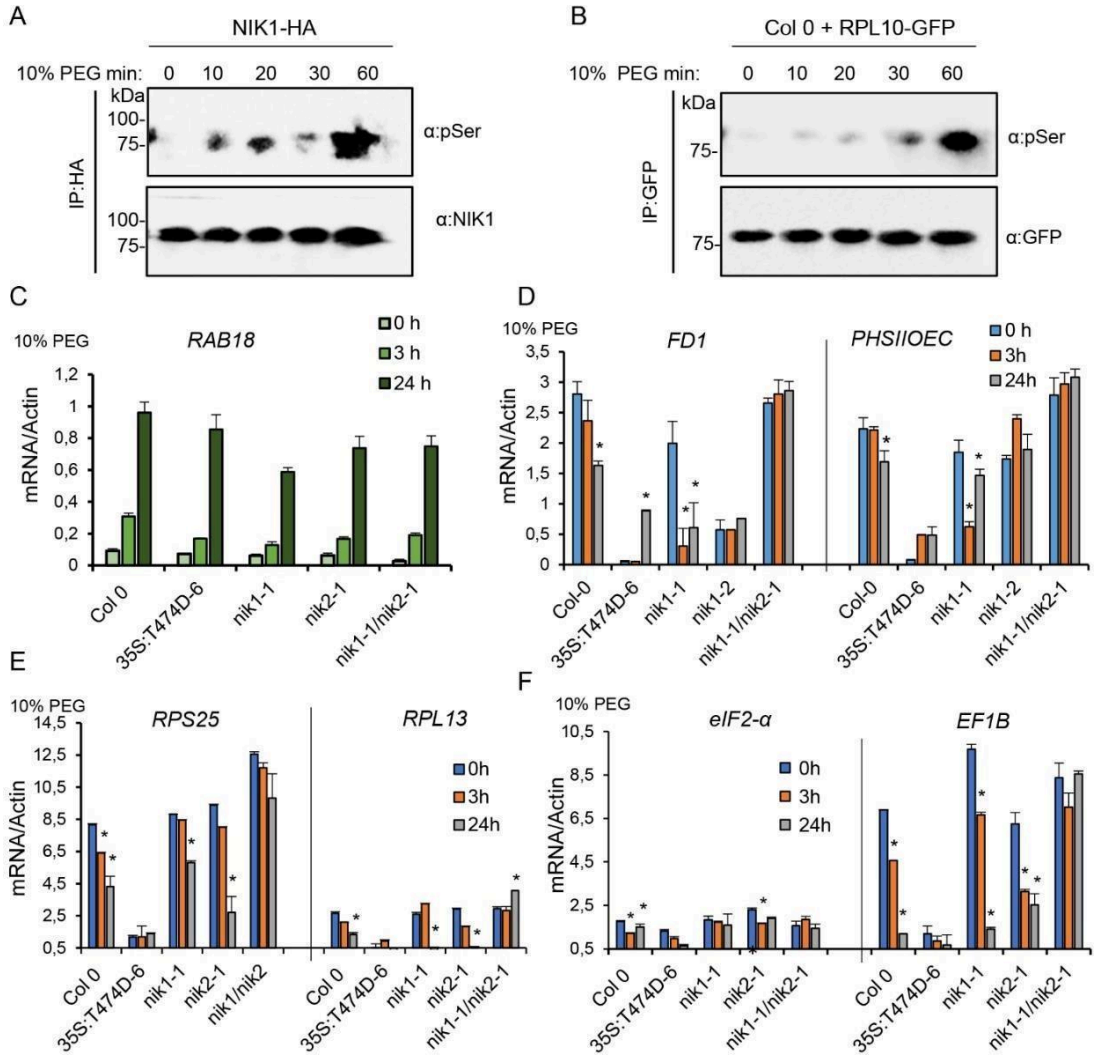

Figure 5. The osmotic signal triggers the NIK1 antiviral signaling. **(A)** NIK1 is phosphorylated by osmotic stress. Arabidopsis seedlings expressing NIK1-HA were treated with 10% PEG for the intervals indicated in the Figure. NIK1 phosphorylation was monitored by probing immunoprecipitated NIK1-HA with an α-pSer antibody (top panel). An α-NIK1 antibody (bottom panel) was used to visualize the immunoprecipitated NIK1-HA. **(B)** Osmotic stress induces RPL10 phosphorylation. Osmotic stress was induced in Arabidopsis seedlings expressing RPL10-GFP by PEG treatment, and then RPL10 phosphorylation was monitored by immunoblotting immunoprecipitated RPL10-GFP (bottom panel) with an α-pSer antibody (top panel). **(C)** Induction of osmotic stress by PEG treatment in all genotypes examined. The expression of the osmotic stress-associated marker gene *RAB18* was examined by RT-qPCR 3h and 24h post- treatment. **(D)** Osmotic stress suppresses the photosynthetic genes *PHSII-OEC* and *FD1* in Col-0 but not in *nik1nik2* double knockouts. Transcript accumulation of *PHSII-OEC* and *FD1* was determined by RT-qPCR 3h and 24h after PEG treatment. The T474D-overexpressing line was used as a positive control. **(E)** Osmotic stress repression of ribosomal protein genes requires the function of NIK1 and/or NIK2. Expression of *RPS25* and *RPL13* was quantified by RT-qPCR 3h and 24h after PEG treatment in the indicated genotypes. **(F)** Osmotic stress suppresses translation regulation-associated genes. Expression of *eIF2-α* and *EF1B* was quantified by RT-qPCR 3h and 24h after PEG treatment in the indicated genotypes. For C, D, E, F, data are shown as the mean ± SE ($n=3$). Asterisks indicate statistically significant differences to the untreated sample (test t, $P<0.05$)

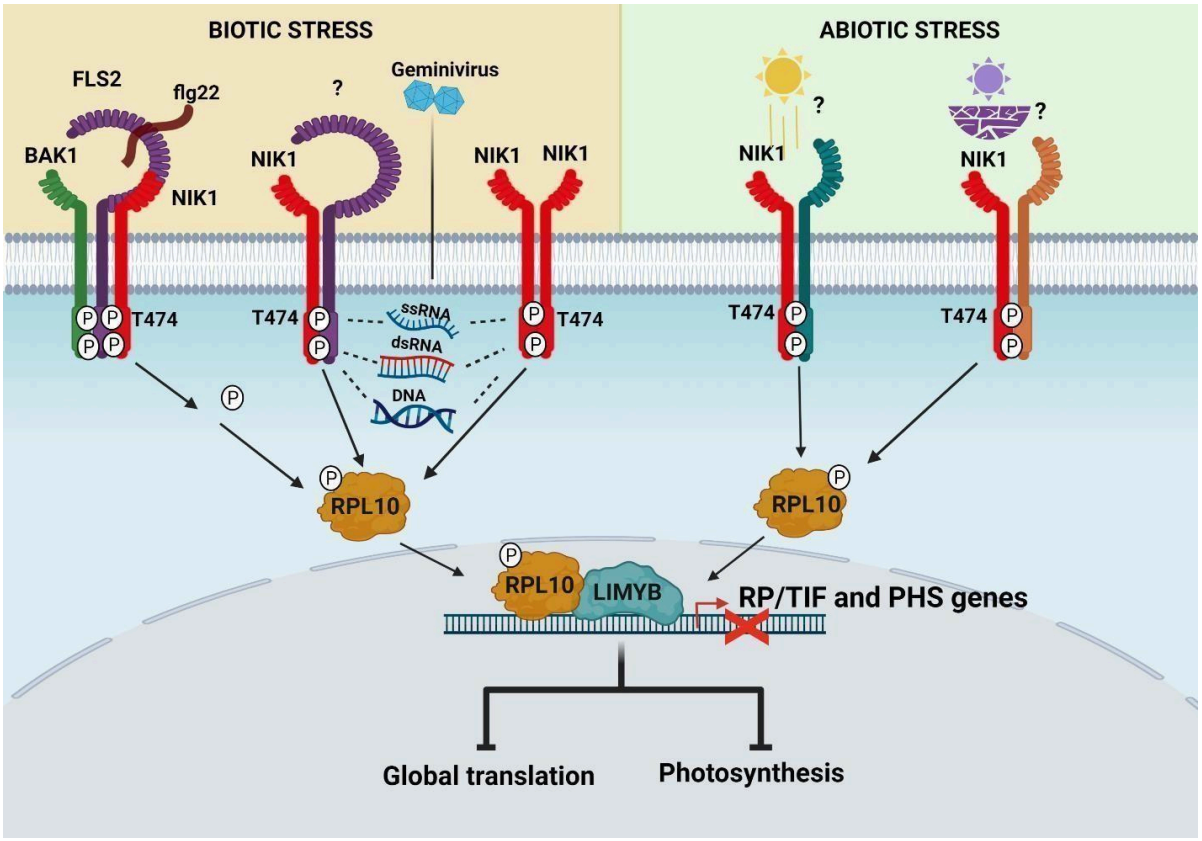

Figure 6. Multiple abiotic and biotic stimuli activate the NIK1/RPL10/LIMY signaling circuit,which regulates coordinately translation and photosynthesis in plant cells. NIK1 has also beenrevealed to interact with different LRR-RLK forming a hub with high centrality. NIK1 transduces different abiotic and biotic signals by relaying information from different stress- sensing receptors. The perception of PAMP flg22, but not viral PAMP needs of the immune complex FLS2-BAK1 for mediating NIK1 phosphorylation and activation. Most likely, a yet to be determined viral pattern recognition receptor, or the interaction of NIK1 with itself, can detect viral PAMPs of nuclei acids to mediate NIK1 activation in response to viral infection. Similarly, NIK1 along with other receptors is activated in the perception of abiotic signals, heatstress and biotics as shown here.NIK1 is propose as a central signaling hub that integrates signals from multiple stress-sensing receptors to control growth under stress conditions. This figure was created with Biorender.com

Table 1- Primers used in Materials and methods

Primers used in methods		
Primers for RT-qPCR		
	Fwd Primer	Rvs Primer
qRT- At2G21580 RPS25B	CCGATCGTTACTCCGTCGAA	AGATTTGGCCGGCTTTGAT
qRT- At3G07110 RPL13A	GGCTGATCCAGAGCTGAGTG AAA	GTGGTGACGAGCATCAACCA
qRT-Ef1B	GTGGTACGATTCTGTTGCT	CAGTATGTGGATGAGCTTCAG
qRT-eIF2α	CTGCTCCGAATCTAGAATGTC	ATACGTAAGCTCCCATGTCA
RT-qPCR Luci. Fire	GCGAAGGTTGTGGATCTGGA	CGTCTTCGTCCCAGTAAGCT
RT-qPCR Actina	ATGTCGTGAGCCATCCTGTC	ACACCGGATTCGTGCGGCAT
qRT-FD1	CAATCTCTCTTCGGCCTC	GTCGAGGACGTAGACATCT
qRT-PSIIOEC 1	AGCTTATCAACGCAGAGAA	TTGTTGTCCTAATCCTGCT
qRT-Hsp70	GGCTGAGGCAGATGAGTTC	GTGTCGTCATCCATTCCTC
qRT-RAB18	ACGAGTACGGAAATCCGATG	ACCACCACTTTCCTTGTGGA
Primers for cloning of gene		
LIMYB At5g05800B	AAAAAGCAGGCTTCACAATG AGGCCAAAAGCAGT	AGAAAGCTGGGTCCTATGTTGT AGTAGGAATAGG
Primers for cloning of promoters		
pRL18-TGW-FWD(1)	GGGGACAACTTTGTATAGAA AAGTTGTCGGAAGATGAGTAT ACGTAAATA	GGGGACTGCTTTTTTGTACAAA CTTGCAATTGAGATCCGATTAA CCTAA
pRL18-TGW-FWD(2)	GGGGACAACTTTGTATAGAA AAGTTGTCGTGTACCAGTAAA ATGTTGTTG	
pRL18-TGW-FWD(3)	GGGGACAACTTTGTATAGAA AAGTTGTCGACCATAATCATA TTCATTGAAGTG	
PSIIOEC-TGW-FWD(1)	GGGGACAACTTTGTATAGAA AAGTTGTCGTCCCCTCCAATT CTGACA	GGGGACTGCTTTTTTGTACAAA CTTGCTGCTTCTTTCTCCTTATC AAC
FD1 TGW-FWD(1)	GGGGACAACTTTGTATAGAA AAGTTGTCGGACCCCTCCAGT GTTAC	GGGGACTGCTTTTTTGTACAAA CTTGCTGTTGAAAGATGATTCT ACAGA

Supplementary Material

Supplementary figure

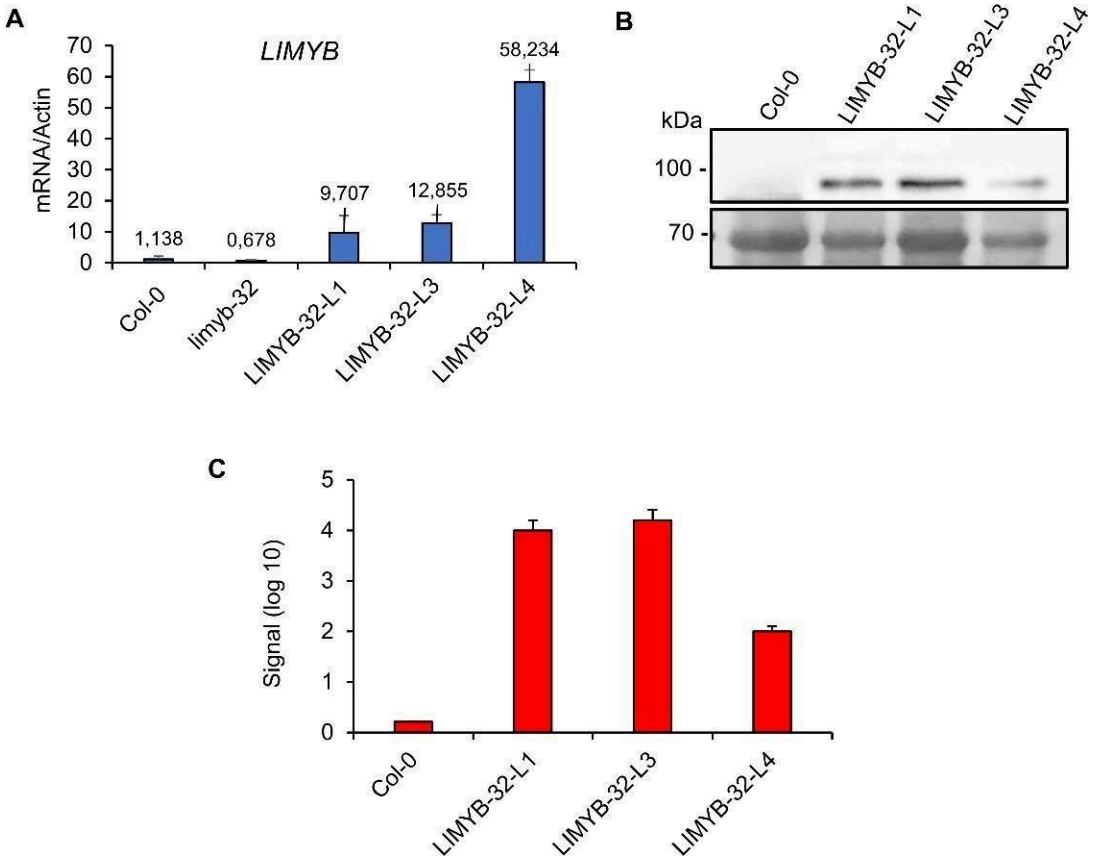

Figure S1. Accumulation of YFP-LIMYB in transgenic lines. (**A**) Accumulation of YFP-LIMYB transcripts in the transgenic lines LIMYB-32-L1, L3, and L4. Gene expression was analyzed by RT-qPCR. Absolute expression was calculated using the $2^{-\Delta Ct}$ method and actin as an endogenous control. The bars represent 95% confidence interval based on replicates from 3 independent experiment samples. (**B**) Accumulation of recombinant protein YFP-LIMYB in LIMYB-32-L1, LIMYB-32-L3, and LIMYB-32-L4. Total protein extracted from the transgenic lines was separated by electrophoresis, transferred to membranes, and probed with polyclonal α-GFP antibody. (**C**) Quantification of YFP- LIMYB protein level in LIMYB-32- L1, L3, and L4. Bands were quantified using the Quantity One BioRad program.

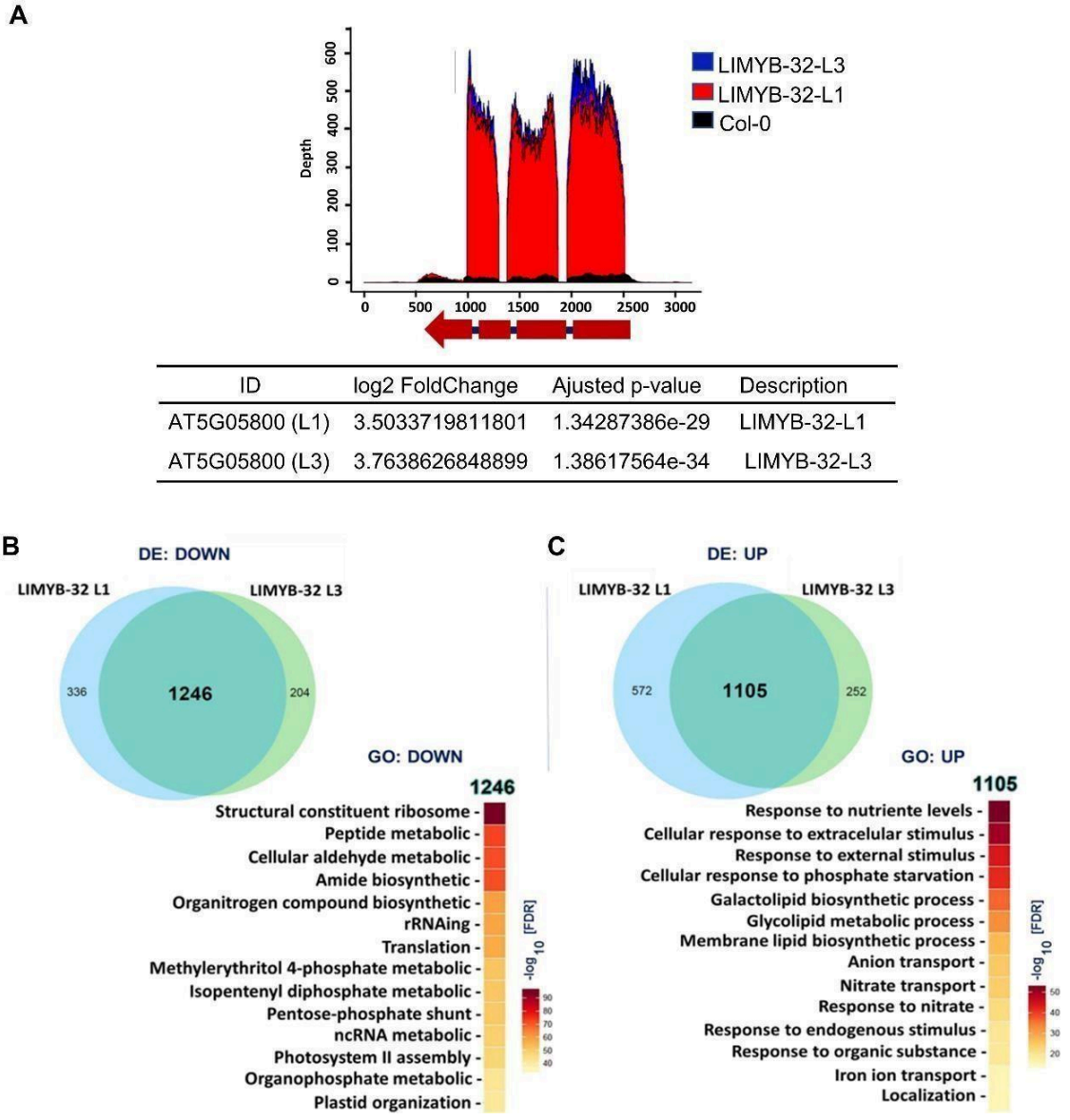

ID	log2 FoldChange	Ajusted p-value	Description
AT5G05800 (L1)	3.5033719811801	1.34287386e-29	LIMYB-32-L1
AT5G05800 (L3)	3.7638626848899	1.38617564e-34	LIMYB-32-L3

Figure S2. Induced transcriptome by LIMYB overexpression. (**A**) Schematic representation of the LIMYB Locus (At5g05800) with the RNA sequencing hits. The gene contains three intronsand four exons. The relative abundance of RNA hits at the At5g05800 locus is shown in black for Col-0, red for L1, and blue for L3. (**B**) Venn diagram depicting the overlap between down-regulated genes in LIMYB-32-L1 and LIMYB-32-L3. Significantly enriched GO terms (false discovery rate, FDR of - log 10) derived from genes that were downregulated in both LIMYB- 32-L1 and LIMYB-32-L3 lines compared to Col-0. (**C**) Venn diagram indicating the overlap between up-regulated genes in LIMYB-32-L1 and LIMYB-32-L3. Heat map of gene ontology(GO), representing the distribution of functional categories of commonly up-regulated genes; DE analyses of GO used an FDR value of - log 10.

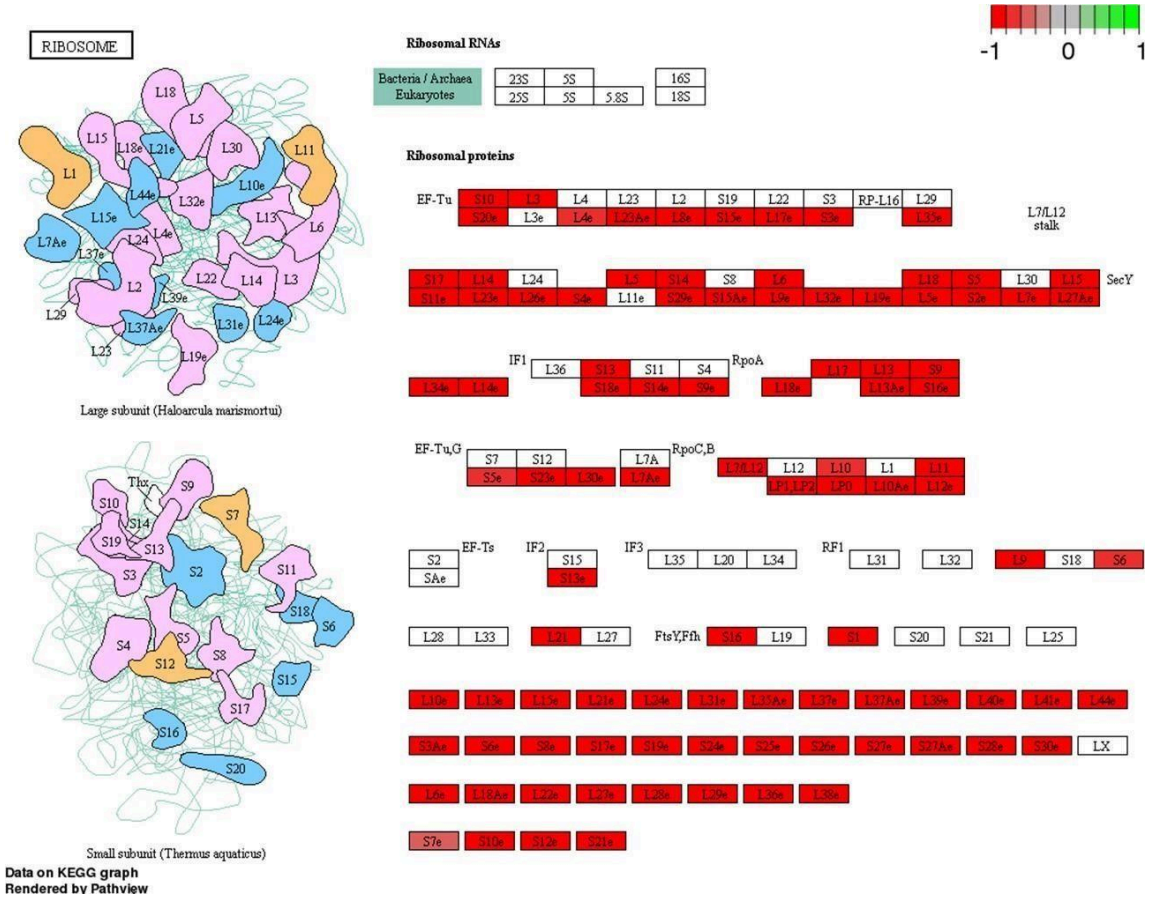

Figure S3. LIMYB overexpression down-regulates ribosomal protein genes. The differential expression analysis is represented via KEGG, demonstrating that the ribosomal protein gene network predominates in the down-regulated changes by LIMYB.

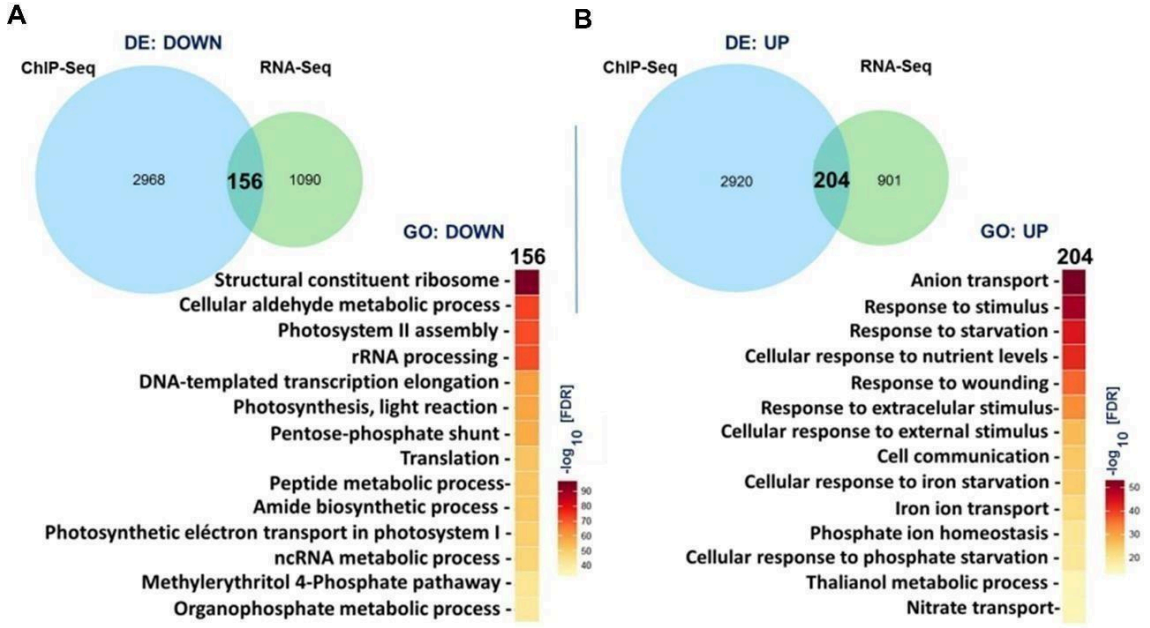

Figure S4. Integrative analysis between ChIP-seq and RNA-seq on LIMYB- overexpressing lines defines the LIMYB regulon. (A) Venn diagram indicating the overlap between down-regulated genes by LIMYB (RNA-seq) and LIMYB target genes (ChIP-seq). Heat map of significantly enriched GO terms (false discovery rate, FDR of - log 10) derived from the LIMYB down-regulon (B) Venn diagram indicating the overlap between up-regulated genes by LIMYB (RNA-seq) and LIMYB target genes (ChIP-seq). Heat map of significantly enriched GO terms (false discovery rate, FDR of - log 10) derived from the LIMYB up-regulon.

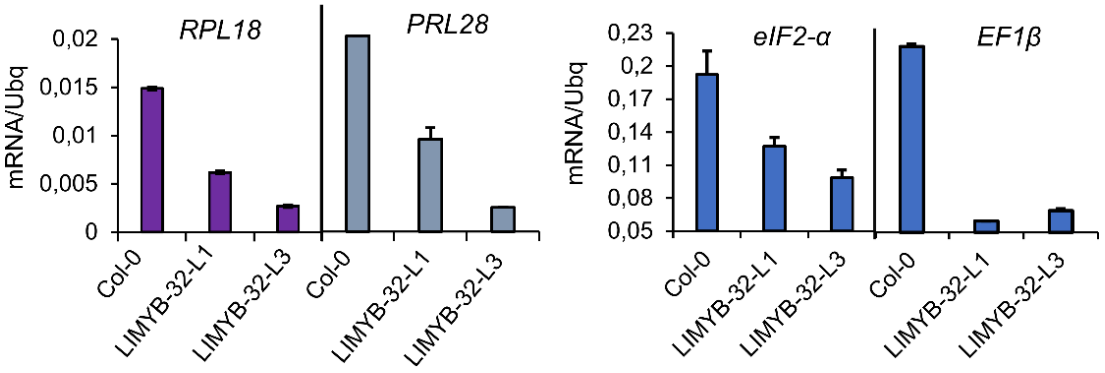

Figure S5. LIMYB overexpression represses the expression of ribosomal protein genes and translation initiation and elongation factor-encoding genes. Gene expression was determined by RT–qPCR of mRNA from LIMYB-overexpressing and Col-0 seedling. Values represent themean ± SD of five biological replicates.

A

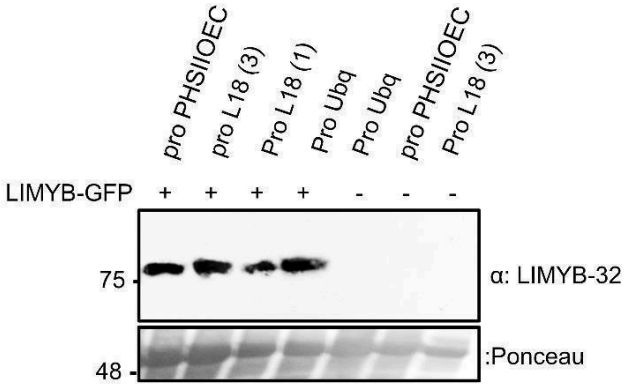

B

ChIPSeq/RNASeq

Id gene	Upstream	log2FC	Log10 q-value	padj
proL18Ae	- 455	- 0.62	28.30	5.5e-15
proPHSIIOEC	- 1574	-1.67	15.14	4.1e-19

Figure S6. *LIMYB* expression in *N. benthamian* leaves for the promoter transactivation assay. LIMYB protein expression was detected by immunoblotting protein extracts from agroinfiltrated leaves using an α-GFP antibody. (**B**) Upstream position of LIMYB motifs and level expression detected by ChIP-seq and RNA-seq, respectively.

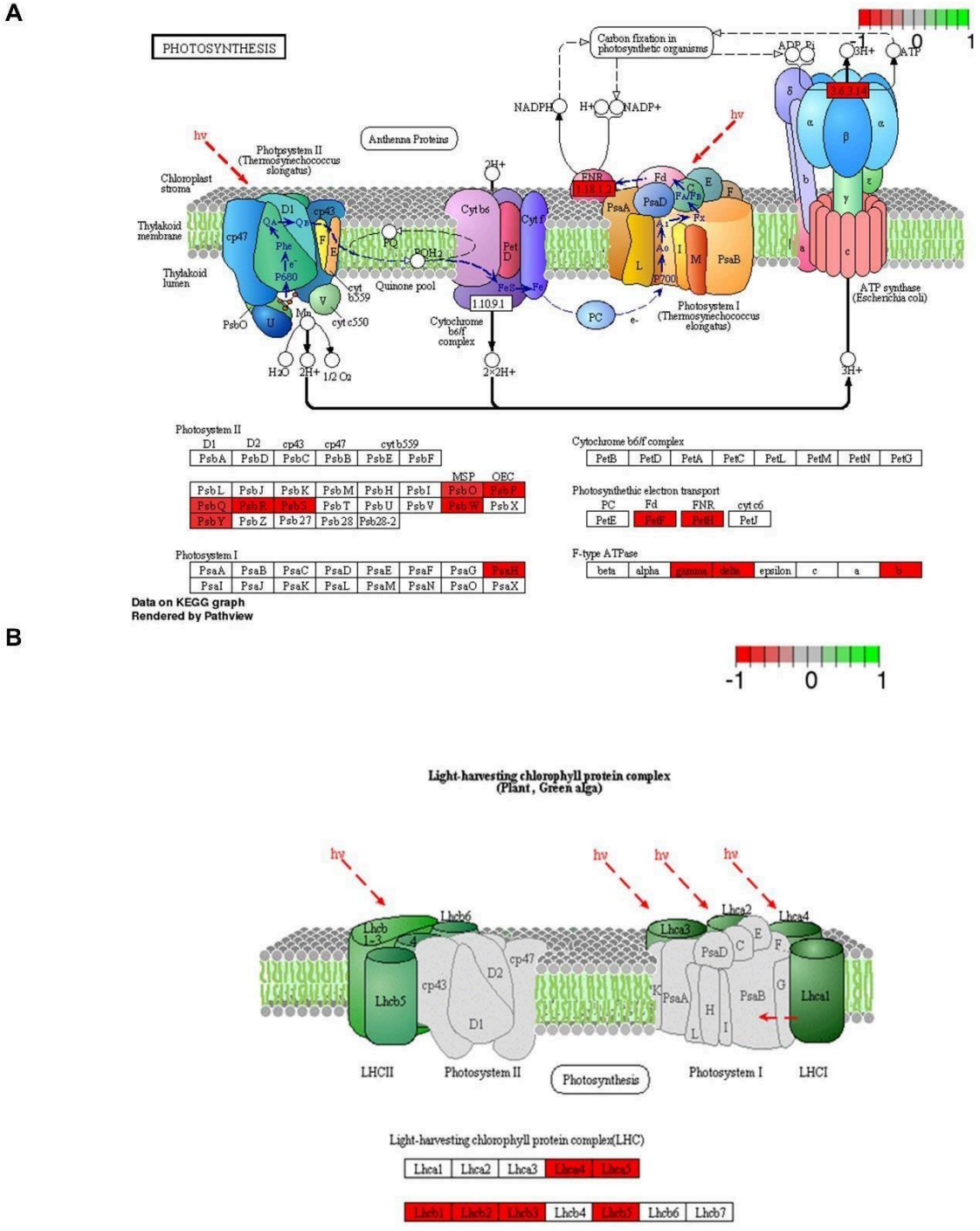

Figure S7. Representation of photosynthetic apparatus-related genes in the LIMYB down-regulon. (**A**) Significant repression of subunits of PSII, PSI, and ATPsintase. (**B**) Expression of light-collecting complex (LHC I and LHC II). Differential expression analysis demonstrates that LIMYB regulates the expression of proteins related to the assembly of photosynthetic complexes.

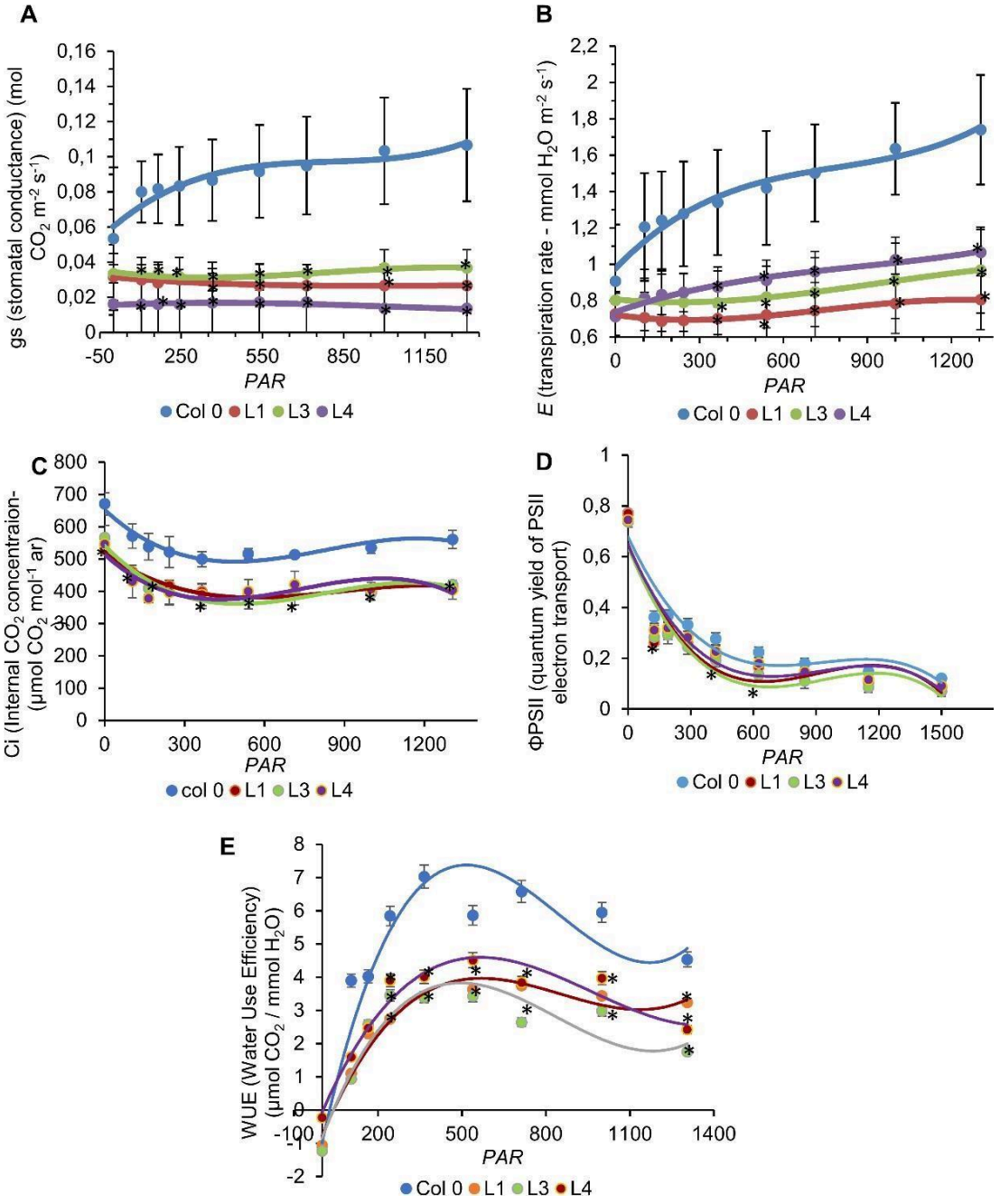

Figure S8. LIMYB affects the photosynthetic activity in plants. (**A**) stomatal conductance(**gs**), transpiration rate (E), (**C**) internal concentration of CO_2 (Ci), (**D**) the quantum efficiency of yield (ΦPII), and (**E**) the use of water efficiency (WUE), in LIMYB-overexpressing lines and Col-0. Data are mean values ±SD (*n=6*). Col-0, Columbia. L1, LIMYB-32-L1. L3, LIMYB- 32-L3. L4, LIMYB-32-L4.

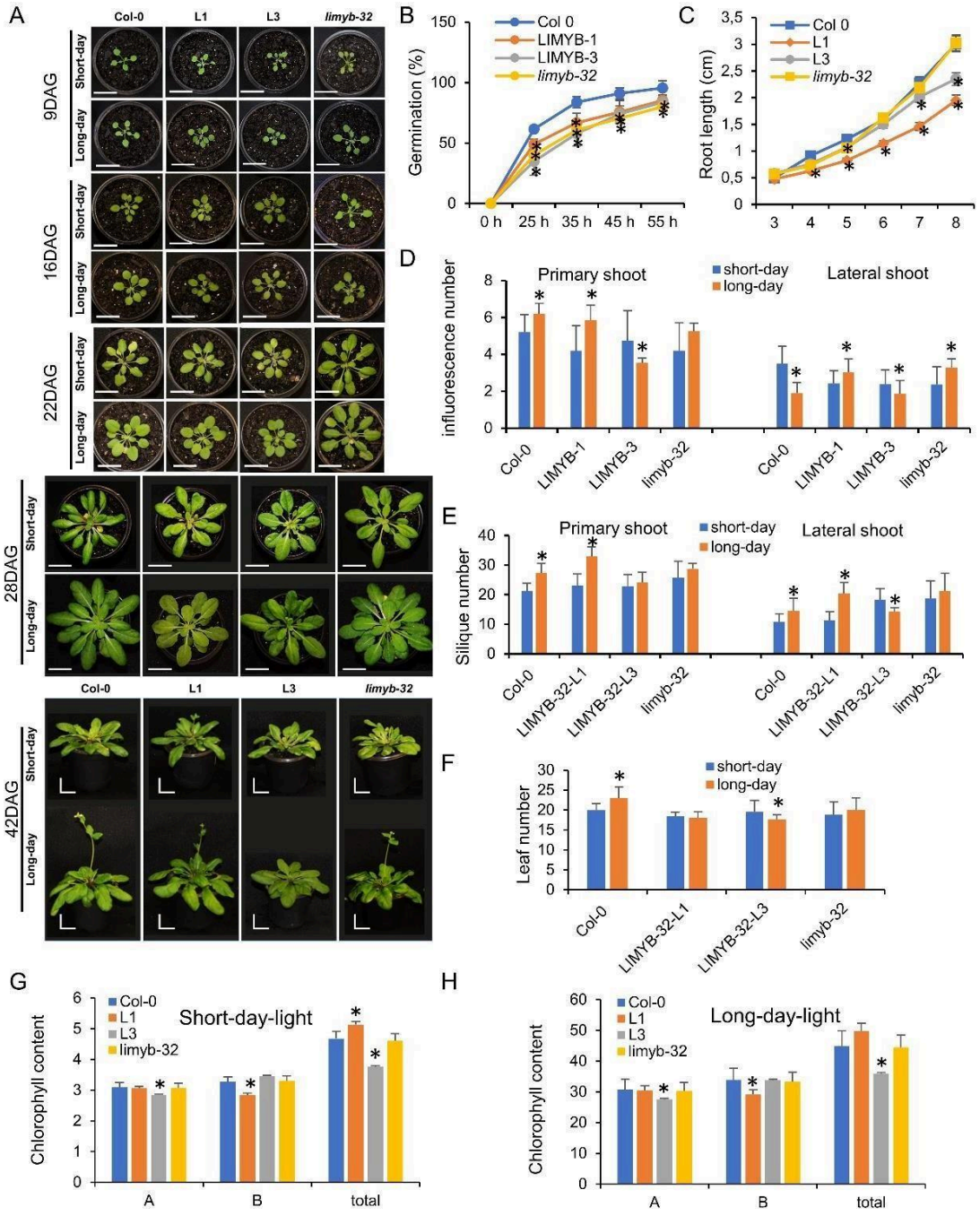

Figure S9. LIMYB overexpression affects growth and development. (**A**) The growth phenotypes of transgenic lines during the vegetative and reproductive phases were recorded from 9 to 48 days after germination under short-day and long-day photoperiods. Seed germination (**B**), root length (**C**), inflorescences number (**D**), silique number (**E**), the number of leaves (**F**), Chlorophyll content in short-day (**G**) and long-day (**H**) photoperiod were determinedin LIMYB overexpressing lines and *limyb* knockout line in comparison with Col-0. Statistical analysis was performed using a Student's t-test ($p < 0.05$). Asterisks denote significantdifferences from the control.

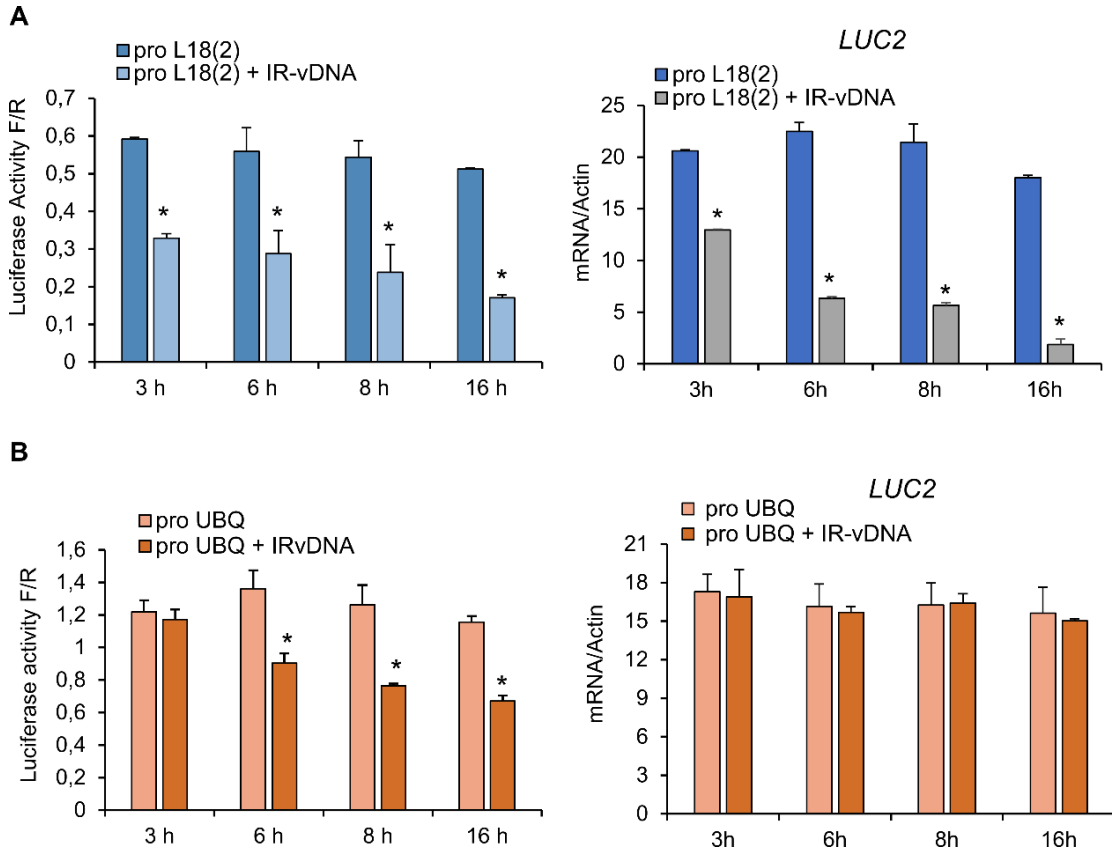

Figure S10. Protein synthesis inhibition by LIMYB is a late response. Protoplasts co-transformed with 35S:LIMYB-GFP + proL18(2) –Luciferase (proL18(2)) or proUBQ-Luciferase (proUBQ) were treated with a viral PAMP (IR-vDNA; intergenic Region from Component B of Begomovirus), and luciferase activity and mRNA accumulation were measured in the intervals of 3, 6, 8 and 16 h. (**A**) Time course of LIMYB-controlled luciferase activity and mRNA accumulation under the control of RPL18 promoter. F/R, firefly luciferase activity to Renilla activity ratio. (**B**) LIMYB does not target the UBQ promoter but represses luciferase activity as a late response. Progression time of luciferase activity and mRNA accumulation of the UBQ promoter after LIMYB expression. Three independent replicates were used. Asterisks indicate statistically significant differences to the control by the test-t ($p < 0.05$)

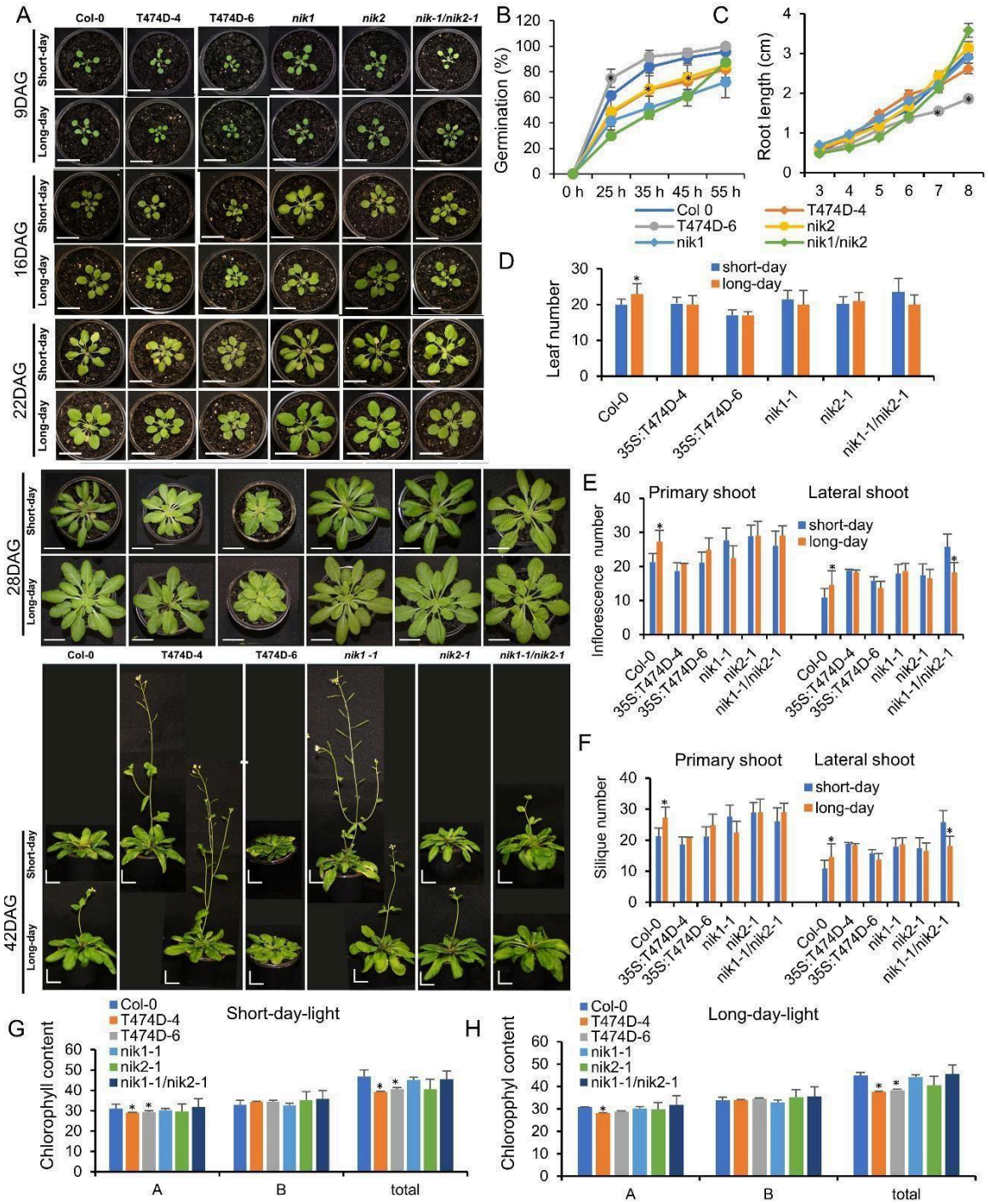

Figure S11. Activation of NIK1 antiviral signaling affects growth and development. (**A**)The growth phenotypes of T474D-expressing lines, nik1, nik2, and nik1nik2 knockout lines and Col-0 during the vegetative and reproductive phases were recorded from 9 to 48 days after germination under short-day and long-day photoperiods. Seed germination (**B**), root length (**C**),leaves number (**D**), inflorescences number (**E**), silique number (**F**), Chlorophyll content in short-day (**G**), and long-day (**H**) photoperiod were determined inT474D-expressing lines in comparison with Col-0. Statistical analysis was performed using a Student's t-test ($P < 0.05$). Asterisks indicate significant differences from the control

Supplementary Table

Table S1. Categories down regulated under LIMYB overexpression, by integrative analysis RNA-seq/ChIP-seq.

Down regulated GO_ID	Pvalue	Odds Ratio	Exp Count	Count	Size	Term
GO:0003735	0.000	17.270	22	187	398	structural constituent of ribosome
GO:0006081	0.000	6.955	19	95	339	cellular aldehyde metabolic process
GO:0010207	0.000	6.512	2	12	177	photosystem II assembly
GO:0006364	0.000	6.907	3	18	256	rRNA processing
GO:0006354	0.000	4.981	7	30	133	DNA-templated transcription, Elongation
GO:0019684	0.002	4.293	2	7	156	photosynthesis, light reaction
GO:0006098	0.000	4.673	2	10	200	pentose-phosphate shunt
GO:0006412	0.000	4.761	6	25	526	Translation
GO:0006518	0.000	5,298	7	31	566	peptide metabolic process
GO:0043604	0.000	5	7	30	578	amide biosynthetic process
GO:0009773	0.000	22.606	3	29	51	photosynthetic electron transporting PHS I
GO:0034660	0.000	6.546	23	110	413	ncRNA metabolic process
GO:0019288	0.005	3.186	3	8	229	methylerythritol 4-phosphate pathway
GO:0046490	0.006	3.129	3	8	233	isopentenyl diphosphate metabolic process
GO:0090407	0.003	1.684	24	38	446	Organophosphate biosynthetic process

Table S2. Categories up regulated under LIMYB overexpression, by integrative analysis RNA-seq/ChIP-seq.

Up regulated GO_ID	Pvalue	Odds Ratio	Exp Count	Count	Size	Term
GO:0006820	0.00	4.271	32	110	619	anion transport
GO:0050896	0.00	1.895	74	126	1814	Response to stimulus
GO:0042594	0.00	9.613	16	100	306	response to starvation
GO:0031669	0.00	9.878	16	103	310	Cellular response to nutrient levels
GO:0009611	0.00	2.845	17	44	335	response to wounding
GO:0009991	0.00	8.089	19	105	363	response to extracellular stimulus
GO:0071496	0.00	8.795	18	107	349	cellular response to external stimulus
GO:0007154	0.00	6.558	21	102	439	cell communication

GO:0010106	0.00	6851	6	31	116	cellular response to iron ion starvation
GO:0006826	0.00	5.413	1	6	99	iron ion transport
GO:0030643	0.00	3.412	5	7	362	phosphate ion homeostasis
GO:0016036	0.00	2.657	3	7	124	cellular response to phosphate starvation
GO:0080003	0.00	5.897	2	3	3	thalianol metabolic process
GO:0010167	0.00	6.295	10	49	197	response to nitrate
GO:0015706	0.00	6.564	11	53	207	nitrate transport

Table S3. Ribosomal protein and translation-associated genes under LIMYB overexpressionwere downregulates in integrative analysis RNA-seq/ChIP-seq.

Gene_id	width	Fold enrich	log10 q-value	Distance to feature	log2 FC	padj	Description
AT1G09690	185	4.13	10.52	-152	-0.77	0.00	Translation protein SH3-like family protein
AT1G22780	173	4.74	13.92	-867	-1.65	0.00	Ribosomal proteinS13/S18 Family
AT1G74060	371	6.04	23.03	-79	-0.33	0.03	Ribosomal protein L6family protein
AT2G27530	184	5.23	16.85	-144	-1.40	0.00	Ribosomal protein L1p/L10e family E
AT2G34480	222	6.93	28.30	-1334	-0.55	0.00	Ribosomalprotein L18ae/LX family protein
AT2G36620	184	4.62	13.22	-1250	-1.26	0.00	ribosomal protein L24RPL24A
AT2G37270	271	7.79	36.16	-75	-0.69	0.00	ribosomal protein 5B
AT3G07110	172	5.11	16.10	-350	-1.16	0.00	Ribosomal protein L13family protein
AT3G09200	188	4.27	15.26	-75	-0.66	0.00	Ribosomal protein L10family protein
AT3G25520	173	5.84	20.74	-455	-1.18	0.00	ribosomal protein L5
AT3G27830	212	6.69	26.56	-220	-1.15	0.00	ribosomal protein L12-A
AT3G44590	279	9.70	54.85	-1091	-1.69	0.00	60S acidic ribosomal protein family
AT3G53890	201	5.71	19.94	-340	-1.68	0.00	Ribosomal protein S21e
AT3G55280	184	5.18	19.86	-1065	-0.72	0.00	60S ribosomal proteinL23(RPL23 aB)
AT4G13170	237	7.05	29.18	-595	-1.56	0.00	Ribosomal protein L13family protein
AT4G31985	193	6.80	29.21	-2389	-1.46	0.00	Ribosomal protein L39family protein
AT4G35490	180	5.96	21.54	-302	-0.67	0.00	mitochondrial ribosomal protein L11

AT4G39200	230	5.59	19.15	-793	-1.22	0.00	Ribosomal protein S25family protein
AT5G02870	264	9.24	46.22	-402	-0.50	0.01	Ribosomal proteinL4/L1family
AT5G13510	230	8.66	54.93	-630	-1.08	0.00	Ribosomal protein L10family protein
AT5G22440	235	10.45	60.19	-693	-1.34	0.00	Ribosomal protein L1p/L10eFamily
AT5G27770	303	4.28	11.84	-364	-1.49	0.00	Ribosomal L22e protein
AT5G46160	205	8.51	40.31	-972	-1.07	0.00	Ribosomal protein L14p/L23e Family
AT5G59850	266	11.19	62.97	-624	-1.44	0.00	Ribosomal protein S8 family protein
AT5G64140	170	5.35	17.61	-222	-0.99	0.00	ribosomal protein S28(RPS28);
AT1G09690	185	4.13	10.52	-152	-0.77	0.00	Translation protein SH3-like family protein
AT1G22780	173	4.74	13.92	-867	-1.65	0.00	Ribosomal protein S13/S18 family
AT1G74060	371	6.04	23.03	-79	-0.33	0.03	Ribosomal protein L6 family protein
AT2G27530	184	5.23	16.85	-144	-1.40	0.00	Ribosomal protein L1p/L10e Family
AT2G34480	222	6.93	28.30	-1334	-0.55	0.00	Ribosomal protein L18ae/LX family protein
AT2G36620	184	4.62	13.22	-1250	-1.26	0.00	ribosomal protein L24.Cytosolic
AT2G37270	271	7.79	36.16	-75	-0.69	0.00	ribosomal protein 5B

Table S4. LIMYB overexpression downregulates associated-genes photosystem II assembly, light reaction, and photosynthetic electron transport observed in integrative analysis RNA-seq/ChIP-seq.

Gene_id	width	Fold enrich	log10 q-value	Distance to feature	log2 FC	padj	Description
AT1G15120	173	465	16.49	-305	-0.72	0	Ubiquinol-cytochrome Reductase hing
AT1G16700	194	851	40.31	-957	-0.72	0	Alpha-helical ferredoxin
AT1G75630	186	547	18.37	-408	-0.96	0	vacuolar H+-pumping ATPase
AT4G04640	237	752	35.64	-2103	-0.76	0	ATPase, F1 complex, gammasubunit pr
AT4G09650	400	1133	6.67	-1043	-1.33	0	ATP synthase delta-subunit gene Encod
AT4G11150	189	6 2	23.18	-1200	-0.63	0	vacuolar ATP synthase subunit E1Encod
AT4G32260	331	1101	76.31	-236	-0.98	0	ATPase, F0 complex, subunit
AT5G40810	173	559	19.15	-2033	-0.07	0	Cytochrome C1 family
AT5G40810	170	438	11.85	-273	-0.07	0	Cytochrome C1 family
AT5G47890	234	5 8	21.81	-1038	-1.04	0	NADH-ubiquinone oxidoreductase B8
AT5G47890	200	584	22.34	-676	-1.04	0	NADH-ubiquinone oxidoreductase B8
AT5G66570	368	802	43.63	-1109	-0.07	0	PS II oxygen-evolving complex 1Encodes a p
AT1G06680	205	822	38.21	-208	-1.11	0	photosystem II subunitP-1
AT4G05180	300	681	28.34	-878	-0.59	0	photosystem II subunitQ-2
AT1G79040	170	486	14.64	-586	-1.34	0	photosystem II subunit R
AT1G44575	229	651	25.96	-1501	-1.08	0	Chlorophyll A-B binding family protein
AT2G30570	170	486	14.64	-88	-1.34	0	photosystem II reaction center WEncodes P

AT1G67740	257	1155	66.25	-1158	-0.67	0	photosystem II BY
AT1G52230	264	1153	68.15	-2151	-0.97	0	photosystem I subunitH2 Phosphorylation o
AT1G10960	283	995	52.27	-398	-1.79	0	ferredoxin 1
AT1G20020	243	588	21.69	-1150	-1.16	0	ferredoxin-NADP(+)-oxidoreductase 2
AT4G04640	237	752	35.64	-2103	-0.76	0	ATPase, F1 complex, gamma subunitprotein
AT4G09650	400	1133	6.67	-1043	-1.33	0	ATP synthase delta-subunit gene Encodes
AT4G32260	331	1101	76.31	-236	-0.98	0	ATPase, F0 complex, subunit B/B., bacterial/
AT1G29910	372	1072	104.41	-889	-0.92	0	chlorophyll A/Bbinding protein 3
AT1G45474	206	62	23.18	-964	-0.13	0	photosystem I light harvesting complex
AT3G27690	473	737	31.72	-482	-0.93	0	photosystem II light harvesting complex g
AT3G47470	699	567	19.79	-1654	-1.03	0	light-harvesting chlorophyll-protein
AT4G10340	336	854	40.96	-291	-0.88	0	light harvesting complex of photosystem
AT4G10340	180	426	11.18	-1234	-0.88	0	light harvesting complex of photosystem
AT5G54270	462	571	2.11	-672	-0.85	0	light-harvesting chlorophyll B-binding protein
AT5G54270	217	492	17.51	-2445	-0.85	0	light-harvesting chlorophyll B-binding

CHAPTER IV

LIMYB induces lignin accumulation via NIK1antiviral signaling

LIMYB induces lignin accumulation via NIK1 antiviral signaling

Abstract

The cell wall represents a first obstacle count attack by pathogens in plants. These attacks induce the thickening of the cell wall in order to hinder the entry of the invading organism. Onestrategy of this thickening is the increase in lignification of the cell wall. This process is predominantly controlled by MYB-type factors, which act on primary and secondary metabolism. Previous studies identified a MYB factor designed *L10-INTERACTING MYB DOMAIN-CONTAINING PROTEIN* (LIMYB) that is involved in the response of the antiviral immunity pathway mediated by the *NSP-INTERACTING KINASE* receptor (NIK1). After the perception of elicitors of viral nucleic acids derived from begomoviral, leads to phosphorylationof receptor NIK1, and triggers phosphorylation cascade that phosphorylates the *RIBOSOMALPROTEIN L10* (RPL10), which is translocated to the nucleus and interacts with LIMYB, which binds to ribosomal protein gene promoters, inhibiting transcription of these genes and leading to global inhibition of translation. In addition to this regulatory process, we observed by interactive analysis by RNA-Seq and ChIP-Seq that LIMYB binds to gene promoters related to the lignin synthesis process and positively induces its expression. We have shown that overexpression lines of LIMYB and mutant NIK1 T474D influenced the enrichment of phenylpropanoid biosynthesis components by monitoring transcript accumulation and direct interaction in gene promoters related to lignin synthesis. We show that LIMYB also upregulates the activation of phenylpropanoid pathway genes, under the activation of the NIK1 path way by nucleic acid elicitors from begomoviral. We show that the products processed by target enzymes *4-COUMARATE-COA-LIGASE* (4CL) and *PEROXIDASE* (POD) involved in the pathway, accumulate in greater quantity in LIMYB and T474D lines. We also show that transgenic lines contain higher total lignin content than wild type and knockout plants, through quantification of total lignin and analysis of histological profiles of tissues of plants overexpressing LIMYB.

Introduction

The cell wall contributes to plant cell stiffness, constituting a physical barrier against mechanical stress, herbivores, and pathogens (Lucas et al., 2000; Malinovsky, Fangel and Willats, 2014). During biotic stresses, a plant defense strategy against the herbivorous attack isactivating cell stiffness-mediated processes to provide a mechanical barrier, mainly in the pest target tissues (Liu, Osbourn e Ma, 2015). This strategy is highly relevant against the predator action; it can prevent a highly cost-effective response of the host as most herbivorous function as vectors of many pathogens (Humphrey, 2007). Very often, the predator attack induces lignification via the increase in the monolignol precursors needed for the biosynthesis of the polymer (Boerjan et al., 2003; Vogt, 2010). This mechanism is predominantly controlled by MYB transcriptional factors, which regulate the expression of phenylpropanoid biosynthesis- related genes, from which the precursors for lignin composition derive (Dubos et al., 2010). MYBs are implicated in the secondary and primary metabolism in plant cells and assist the flavonoid and phenolic acid biosynthesis, which also depend on phenylpropanoid biogenesis. Therefore, phenylpropanoids are also involved in plant development and defense against bioticand abiotic stresses (Liu, Osbourn e Ma, 2015).

The MYB domain-containing transcription factors (TFs) play major role in controlling thecell wall biogenesis. The superfamily of proteins harboring the MYB domain has been characterized in the model plant *Arabidopsis thaliana* and crops like rice, sorghum, and wheat.The MYB superfamily members maintain functional conservation among these plant species, also participating in a range of processes such as plant development, biotic and abiotic stress responses (Brownfield et al., 2009; Ibraheem et al., 2015; Li, Ng and Fan, 2015; Shan et al., 2016; Baillo et al., 2019; Tang et al., 2019;Kim et al., 2020).

Among members of the MYB superfamily, LIMYB (L10-interacting MYB domain-containing protein), belonging to the R2R3-Myb group, has been characterized as a downstream component of an antiviral signaling pathway that protects plants against begomoviruses (Zorzatto et al., 2015). Activation of the LIMYB repressing transcriptional activity down-regulates the expression of transcriptional machinery- related genes, causing suppression of host and viral mRNA translation compromising begomovirus infection (Zorzatto et al., 2015). The infection signal (begomovirus-derived nucleic acids) is sensed by transmembrane receptors that might form receptor/coreceptor complexes to activate and phosphorylate the nuclear shuttle protein-interacting kinase 1 (NIK1; Li et al., 2019). Viral PAMPs induce NIK1 phosphorylation at a critical threonine residue at position 474 in

the activation loop of the NIK1 kinase, thereby activating the antiviral signaling pathway (Fontes et al., Santos et al., 2009). Activated NIK1 mediates the phosphorylation of the downstream component, the ribosomal protein L10 (RPL10), which in turn is redirected to the nucleus, where it interacts with LIMYB. The RPL10- LIMYB transcriptional complex fully represses the expression of translational machinery-related genes, leading to suppression of global translation under prolonged NIK1 activation (Rocha et al., 2008; Carvalho et al. 2008; Zorzattoet al., 2015).

RNA-seq and ChIP-seq combined results have recently identified the LIMYB wide-genome transcriptional landscape. From the LIMYB down-regulon, we demonstrated that the repressing transcriptional activity of LIMYB was also involved in down-regulating photosynthetic apparatus-related genes and hence photosynthesis in a coordinated manner withglobal translation suppression. Here, we examined further the LIMYB up-regulon and showedthat LIMYB is also involved in the modulation of the phenylpropanoid biosynthetic chain. Thischapter investigates the LIMYB-mediated upregulation of genes involved in the synthesis of phenylpropanoids, the precursors of lignin production.

Results

The phenylpropanoid biosynthesis-related genes are enriched in then LIMYB upregulation

The transcriptome analysis of LIMYB-overexpressing *A. thaliana* lines revealed upregulated genes that belong to the phenylpropanoid pathway (Figure 1A). Among the upregulated genes, enzymes of important steps of the phenylpropanoids pathway associated with lignin biosynthesis were found to be differentially expressed (DE) (Table1). We selected two up-regulated genes, an oxidizing enzyme *PEROXIDASE* (POD), involved in defense to several pathogens, and *4-COUMARATE-CoA LIGASE 2* (4CL2), which is involved in the synthesis of CoA thioesters, used to synthesize several phenylpropanoid-derived compounds (Figure 1B) tovalidate the RNA-seq results. The enzyme 4CL2 is one of the enzymes of the set that synthesizes p-coumaroyl alcohol, a monolignol precursor; and POD is a very important component for lignin deposition (Zhao, Q. 2016). The lignification process has the central function of increasing the structural integrity of the vascular bundle, serving as a barrier against pathogens (Wainhouse et al. , 1990; Boerjan et al., 2003; Vogt, 2010).

LIMYB overexpression in L1 and L3 lines (Chapter III) induces POD and 4CL2 transcriptaccumulation (Figure 2A). These genes were significantly upregulated, reinforcing

LIMYB asan important biological regulator of the phenylpropanoid synthesis process, and consequently lignification. Interestingly, the peaks of all three LIMYB DNA-binding motifs (Chapter III) were mapped on the POD and 4CL2 promoter region, whereas the hits from the RNA-seq liedon the coding region and were upregulated in the LIMYB-overexpressing line as compared with their abundance in the wild-type control (Figure 2B). To further confirm that LIMYB directly target the 4CL2 and POD promoters, we performed a luciferase reporter transactivationassay in *Nicotiana benthamiana* (Figure 2C). *Nicotiana benthamiana* leaves were agroinfiltrated with constructs containing the Luciferase gene under the control of -2000 bp 5' flanking sequences of 4CL2 and POD genes (pro4CL:Luciferae and pro POD: Luciferase). As a positive target of LIMYB transcriptional activity, we used proL18(1):Luciferase and as a negative control proUBQ: Luciferase. The analysis showed that LIMYB interacts with promoters of monolignol biosynthesis genes and acts as a positive regulator of 4CL and POD genes, which are directly responsible for the production of essential intermediates in the lignin biosynthesis pathway and its allocation to the cell wall, respectively (Zhao, 2016).

LIMYB upregulates POD and 4CL2 via activation of NIK1 signaling

The lignification process plays an important role in the mechanical defense against pathogens (Wainhouse et al. , 1990; Boerjan et al., 2003; Vogt, 2010), and both the cell wall and the lignification process can undergo remodeling due to the activation of pattern-triggered immunity (PTI) and effector-triggered immunity (ETI) (Nicholson and Hammerschmidt, 1992; Torres, 2010; Tsuda and Katagiri, 2010). Lignification is also enhanced in response to differentbiotic stresses, and can be used for a spatial restriction for pathogens, therefore increasing mechanical resistance (Lee et al., 2019). As a downstream component of the NIK1 signaling, which has been shown to transduce biotic and abiotic signals, we investigated whether the LIMYB-mediated up-regulation of *POD* and *4CL2* was linked to NIK1 activation.

NIK1 activation was induced by using nucleic acid elicitors isolated from begomovirus-infected (InRNA) and uninfected (UnRNA) plants. The transcript accumulation analysis detected increased mRNA accumulation of POD and 4CL genes in samples treated with RNA prepared from begomoviral-infected plants, but not from mock-inoculated leaves, in wild-typeplants, but not in *nik1-1/nik2-1* double mutant and *nik1* knockout lines (Figure 3A and 3B). POD and 4CL2 genes were also induced by the viral PAMP in *nik2* mutant, although to a lesserextent than in Col-0, reflecting partial overlap with NIK1 function. The

viral PAMP-mediated increase in gene expression of the LIMYB targets was dependent on the NIK1 function and activation. Therefore, these enzymes involved in lignin biogenesis may be upregulated by viral infection in a NIK1 receptor-dependent fashion. This hypothesis is reinforced by the analysis of the expression level of POD and 4CL2 genes in NIK1 mutants and in T474D-expressing lines (Figure 3C and 3D). As previously shown, NIK1 harboring the T474D mutation is constitutively activated and capable of sustaining the transcriptional repressing activity of LIMYB (Zorzatto et al., 2015). We showed here that T474D also constitutively regulates the transcriptional activating function of LIMYB on target genes encoding enzymes involved in the phenylpropanoid pathway.

We next examined whether the transcriptional activity of LIMYB on the promoters of lignin biosynthesis-related genes was also regulated in response to viral PAMPs (Figure 3E). For the promoter transactivation assay, protoplasts prepared from *limyb-32* leaves were co- transformed with promoter(Target):Luciferase + 35:LIMYB- GFP DNA constructs, and treated with begomovirus-derived viral nucleic acid elicitors (InRNA, viral PAMP) and RNA from mock-inoculated plants (UnRNA) for 3h. 35:LIMYB-GFP was transformed along with the promoter target constructs, pro L18:Lucfierase, pro4CL:Luciferase, proPOD:Luciferase, and the unrelated promoter construct, proUBQ (Figure 3E). The promoter activity transactivation assay via the luciferase reporter gene showed a significant viral PAMP (IN)-induced increase in the luciferase enzyme expression from the 4CL and POD promoters, a decrease from the proL18 promoter and without significant changes from proUBQ in LIMYB expressing protoplasts. The analysis demonstrates that the LIMYB transcriptional activity targeting genes from the lignin biogenesis can be triggered by viral elicitors, thus associating the activation of the NIK1-mediated immunity pathway with the deposition of lignin in the cell wall (Nicholson and Hammerschmidt, 1992; Sattler and Funnell-Harris, 2013).

LIMYB overexpression enhances POD activity via NIK1 activation

POD-enriched protein extracts were prepared from LIMYB-overexpressing lines and NIK1 gain- and loss-function mutants. POD activity was initially evaluated using o-phenylenediamine (OPD) as substrate and the increase in absorbance of the generated products (diaminophenazine) was observed for up to 35 min (Figure 4A and 4B). POD activity was significantly higher in LIMYB 28-day-old overexpressing lines than in Col- 0 at each time recorded. Adult plants with 28 days were deployed to check for possible changes due to physiological status changes associated with development (Figure 4C, D).

The highest accumulation of products was observed in the LIMYB-32-L1 and LIMYB-32-L3 lines in 12- day-old plants (Figure 4C), while for the 28-day-old plants, the three lines overexpressing LIMYB showed higher accumulation of products generated from POD's activity.

NIK1 mutants were also evaluated under the same developmental stages mentioned above. In seedling extracts the highest accumulation tetraguaicol, reaction product of oxidation of guaiacol (2-methoxyphenol) for POD, was observed in T474D-6, and an increase in *nik1*-1, and*nik2-1* knockouts, but no changes in Col -0 and *nik1-1/nik2-1*. In the 28-day-old plants, the transgenic lines T474D-6 and NIK1-6HA showed greater accumulation of the products. The accumulation in NIK1 transformants confirms that the receptor maintains communication with the LIMYB factor, since it binds directly to the peroxidase promoter and positively regulates its expression. In Arabidopsis, MYB factorsR2R3-MYB, the group to which LIMYB belongs, have several members such as MYB46 and AtMYB15, which bind directly to MYB-responsiveelements, present in genes associated with the secondary cell wall and control of defense- induced lignification and basal immunity (Zhong et al., 2007; McCarthy et al., 2009; Chezem et al., 2017).

LIMYB-overexpressing lines and T474D lines display enhanced 4CL2 activity and lignin

The 4CL2 activity was monitored by measuring.4-Coumaroyl-CoA accumulation in the transgenic lines. LIMYB-overexpressing young plants displayed a higher accumulation of intermediates in lignin biosynthesis pathway than Col-0, similar to *limyb*-32 (Figure 5A). In 28 days-old plants, 4CL2 activity remained higher in LIMYB- overexpressing lines than Col-0, whereas in *limyb* lines, enzyme activity was lower than Col-0 (Figure 5B). Expression of T474D-6 and NIK1-6HA overexpression enhanced 4CL2 activity, as judged by the increased accumulation of 4-Coumaroyl-CoA in both young and adult plants compared to Col-0. Although *nik2* also displayed higher accumulation of 4-Coumaroyl-CoA than Col-0, young *nik1-1/nik2-1* accumulated similar levels of the enzymatic product as Col-0 but displayed lower 4CL2 enzyme activity in the adult phase (Figure 5C, D). In Arabidopsis, overexpression of regulators of lignin biosynthesis during secondary cell wall formation up-regulated the genes in the lignin biosynthetic pathway, as *PAL1, C4H, 4CL1, C3'H, HCT*, and *CCoAOMT1* (Zhou et al.,2009).

The quantification of the products of 4CL2 and POD are indicative of the lignin profile inplants as they are precursors in the biosynthetic pathway (Zhao, Q. 2016). To confirm that

the transcriptional activity of LIMYB resulted in lignin deposition in the cell wall, we quantified lignin polymer in the genotypes exhibiting alterations in 4CL2 and POD activities. In both developmental stages, lignin accumulate to higher levels in the genotypes ectopically expressing LIMYB and T474D, than in Col-0, and no significative alterations were observed in knockout lines (Figure 5E, F, G, H). These results were correlated with the enzymatic activity of 4CL2 and POD and demonstrated that LINYB regulates lignin biosynthesis via NIK1 activation.

To examine whether LIMYB overexpression would influence the lignification process, lignin was histologically staining by toluidine blue in cross sections of Col-0, LIMYB-32-L1, LIMYB-32-L3, LIMYB-32-L4 and *limyb-32* leaves, and lignin deposition were visualized by microscopy. LIMYB overexpression was associated with a higher staining intensity of lignification (Figure 6A). The LIMYB-overexpressing leaves displayed an altered histological phenotype of the leaf sections, including alteration in the palisade parenchyma and increased spacing between sheath cells (Figure 6A). Mesophyll thickness increased in the LIMYB- overexpressing lines (Figure 6B), possibly due to the deposition of higher lignin levels, which was in contrast with the lower thickness in *limyb-32* plants as compared to Col-0. Tissue lignification is crucial for the development, as defective genes of the enzymes involved in the biosynthesis of monolignols result in defective phenotypes, which obviously demonstrates thatdifferent levels of lignification will lead to differences in anatomical profiles, making lignin essential for development (Schilmiller et al, 2009; Huang et al, 2010; Bonawitz et al, 2014).

In the vein sections (Figure 7), the organization profile of the vascular bundle was altered, and greater thickness and diameter of the xylem vessels were observed in the LIMYB- 32 lines.These lines also exhibited greater color intensification around the vascular bundle, in the regions around the phloem. The same characteristics were observed in the cross sections of thepetiole, however the staining by Toluidine Blue intensifies even more in the cell walls and around the vascular bundle, indicating considerable lignin content in the LIMYB-overexpressing lines. Collectively, these results indicated that LIMYB controls the level and pattern of lignin deposition in response to NIK1 activation which has been shown to be inducedby biotic and abiotic signals.

Discussion

LIMYB is a component of the NIK1 antiviral signaling, which has been shown to be induced by different biotic signals, viral and bacterial PAMPs, and abiotic signals, high temperature and osmotic stress (Teixeira et al., 2019, Li et al., 2019, Chapter III). We have recently shown that NIK1 activation by these pathogen and environmental signals leads to coordinate suppression of photosynthesis and translation via the repressing transcriptional activity of LIMYB. Here we showed that LIMYB also functions as a transcriptional activator and induces the expression of genes encoding enzymes involved in the phenylpropanoid biosynthetic pathway, particularly involved in the synthesis of lignin precursors. LIMYB overexpression enhances 4CL2 and POD enzymatic activity, a phenotype that was associated with a higher accumulation of lignin and NIK1 signaling. Therefore, the NIK1 signaling- mediated responses were expanded to include regulation of phenylpropanoid biosynthesis- related genes and enhanced deposition of lignin. In addition to its crucial role in plant growth, lignin is implicated in mechanical defense, a physical barrier against pathogens (Nicholson & Hammerschmidt, 1992; Sattler & Funnell-Harris, 2013; Malinovsky et al., 2014; Cesarino, 2019). Lignification has been shown to be induced by biotic stress as a strategy of plant defense (Nicholson e Hammerschmidt, 1992; Sattler e Funnell-Harris, 2013). Lignin provide a mechanical barrier to pathogen ingress, limit the digestibility of plant tissues by herbivores, and presumably decrease the plant attractiveness as a foodstuff. Thus, the biosynthesis of ligninis relevant not only for plant support and water transport but also in plant defense.

LIMYB and T474D plants showed an increase in the accumulation of precursors, and final amounts of lignin polymer, which shows the positive relationship of the NIK1/RPL10/LIMYB components in the lignification process, mainly due to the fact that MYB factors are the most prominent components in the lignification process. association with the process of lignin biosynthesis (Shigeto et al., 2015). Peroxidases from the lignin biosynthesis process are key enzymes that participate in the polymerization of monomers(Berthet et al., 2015;Zhao et al., 2013). The overexpression of POD in Tobacco increased the content of phenolic acids and lignin in plants, as well as promoting increased tolerance to stress, and the depletion of this protein seriously affected the development of Arabidopsis plants (Kim et al., 2008; Shigeto et al., 2015). The 4CL gene was found to be highly expressed, among genes associated with increased lignification from plant treatments with *Pseudomonas Syringae*, which activated ETI, and among the effects, there was an increase in lignification (Vanholme et al., 2012; Kim et al., 2020). The suppression of

transcription of the 4CL gene in *Pinus radiata*, in addition to drastically reducing the lignin content by about 36 to 50%, resulted in severely defective phenotypes (Wagner et al., 2009). These findings, associated with those presented here, reinforce the role of MYB factors in the cell wall thickening process, given its relevance in plant development and possible biotechnological applications, lignin metabolism has been extensively studied, both in model plants, with in woody trees and grass biomass crops (Vanholme et al., 2010; Umezawa, 2018).

As an antiviral immunity mechanism of plant cells, NIK1 signaling protects begomovirus infection via suppression of host and viral mRNA translation (Brustolini et al., 2015). NIK1 signaling has also been shown to be effective against RNA viruses that nevertheless have developed several translational strategies to escape the translational regulatory mechanisms of plant cells (Li et al., 2019). Therefore, it is not clear how NIK1 signaling combats RNA virus infection. It is possible that NIK1-mediated lignification provides a mechanism to interfere with the vector-directed mechanical entry of RNA viruses into plant cells. This hypothesis is worth investigating further. Recently, Lee et al. (2019) demonstrated that the MYB15 transfactor, belonging to the same R2R3-MYB group as LIMYB, regulates positively bacterial PAMP flg22-induced lignification (Chezem et al., 2017). Interestingly, the NIK1-mediated immunity has been recently shown to be induced by the bacterial PAMP flg22 (Li et al., 2019). Upon bacterial treatment, the pattern recognition receptor (PRR) FLS2 recognizes the bacterial flg22 epitope driving dimerization with BAK1 forming the active FLS2-BAK1 immune complex that phosphorylates each other to initiate PAMP-triggered immunity (Li et al., 2019). Activated BAK1 phosphorylates NIK1 on its crucial residue Thr- 474 at the activation loop of the NIK1 kinase domain to activate antiviral immunity via LIMYB that is also linked to lignin accumulation (Li et al., 2019). Therefore, the NIK1 mediated signaling may assembly a defense strategy against non-viral pathogens via LIMYB- mediated regulation of lignin accumulation.

Material and Methods

Plant material and growth conditions

Arabidopsis thaliana plants ecotype Columbia-0 (Col-0), knockouts lines *nik1-1* (SALK_060808), *nik2-1* (SALK_044363), and *limyb-32* (SALK_032054) used, were obtained from Arabidopsis Biological Resource Center, previously described (Fontes et al., 2004; Li et al., 2015; Zorzatto et al., 2015). The double mutant *nik1-1/nik2,* complementation line T474D- 6, which harbor a 35S:NIK1-GFP construct in the nik1 genetic background, described previously (Zorzatto et al., 2015; Li et al., 2019). Plants were grown in soil (Metro Mix 366) in a growth chamber at 23 °C, 45% humidity, and 75 µE/m2/s1 light with a 10-h-light/14-h-dark photoperiod. Four-week-old plants were used for enzymatic assays, lignin analysis and treatments with viral nucleic acid elicitors, and protoplast isolation. Seedlings were germinated for up to 12 days on half-strength Murashige and Skoog (MS1/2) plates containing 1% (w/v) sucrose and 0.8% (w/v) agar, grown under the equivalent conditions.

Plasmid construct for transient expression in protoplast

The construction of pK7F-NIK1T474D (pUFV 632), which expresses a T474Dmutant fused in frame with the N-terminal of GFP under the control of CaMV 35S promoter, has been previously described (Santos et al., 2009). The recombinant plasmid pYFP-LIMYB (pUFV1886), containing LIMYB ORF fused in-frame to the C-terminus of YFP under the control of the 35S promoter and inserted into the binary vector 35S- YFP- casseteA-Nos-pCAMBIA1300, has been previously described (Zorzatto et al., 2015). The recombinant plasmid AT5G05800NS-pK7FWG2 (pUVF 1395), containing LIMYB ORF fused-in frame tothe N-terminal of GFP under control of the 35S promoter (Zorzatto et al., 2015).

Plasmid construct for promoter transactivation assay in protoplast

The clone prAt1g29970-Lucif-term-2X35S RLucifpH7M34GW (pUVF 2231), previously described (Zorzatto et al., 2015), contains the firefly luciferase cDNA under the control of the rpL18A promoter, as well as the Renilla luciferase cDNA under the control of a 2 x 35S promoter. Likewise, the clones containing the firefly luciferase cDNA under the control of the RPL28e and ubiquitin promoters for luciferase transactivation assays were previously obtained(Zorzatto et al., 2015). The At3g21240 (4CL) promoter (-2000 pb) was obtained from Arabidopsis DNA by PCR using the gene-specific primers (Table 1), and cloned into pDONR-P4-P1R vector, generating pUFV 3413 clone. The clone LUCF-

term-pDON221 (pUFV 2132) harbors the firefly luciferase cDNA in the entry vector pDON221, whereas the clone 2×35S-RLUCF-pDONR-P2R-P3 (pUFV2131) contains Renilla luciferase cDNA under the control of a 2× 35S promoter. The At3g21240 (4CL) promoter (-2000 pb) was inserted into the destination vector pH7m34GW (pUFV 1918), along with 2×35S- RLUCF-pDONR-P2RP3 (pUFV 2131) and LUCF-term-pDON221 (pUFV 2132), by triple recombination using the gateway system (Promega, Gateway™ LR Clonase™ Enzyme mix, cat # 11791019). The resulting clone, pro4CL:Lucif-term-2X35S:RLucif pH7M34GW (pUFV 3429), contains the firefly luciferase cDNA under the control of the 4CL promoter (2000 5' flanking sequences), as well as the Renilla luciferase cDNA under the control of a 2× 35S promoter. The same procedure was used to clone the firefly luciferase cDNA under the control of the POD promoter(-2000 pb), yielding the clone proPOD:Lucif-term- 2X35S:RLucif pH7M34GW (pUFV 3421). Promoter-specific primers used for amplifying promoter sequences are listed in Table 1.

Plant transformation

The *limyb-32* knockout lines were transformed with pYFP-LIMYB (pUFV 1886) by floral dip method, generating LIMYB-32-L1, LIMYB-32-L3 and LIMYB-32-L4 lines. For overexpressing lines, also were Col-0 transformed with 2×35S::NIK1-6HA-containing pH7m34GW (pUFV 2226), previously described (Li et al., 2019). Primary transformants were selected using the appropriate antibiotic, 30 µgmL-1 hygromycin, and transgene stable insertionwas monitored by PCR with gene-specific primers (Table 1). Transgene expression level was confirmed by immunoblotting and real-time qPCR with gene-specific primers (Table 1).

Whole-genome chromatin immunoprecipitation sequencing (ChIP-Seq) and data analysis

Seedlings (600 mg) of LIMYB lines were crosslinked by 1% formaldehyde in PBS solution (Sigma-Aldrich, cat. # F8775) under vacuums for 1-3 min, as previously described (Yamaguchi et al., 2014). Subsequently, extraction and nuclei isolation, and chromatin sonication up to 100– 800 bp fragments. Targets in LIMYB-32-L1, LIMYB- 32-L3 and LIMYB-32-L4 transgenic lines were immunoprecipitated using rabbit polyclonal anti-GFP - IgG antibody (Thermo Fisher Scientific, MA, USA, cat. # A11122) captured with protein-A agarose beads (Invitrogen TM, Cat # 15918014). Subsequently elution, reverse crosslinking and DNA purification. ChIPed- DNA was used to generate sequencing libraries through

Illumina TruSeq kit (Illumina, cat # IP-202-1012, IP-202- 1014) according to manufacturer's protocols. The quality of the reads was estimated through the statistical metrics employed in the FastQC data quality analysis tool (Andrews, 2017); low quality sequencing reads were filtered using the printSEQ software package (Schmieder & Edwards, 2011). The read mapping process was performed using the program Bowtie 2 (Langmead et al., 2009). ChIP-seq peaks were calculated with the software ChIPpeakAnno (Zhu et al., 2010; Zhu L., 2013) using MACS2 (Zhang et al., 2008) was used to analyze the ChIP-seq data. Putative target genes and peak distribution of the ChIP-seq data were figured out using the ChIPpeakAnno software (Zhu et al., 2010; Zhu L., 2013). ChIP-seqdata have been deposited in the Gene Expression Omnibus under accession number GSE197332.

RNA-sequencing (RNA-seq) method and data analysis

RNA-seq experiments were conducted with three biological replicates of a pool of 12-day- old Col-0, LIMYB-32-L1 and LIMYB-32-L3 seedlings and examined differential expression between Col-0 and LIMYB lines using the Deseq2 differential gene expression method (Robinson and Oshlack, 2010; Anders and Huber, 2010). RNA- seq data were obtained using an Illumina Hi-seq 2500 platform. The Libraries construction were prepared with the kit TrueSeq-RNA Sample Prep Kit Illumina (Illumina, cat # 20020595). The paired-end 100-bp protocol was used with the following quality filter parameters: 5 bases trimmed at the 3′ and 5′ends of the reads and a minimum average Phred score of 30. Reads quality was evaluated by FastQC (Andrews, 2010). Illumina adapters were removed using Trimmomatic software (Bolger et al., 2014) and as low-quality sequencing reads were filtered and trimmed using prinSEQ software package (Schmieder & Edwards, 2011). Read mapping was performed using the Bowtie 2 program (Langmead et al., 2009). The global analysis of differential gene expression (DGE) was performed using the edger package (Robinson et al., 2010) and DEseq2 (Anders & Huber, 2010). Differential expression was determined using the p-value adjusted bythe "False discover rate" (FDR). Log2.Fold Change p-value < 0.01 e log2- fold-change >1.0 for up-regulated genes e log2-fold-change <1.0 for down-regulated gene, were used as the cutoff point. Differentially expressed (DE) genes were stored using SQL tables in the Postgre SQL relational data base (http://200.235.143.46/LiMyb/ or https://inctipp.bioagro.ufv.br/maloni/), which listed corresponding log2 FC (fold change) andp values corrected by false discovery rate (q value) for all DE genes. The classification of gene ontology (GO) and analysis of enrichment of pathways were performed using the packages GoStats (Falcon & Gentleman, 2007) and

PathView (Luo & Brouwer, 2013) both present in the R/Bioconductor GOstats repository.

Protoplast preparation from *A. thaliana* leaves

Well-expanded leaves from 3–4-week-old plants were cut in 0.5–1-mm pieces and digested with 5–10 ml enzyme solution (20 mM MES pH 5.7; 1.5% cellulase R10; 0.4% macerozyme R10; 0.4 M mannitol and 20 mM KCl). The leaf strips were vacuum-infiltrated for 30 min in the dark using a desiccator. Then, the digestion was conducted without shaking, in the dark for at least 3 h at room temperature and the integrity of the protoplasts were examined under a lightmicroscope. The protoplasts were filtered to remove undigested leaf tissues and recovered by centrifugation. The protoplasts were transformed using the protocol of DNA-PEG–calcium transfection, in which 10 µl DNA (10–20 µg of plasmid DNA) were mixed with 2 × 104 protoplasts along with the 15% PEG solution 4000 (Polyethylene glycol 4000, sigma, Cat # 25322-68-3) at room temperature for up to 15 min and then incubated for recovery during 12 h (Yoo and Sheen,2007).

RNA isolation and transcript accumulation analysis by RT-qPCR

Genes related from phenylpropanoids metabolic pathway associated to lignin biosynthesis were selected for validation by quantitative real-time PCR (RT-qPCR), using primers showed in Table 1. RNA was extracted using method TRIzol reagent (InvitrogenTM, cat # 15596018, USA) and quantified with a NanoSpecspectrophotometer. Total RNA was treated with DNase I, RNase-free (Thermo Scientific™, cat # EN052) for 30 min at 37 °C and then reverse transcribed with M-MLV Reverse Transcriptase (Invitrogen™, cat # 28025013). Real-time PCR was performed using iTaq Universal SYBR Green Supermix (Bio-Rad, cat # 1725121, USA) and a 7500 Fast Real-Time PCR System (Applied Biosystems™, cat # 4351106, USA). Expression of each gene was normalized to expression with endogen Actin or UBQ10.

Regulation of the NIK1 signaling pathway in phenylpropanoids biosynthesis

Leaf discs were previously injured with an abrasive, and excised by cork borer, then incubated overnight in 12-well plates containing 500 in ultra-pure water. After, the water was substituted by of treatment containing viral nucleic acids (DNA or total RNA infected by begomoviral) at a concentration of 250 ng/µL, 100 mM flg22 and ultra-pure water. Treatmentswere performed for 3 h for the analysis of transcript accumulation of target genes of the pathway.

Luciferase reporter gene assay

The protoplasts were isolated from the *limyb-32* were co-transformed with combinations: pK7F-NIK1T474D; pK7F-NIK1T474D + AT5G05800NS-pK7FWG2 + proL18(2):Lucif-term-2X35S:RLucifpH7M34GW; AT5G05800NS-pK7FWG2 + proL18(2):Lucif-term-2X35S:RLucifpH7M34GW; pro4CL:Lucif-term-2X35S:RLucifpH7M34GW + AT5G05800NS-pK7FWG2; pK7F-NIK1T474D + proUBQ:Lucif-term-2X35S:RLucifpH7M34GW: pK7F-NIK1T474D + AT5G05800NS-pK7FWG2 + proUBQ:Lucif-term-2X35S:RLucifpH7M34GW.

N. benthamiana leaves were agro-infiltrated with A. tumefaciens GV3101 strains containing the following combinations of DNA constructs: pro 4CL-Lucif-term-2×35S RLucif pH7M34GW; pro 4CL-Lucif-term-2X35S RLucif pH7M34GW + AT5G05800NS-pK7FWG2; POD-Lucif-term-2X35S RLucif pH7M34GW and POD-Lucif-term-2×35S:RLucif pH7M34GW + AT5G05800NS -pK7FWG2. Forty-eight hours after infiltration, 200 mg of leaf tissue was harvested for total protein extraction. Luciferase activity was assayed with the Dual-Luciferase Reporter Assay System (Promega) according to the manufacturer's instructions.

Enzymatic assay

POD activity was monitored conform previously described Lurie et al. 1997, with some modification. Approximately 0,5 g from frozen tissue powder was extracted with 1mL PBS (0.05 M, pH 7.8). The mixture was homogenized and centrifuged at 8,000× g for 10 min, and then the was collected supernatant liquid as the enzyme for activity assay. The buffer reaction was prepared containing 25 μL of extract and 150 μL reaction mixture (100 mM, pH 6.0 PBS,25 mM 2-Methoxyphenol, and 30% H2O2) was measured at the absorbance at 470 nm (2- Methoxyphenol, Sigma, cat # W253200-SAMPLE-K). One unit of POD activity was defined as a change in OD470 per minute per gram. For each treatment, three independent replicates were conducted.

4CL activity assay was performed as before described in (Knobloch and Hahlbrock 1977). Frozen tissue was powder with buffer Potassium Phosphate 0,1 M pH7,5 containing 1mM de DTT, 0,1 mM de EDTA, 5 mM de ascorbic acid, 1 mM de PMSF, 0,15% p / v PVP. Após, o misturado foi centrifugado a 12.000 × g por 20 min a 4 ° C e o sobrenadante utilizado como uma fonte de enzimas. The buffer reaction was prepared with 2 μg of protein, 0.33 mM coenzyme A, 5 mM ATP, 25 mM MgCl2, and 500 mM Tris–HCl (pH 7.8)

by addition of 0.5 mM of p-coumarate or 50 mM *o*-phenylenediamine (OPD) as substrate. After incubation at room temperature for 10 up to 40 min, the absorbance was monitored at 333 nm for 4-coumaroyl-CoA.

Analysis of lignin accumulation

The determination of the total amount of lignin was performed by derivatization with glycolic acid as described by Brinkmann et al (2002) with some modifications. Plant tissues were ground in liquids and lyophilized. 20 mg of the plant spray were in 2 mL that will be administered as a suspension wash (100 mM K2HPO4 / KH2PO4 pH 7,8, 0,5% Triton X-100),with gentle agitation for 30 min at room temperature and after centrifugation at 1,500g for 5 minutes. The pellet was washed three times in 100% methanol and the sediment dry to 80°C for 12 h. Then 2 mg aliquots of the dried pellet were mixed with 1.5 ml of 2N HCl and 0.3 ml of thioglycolic acid (Sigma, thioglycolic acid, cat # T3758-100ML). After incubation to 95 ° Cfor 4 h, followed by centrifugation 10 min at 15.000 × g. Next, pellets were washed three timesin distilled water and then incubated with 1 ml of 0.5 M NaOH for 18 hours at roomtemperature. Then the samples were centrifuged and the supernatant mixed with 1.8 mL of HCl,and then incubated at 4 °C for 4 hours and centrifuged. The pellet was solubilized in 1 mL of 0.5 M NaOH and the absorbance read at 280 nm. The calibration curve was prepared with commercial lignin (Sigma, Lignin alkali, cat # 471003-100G).

Light microscopy and Histochemical analysis of lignin profiles

Well-expanded leaves of A. thaliana, closer to the substrate (rosette region), were collected and fixed in FAA (Formalin-Aceto-Alcohol) (formaldehyde, glacial acetic acid,50% ethanol 1:1:18) and then preserved in 70% ethanol (Jensen, 1962). In order to measure the leaf blade thickness and to perform histochemical tests for lignin detection, the material was serially dehydrated in ethylic solution and later incubated in methacrylate (Historesina Leica Microsystems Nussloch GmbH, Heidelberg, Germany). To obtain 5 µm thick transversal sections of petiole, vein and leaf blade, an automatic advanced rotary microtome was utilized (model RM2155, Leica Microsystems Inc., Deerfield, USA). Subsequently, toluidine blue dyepH 4,0 was applied in the samples(O'Brien et al. al., 1964), which therefore stained the lignin to cyan and the cellulosic walls to violet (Sakai, 1973). The permanent slides were mounted in Permount synthetic resin (Permount, Fisher Scientific, New Jersey, USA). Observations and photographic documentation were performed through a light microscope (model AX70TRF, Olympus Optical, Japan) equipped

with an image capture system (Ax Cam, Zeiss, Germany). All measurements were made with the Image- Pro Plus 7 software.

Statistical analysis

Student's t test was used to statistical analysis, performed in Excel 2019 software. The analyses were executed with three-independent experiment, and the data were expressed as means ± sd. A significant difference was considered p-value ≤ 0.05.

References

Anders, S. and Huber, W. (2010). Differential expression analysis for sequence count data. Genome Biol. **11**: 1–12.

Andrews, S. (2010). FastQC: A quality control tool for high throughput sequence data. Ref. Source Assoc. *Bioinformatics*. **23**: 257–258.

Baillo, E.H., Kimotho, R.N., Zhang, Z., and Xu, P. (2019). Transcription factors associated with abiotic and biotic stress tolerance and their potential for crops improvement. *Genes* (Basel). **10**: 1–23.

Berthet S., Demontcaulet N., Pollet B., Bidzinski P., Cezard L., Bris P.L., Borrega N., Herve J., Blondet E., Balzergue S., et al. (2011). Disruption of LACCASE4 and 17 resultsin tissue-specific alterations to lignification of *Arabidopsis thaliana* stems. *Plant Cell.* **23**:1124–1137.

Boerjan, W., Ralph, J., and Baucher, M. (2003). Lignin Biosynthesis. *Annu. Rev. Plant Biol.* **54**: 519–546.

Bonawitz, N.D., Kim, J.I., Tobimatsu, Y., Ciesielski, P.N., Anderson, N.A., Ximenes, E., Maeda, J., Ralph, J., Donohoe, B.S., Ladish, M., and Chapple, C. (2014). Disruption ofMediator rescues the stunted growth of a lignin-deficient Arabidopsis mutant. *Nature* **509**: 376–380.

Carvalho, C.M., Santos, A.A., Pires, S.R., Rocha, C.S., Saraiva, D.I., Machado, J.P.B., Mattos, E.C., Fietto, L.G., and Fontes, E.P.B. (2008). Regulated nuclear trafficking of rpL10A mediated by NIK1 represents a defense strategy of plant cells against virus. *PLoSPathog*. **4**: e1000247.

Cesarino, I. (2019). Structural features and regulation of lignin deposited upon biotic and abiotic stresses. *Curr. Opin. Biotechnol*. **56**: 209–214.

Chezem, W.R., Memon, A., Li, F.S., Weng, J.K., and Clay, N.K. (2017). SG2-type R2R3- MYB transcription factor MYB15 controls defense-induced lignification and basal immunity in Arabidopsis. *Plant Cell* **29**: 1907–1926.

Dubos, C., Stracke, R., Grotewold, E., Weisshaar, B., Martin, C., and Lepiniec, L. (2010). MYB transcription factors in Arabidopsis. *Trends Plant Sci.* **15**: 573–581.

Falcon, S. and Gentleman, R. (2007). Using GOstats to test gene lists for GO term

association. *Bioinformatics* **23**: 257–258.

Fielding, J.L. and Hall, J.L. (1978). A Biochemical and Cytochemical Study of Peroxidase Activity in Roots of Pisum sativum: II. DISTRIBUTION OF ENZYMES IN RELATIONTO ROOT DEVELOPMENT. *J. Exp. Bot.* **29**: 983–991.

Fontes, E.P.B., Santos, A.A., Luz, D.F., Waclawovsky, A.J., and Chory, J. (2004). The geminivirus nuclear shuttle protein is a virulence factor that suppresses transmembrane receptor kinase activity. *Genes Dev.* **18**: 2545–2556.

Fornera, S. and Walde, P. (2010). Spectrophotometric quantification of horseradish peroxidase with o-phenylenediamine. *Anal. Biochem.* **407**: 293–295.

Huang, J., Gu, M., Lai, Z., Fan, B., Shi, K., Zhou, Y.H., Yu, J.Q., and Chen, Z. (2010). Functional analysis of the Arabidopsis PAL gene family in plant growth, development, andresponse to environmental stress. *Plant Physiol.* **153**: 1526–1538.

Ibraheem, F., Gaffoor, I., Tan, Q., Shyu, C.R., and Chopra, S. (2015). A sorghum MYB transcription factor induces 3-deoxyanthocyanidins and enhances resistance against leaf blights in maize. *Molecules* **20**: 2388–2404.

Jensen, W.A. (1962). Preparation of tissue. *Bot. Histochem.*: 55–144.

Jones, J.D.G. and Dangl, J.L. (2006). The plant immune system. *Nature*. **444**: 323–329.

Kim, S.H., Lam, P.Y., Lee, M.H., Jeon, H.S., Tobimatsu, Y., and Park, O.K. (2020). The Arabidopsis R2R3 MYB Transcription Factor MYB15 Is a Key Regulator of Lignin Biosynthesis in Effector-Triggered Immunity. *Front. Plant Sci.* **11**: 1–10.

Kim Y., Kim C.Y., Song W., Park D., Kwon S., Lee H., Bang J., Kwak S. (2008). Overexpression of sweet potato swpa4 peroxidase results in increased hydrogen peroxide production and enhances stress tolerance in tobacco. *Planta.* **227**: 867–881.

Knobloch, K.-H. and Haklbrock, K. (1977). 4-Coumarate:CoA ligase from cell suspension cultures of Petroselinum hortense Hoffm: Partial purification, substrate specificity, and further properties. *Arch. Biochem. Biophys.* **184**: 237–248.

Langmead, B., Trapnell, C., Pop, M., and Salzberg, S.L. (2009). Ultrafast and memory-efficient alignment of short DNA sequences to the human genome. *Genome Biol.* **10**.

Lee, M., Jeon, H.S., Kim, S.H., Chung, J.H., Roppolo, D., Lee, H., Cho, H.J., Tobimatsu, Y., Ralph, J., and Park, O.K. (2019). Lignin-based barrier restricts pathogens to the infection site and confers resistance in plants. *EMBO J.* **38**: 1–17.

Li, B. et al. (2019). The receptor-like kinase NIK1 targets FLS2/BAK1 immune complex andinversely modulates antiviral and antibacterial immunity. *Nat. Commun.* **10**: 1–14.

Li, C., Ng, C.K.-Y., and Fan, L.-M. (2015). MYB transcription factors, active players in abiotic stress signaling. *Environ. Exp. Bot.* **114**: 80–91.

Liu, J., Osbourn, A., and Ma, P. (2015). MYB transcription factors as regulators of phenylpropanoid metabolism in plants. *Mol. Plant* **8**: 689–708.

Lucas, P.W., Turner, I.M., Dominy, N.J., and Yamashita, N. (2000). Mechanical Defencesto Herbivory. *Ann. Bot.* **86**: 913–920.

Luo, W. and Brouwer, C. (2013). Pathview: An R/Bioconductor package for pathway-

based data integration and visualization. *Bioinformatics* **29**: 1830–1831.

Malinovsky, F.G., Fangel, J.U., and Willats, W.G.T. (2014). The role of the cell wall in plant immunity. *Front. Plant Sci*. **5**: 1–12.

McCarthy, R.L., Zhong, R., and Ye, Z.H. (2009). MYB83 is a direct target of SND1 and acts redundantly with MYB46 in the regulation of secondary cell wall biosynthesis in arabidopsis. *Plant Cell Physiol*. **50**: 1950–1964.

Nicholson, R.L. and Hammerschmidt, R. (1992). Phenolic Compounds and Their Role Disease Resistance. *Annu. Rev. Phytopathol*. **30**: 369–389.

O'Brien, T.P., Feder, N., and McCully, M.E. (1964). Polychromatic staining of plant cell walls by toluidine blue O. *Protoplasma*. **59**: 368–373.

Rácz, A., Hideg, É., and Czégény, G. (2018). Selective responses of class III plant peroxidase isoforms to environmentally relevant UV-B doses. *J. Plant Physiol*. **221**: 101–106.

Robinson, M.D. and Oshlack, A. (2010). A scaling normalization method for differential expression analysis of RNA-seq data. *Genome Biol*. **11**: 1–9.

Rocha, C.S., Santos, A.A., Machado, J.P.B., and Fontes, E.P.B. (2008). The ribosomal protein L10/QM-like protein is a component of the NIK-mediated antiviral signaling. *Virology*. **380**: 165–169.

Santos, A.A., Carvalho, C.M., Florentino, L.H., Ramos, H.J.O., and Fontes, E.P.B. (2009). Conserved threonine residues within the A-loop of the receptor NIK differentially regulate the kinase function required for antiviral signaling. *PLoS ONE*. **4**:e5781.

Sattler, S.E. and Funnell-Harris, D.L. (2013). Modifying lignin to improve bioenergy feedstocks: Strengthening the barrier against pathogens? *Front. Plant Sci*. **4**: 1–8.

Schilmiller, A.L., Stout, J., Weng, J.K., Humphreys, J., Ruegger, M.O., and Chapple,
C. (2009). Mutations in the cinnamate 4-hydroxylase gene impact metabolism, growthand development in Arabidopsis. *Plant J*. **60**: 771–782.

Schmieder, R. and Edwards, R. (2011). Quality control and preprocessing of metagenomic datasets. Bioinformatics **27**: 863–864.

Shigeto J., Itoh Y., Hirao S., Ohira K., Fujita K., Tsutsumi Y. (2015) Simultaneously disrupting *AtPrx2*, *AtPrx25* and *AtPrx71* alters lignin content and structure in *Arabidopsis* stem. *J. Integr. Plant Biol.* **57**:349–356

Tang, Y. et al. (2019). Overexpression of a myb family gene, Osmyb6, increases drought and salinity stress tolerance in transgenic rice. *Front. Plant Sci*. **10**: 1–12.

Torres, M.A. (2010). ROS in biotic interactions. *Physiol. Plant*. **138**: 414–429.

Tsuda, K. and Katagiri, F. (2010). Comparing signaling mechanisms engaged in pattern-triggered and effector-triggered immunity. *Curr. Opin. Plant Biol*. **13**: 459–465.

Umezawa T. 2018. Lignin modification in planta for valorization. *Phytochemistry Reviews,* **17**: 1305– 1327.

Vanholme, R., Demedts, B., Morreel, K., Ralph, J. and Boerjan, W. (2010). Lignin biosynthesis and structure. *Plant Physiol*., **153**: 895–905.

Vanholme, R., Storme, V., Vanholme, B., Sundin, L., Christensen, J. H., Goeminne, G., Halpin, C., Rohde, A., Morreel, K., & Boerjan, W. (2012). A systems biology view of responses to lignin biosynthesis perturbations in Arabidopsis. *The Plant cell*, **9**: 3506–3529.

Vogt, T. (2010). Phenylpropanoid biosynthesis. *Mol. Plant* **3**: 2–20.

Wainhouse, D., Cross, D.J., and Howell, R.S. (1990). The Role of Lignin as a Defence against the Spruce Bark Beetle Dendroctonus micans: Effect on Larvae and Adults. *Oecologia* **85**:257–265.

Wagner A., Donaldson L., Kim H., Phillips L., Flint H., Steward D., Torr K., Koch G., Schmitt U., Ralph J. (2009). Suppression of 4-coumarate-CoA ligase in the coniferous gymnosperm *Pinus radiata*. *Plant Physiol.* **149**:370–383.

Yamaguchi, N., Winter, C.M., Wu, M.-F., Kwon, C.S., William, D.A., and Wagner, D. (2014). PROTOCOL: Chromatin Immunoprecipitation from Arabidopsis Tissues. *Arab*. B.**12**: e0170.

Yoo, S.D., Cho, Y.H., and Sheen, J. (2007). Arabidopsis mesophyll protoplasts: A versatile cell system for transient gene expression analysis. *Nat. Protoc*. **2**: 1565–1572.

Zhang, Y., Liu, T., Meyer, C.A., Eeckhoute, J., Johnson, D.S., Bernstein, B.E., Nussbaum, C., Myers, R.M., Brown, M., Li, W., and Shirley, X.S. (2008). Model-based analysis of ChIP-Seq (MACS). *Genome Biol*. **9**.

Zhao, Q. (2016). Lignification: Flexibility, Biosynthesis and Regulation. *Trends Plant Sci*. **21**: 713–721.

Zhao, Q., Nakashima, J., Chen, F., Yin, Y., Fu, C., Yun, J., Shao, H., Wang, X., Wang,Z. and Dixon, R.A. (2013). LACCASE is necessary and nonredundant with PEROXIDASE for lignin polymerization during vascular development in *Arabidopsis*. *Plant Cell.* **25**:3976–3987.

Zhong, R., Richardson, E.A., and Ye, Z.H. (2007). The MYB46 transcription factor is a direct target of SND1 and regulates secondary wall biosynthesis in Arabidopsis. *Plant Cell* **19**: 2776–2792.

Zhou, Y.-H., Zhang, Y.-Y., Zhao, X., Yu, H.-J., Shi, K., and Yu, J.-Q. (2009). Impact of Light Variation on Development of Photoprotection, Antioxidants, and Nutritional Valuein Lactuca sativa L. *J. Agric. Food Chem*. **57**: 5494–5500.

Zhu, L.J. (2013). Integrative analysis of ChIP-chip and ChIP-seq dataset. *Methods Mol. Biol*. **1087**: 105–124.

Zhu, L.J., Gazin, C., Lawson, N.D., Pagès, H., Lin, S.M., Lapointe, D.S., and Green, M.R. (2010). ChIPpeakAnno: A Bioconductor package to annotate ChIP-seq and ChIP-chip data. *BMC Bioinformatics* **11.**

Zorzatto, C. et al. (2015). NIK1-mediated translation suppression functions as a plant antiviralimmunity mechanism. *Nature* **520**: 679–682.

Figure and legends

A

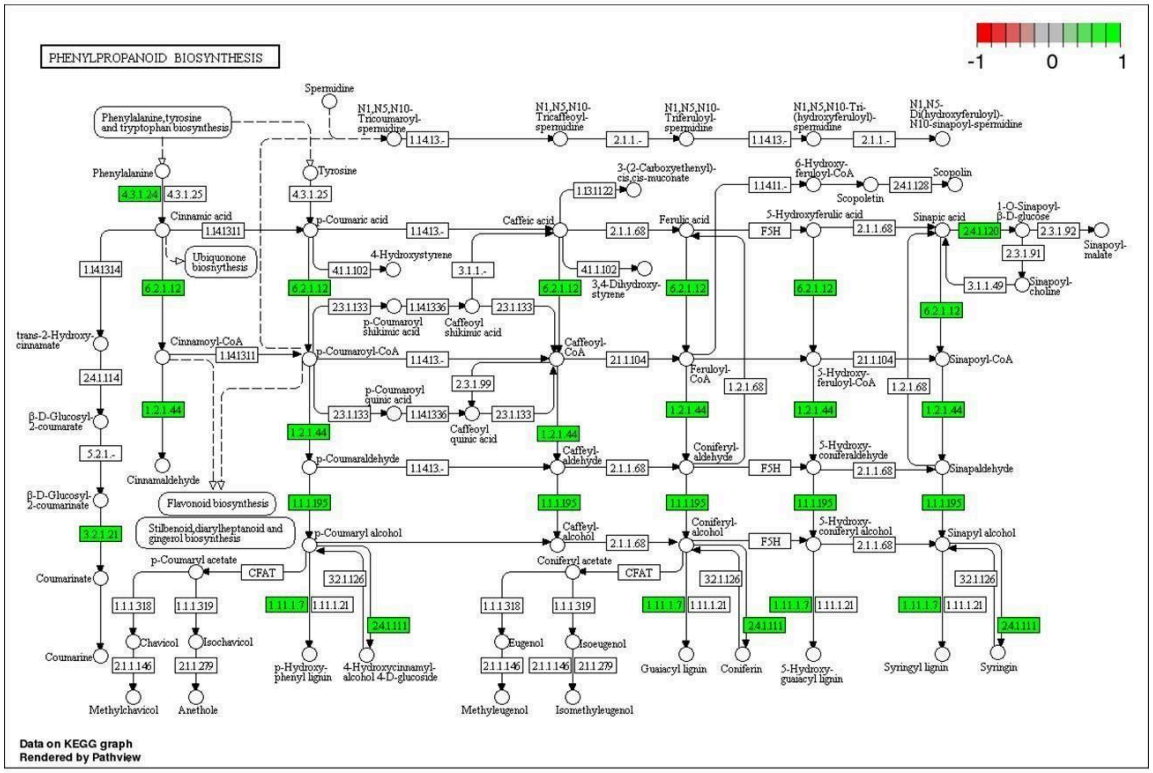

B

Id gene	Upstream	log2FC	Log10 q-value	padj
POD (AT2G35380)	-622	2,63	11,46	0
4CL2 (AT3G21240)	-164	1,92	19,15	0

Figure 1. Genes encoding phenylpropanoid biosynthesis enzymes are enriched in the LIMYB up-regulon, identified by overlapping LIMYB upregulated genes (RNA-seq) and ChIP-seq data. (**A**) The KEGG phenylpropanoid biosynthetic pathway shows the genes differentially expressed by LIMYB overexpression and transcriptional activity. In the schematic representation, red means genes downregulated, and green is upregulated. (**B**) Upstream position of LIMYB DNA-binding motifs and expression levels of selected genes detected by ChIP- Seq and RNA-Seq, respectively.

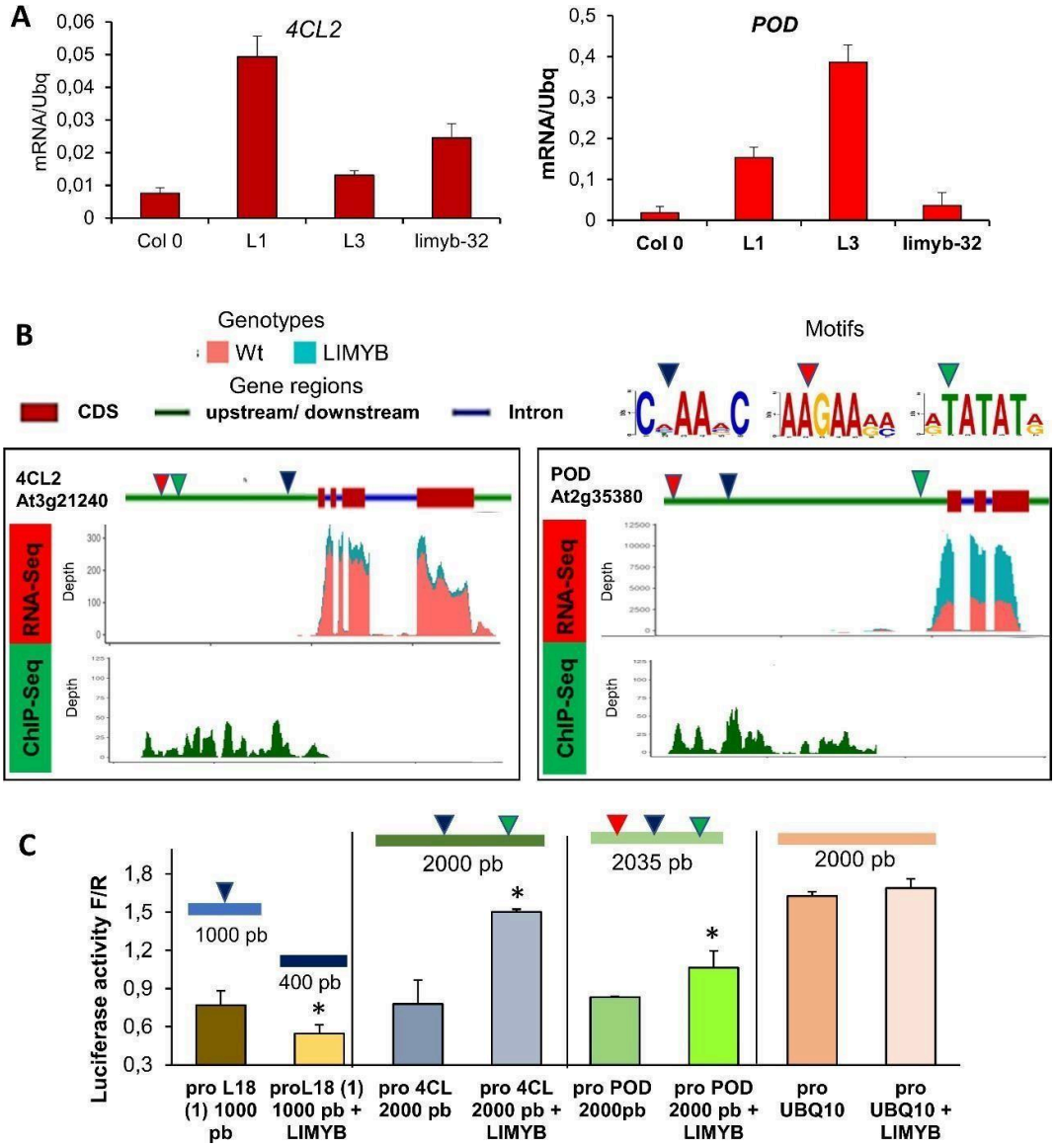

Figure 2. LIMYB induces the selected 4CL2 and POD promoter activities and gene expression. (**A**) Up-regulation of 4CL2 and POD genes by LIMYB. Accumulation of gene transcripts in LYMYB-overexpressing lines L1 and L3 and *limyb-32* knockout line was analyzed by RT-qPCR, and the absolute expression was calculated using the $2^{-\Delta Ct}$ method; ubiquitin was used as an endogenous control for data normalization. The bars represent a 95% confidence interval based on replicates from 3 independent experiment samples. (**B**) The LIMYB binding peaks (ChIP-seq) reside in the promoter region of the selected upregulated genes. Peaks of LIMYB binding sites were mapped to the upstream promoter region and the hits of RNA-sequencing in the coding region of the selected genes, as indicated in the figure. In the schematic representation of the loci, upstream promoter sequences are in green and coding regions in red. RNA-seq hits in red were from Col-0, and in blue, LIMYB-overexpressing lines. (**C**) LIMYB induces the 4CL2 and POD promoters. *N. benthamiana* leaves were co- transformed with either the 2000p4CL2:Luciferase or 2000pPOD:Luciferase construct and a 35S:RPL10 construct. After 48h, the luciferase activity was measured from the total protein extracts of transformed leaf discs. The RPL18 promoter was used as a positive control and the UBQ promoter as a negative control. Data are mean values ±SD. Asterisks indicate significant differences from the control (t-test, $p < 0.05$).

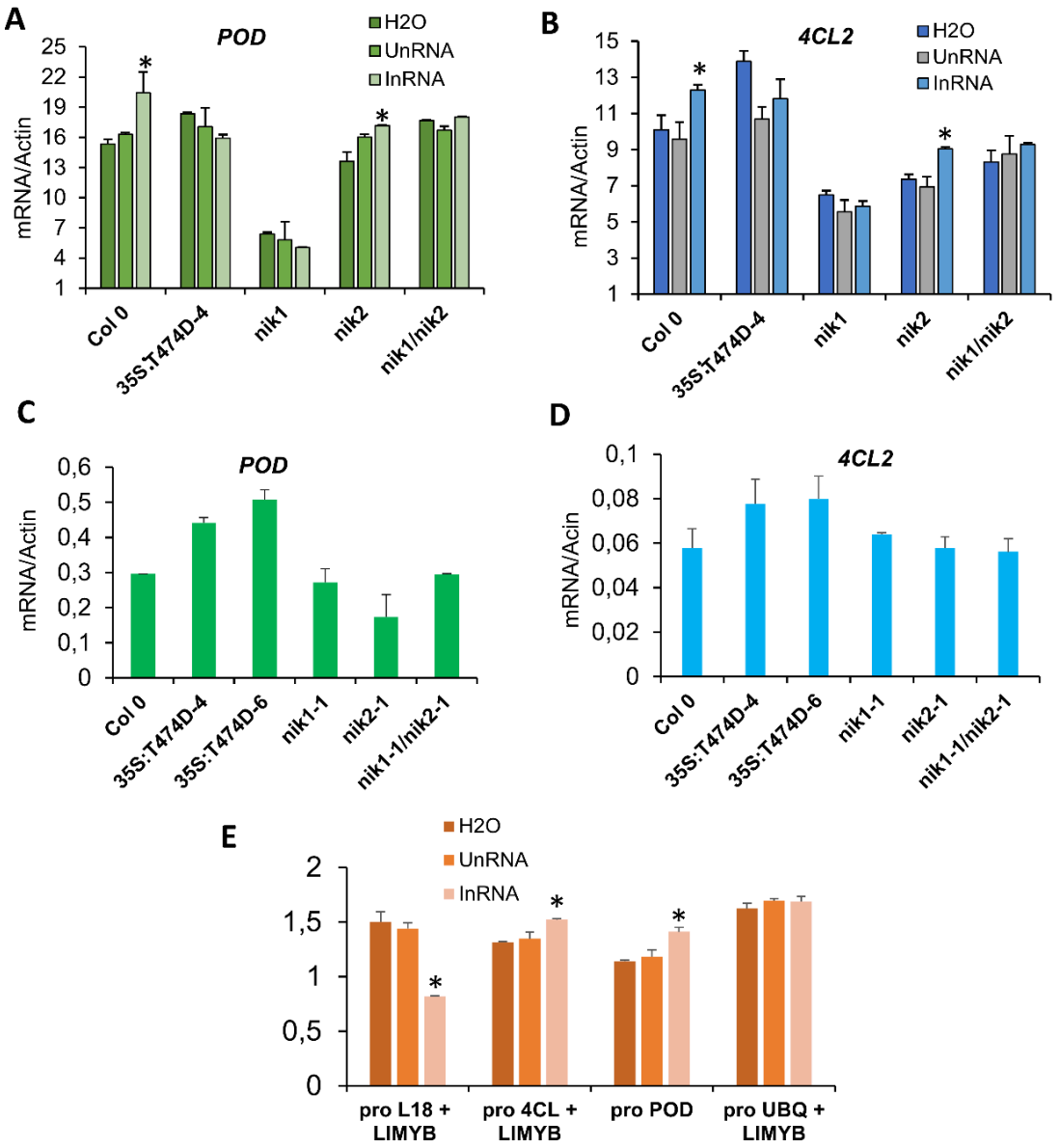

Figure 3. LIMYB-mediated up-regulation of target genes relies on the NIK1 antiviral signalingactivation. **(A)**, **(B)** Viral PAMPs induce the expression of POD **(A)** and 4CL2 **(B)** genes via NIK1 activation. Seedlings of the indicated genotypes were treated with RNA from begomovirus-infected (InRNA) and mock-inoculated plants (UnRNA) for 3h, and gene expression was determined by RT-qPCR, using actin as an endogenous control. The bars represent 95% confidence interval based on replicates from 3 independent experiment samples. **(C)**, **(D)** Constitutive activation of NIK1 up-regulated POD (**C**) and 4CL2 **(D)** genes. Total RNA was extracted from the indicated genotypes, and absolute expression was monitored by RT=qPCR. The bars represent a 95% confidence interval based on replicates from 3 independent experiment samples. **(E)** The viral PAMP InRNA induces promoter activity of 4CL2 and POD genes in the presence of LIMYB. Arabidopsis limyb protoplasts transformed with 35S:LIMYB-GFP were treated with InRNA from begomovirus-infected plants and UnRNA from mock-inoculated plants for3h, and gene expression was monitored by RT-qPCR. Data are mean values ±SD. Asterisks indicate differences from the control (Test-t, $p < 0.05$).

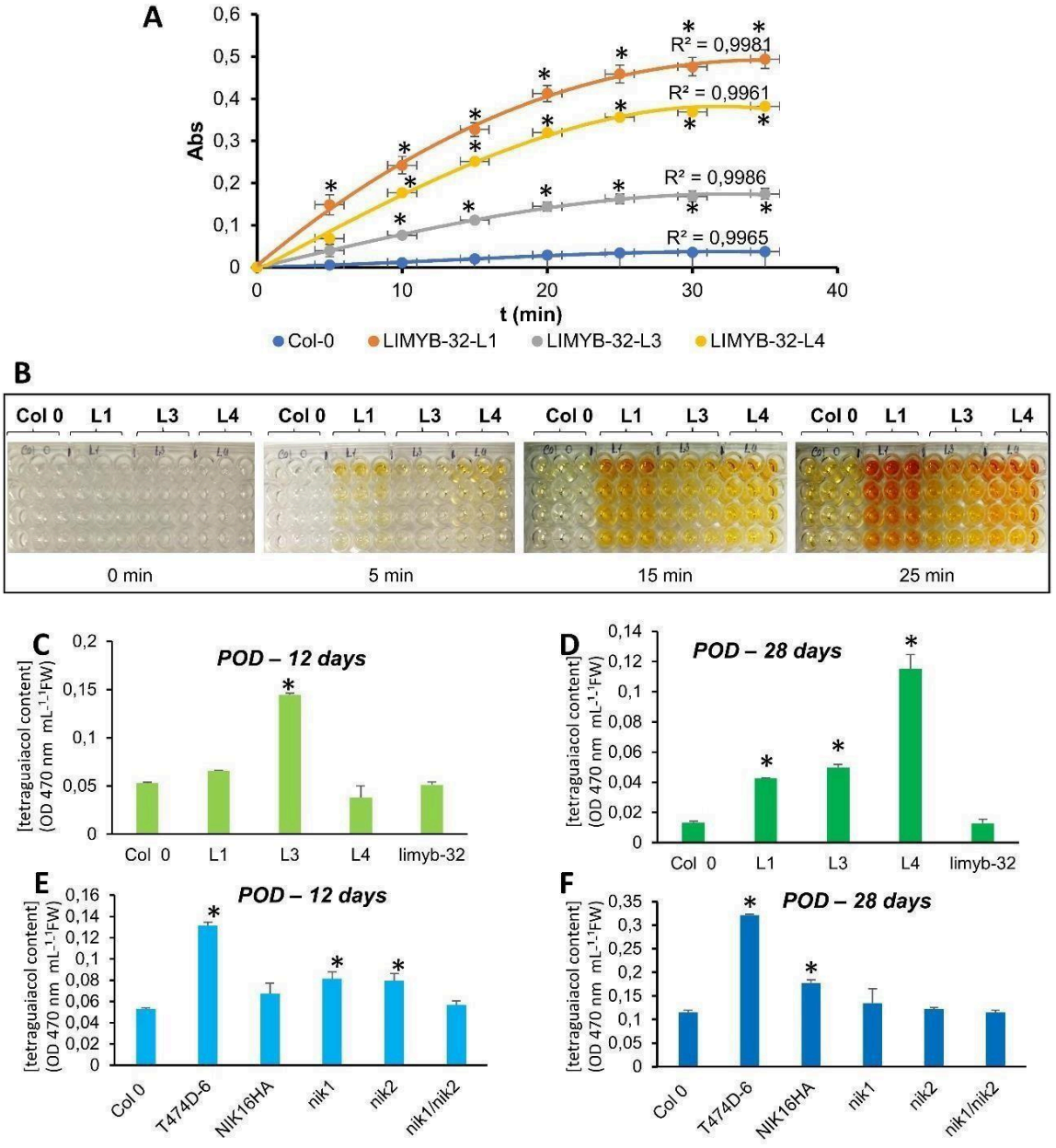

Figure 4. LIMYB-induced POD activity is regulated by NIK1 activation. Analysis POD activity in LIMYB-overexpressing lines and NIK1 lines, measured with POD substrates. **(A)**, **(B)** POD activity was monitored with OPD substrate in LIMYB-overexpressing and knockoutlines for 5 up to 35 min. **(C)**, **(D)**, **(E)** and (**F**) 2-methoxyphenyl (guaiacol) was used to monitor peroxidase activity in plants of 12 and 28-old-days in LIMYB and NIK1 genotypes. Data are mean values ±SD. Asterisks indicate significant differences from the control samples (test-t, $p < 0.05$).

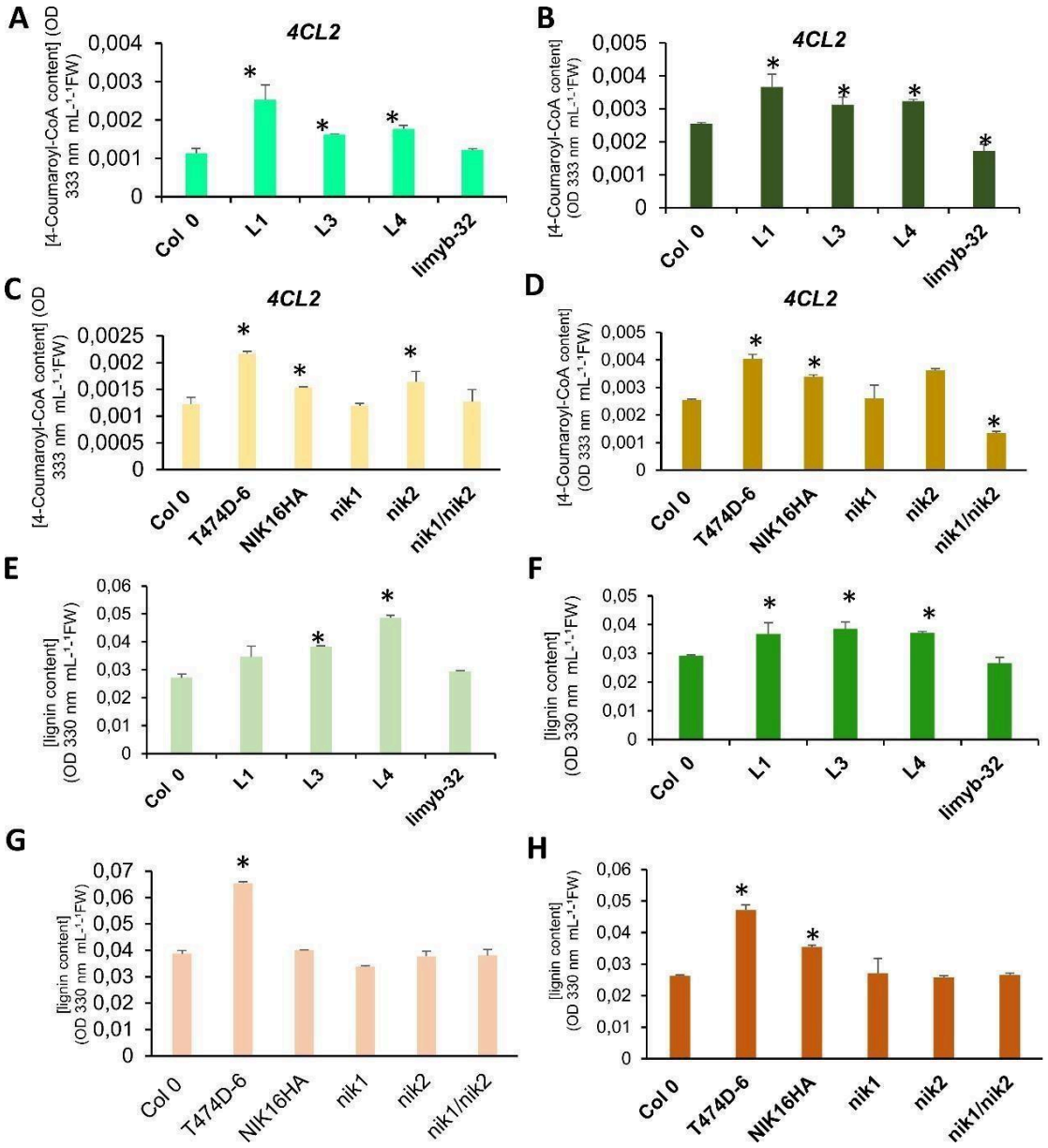

Figure 5. LIMYB-induced 4CL2 activity and lignin accumulation are regulated by NIK1 activation. 4CL2 activity and lignin accumulation were measured in the genotypes indicated inthe figure. (**A**), (**B**), (**C**), and (**D**) 4CL2 activity was measured by determining the content of 4-coumaroyl-CoA for 40 min in 12- and 28-days-old plants. (**E**), (**F**), (**G**), and (**H**) Lignin accumulation was measured by determining the total amount of derivative with to-glycolic acid. Data are mean values ±SD. Asterisks indicate statistically significant differences from the control (test-t, $p < 0.05$).

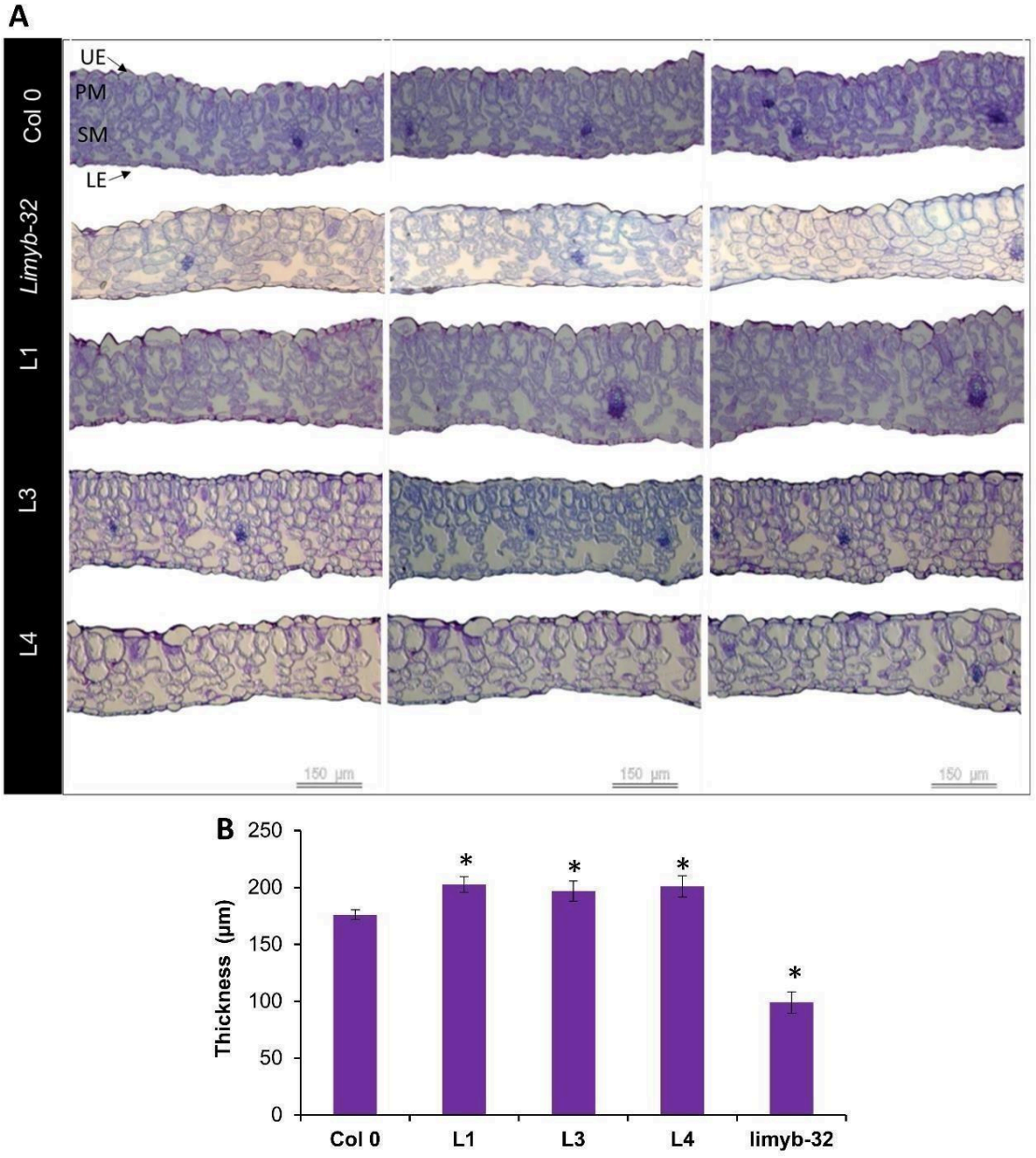

Figure 6. Enhanced lignification in LIMYB-overexpressing transgenic Arabidopsis leaves. (**A**) Transverse leaf sections were photographed with Toluidine Blue O by microscopy to show lignin deposition in the ultrastructure of leaf regions of Col-0, three transgenic lines (L1, L3 e L4), and *limyb-32*. UE, upper epidermis layer; PM, palisade mesophyll layer; SM, spongy mesophyll layer; LE, lower epidermis layer. (**B**) The thickness of foliar mesophyll is affected by lignification in transgenic lines. The thickness of foliar mesophyll of the different genotypes(as indicated in the figure) was measured by Image-Plus 7.

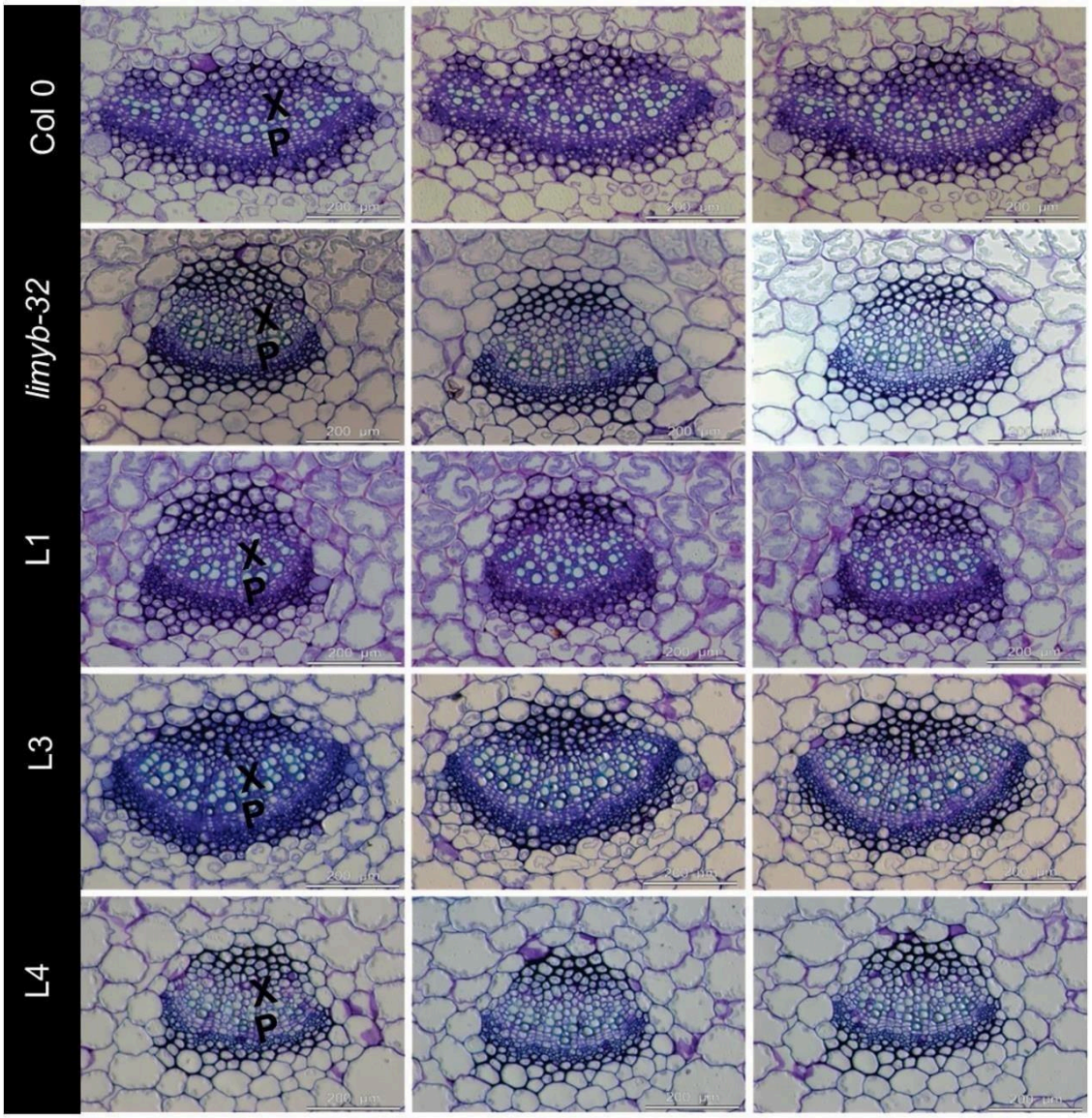

Figure 7. Histological staining for lignin deposition in LIMYB-overexpressing transgenic Arabidopsis plants. Transverse leaf vein sections were photographed with Toluidine Blue O by microscopy to show lignin deposition in the ultrastructure of the xylem of Col-0, three transgenic lines L1, L3, L4, and the *limyb-32* knockout line.

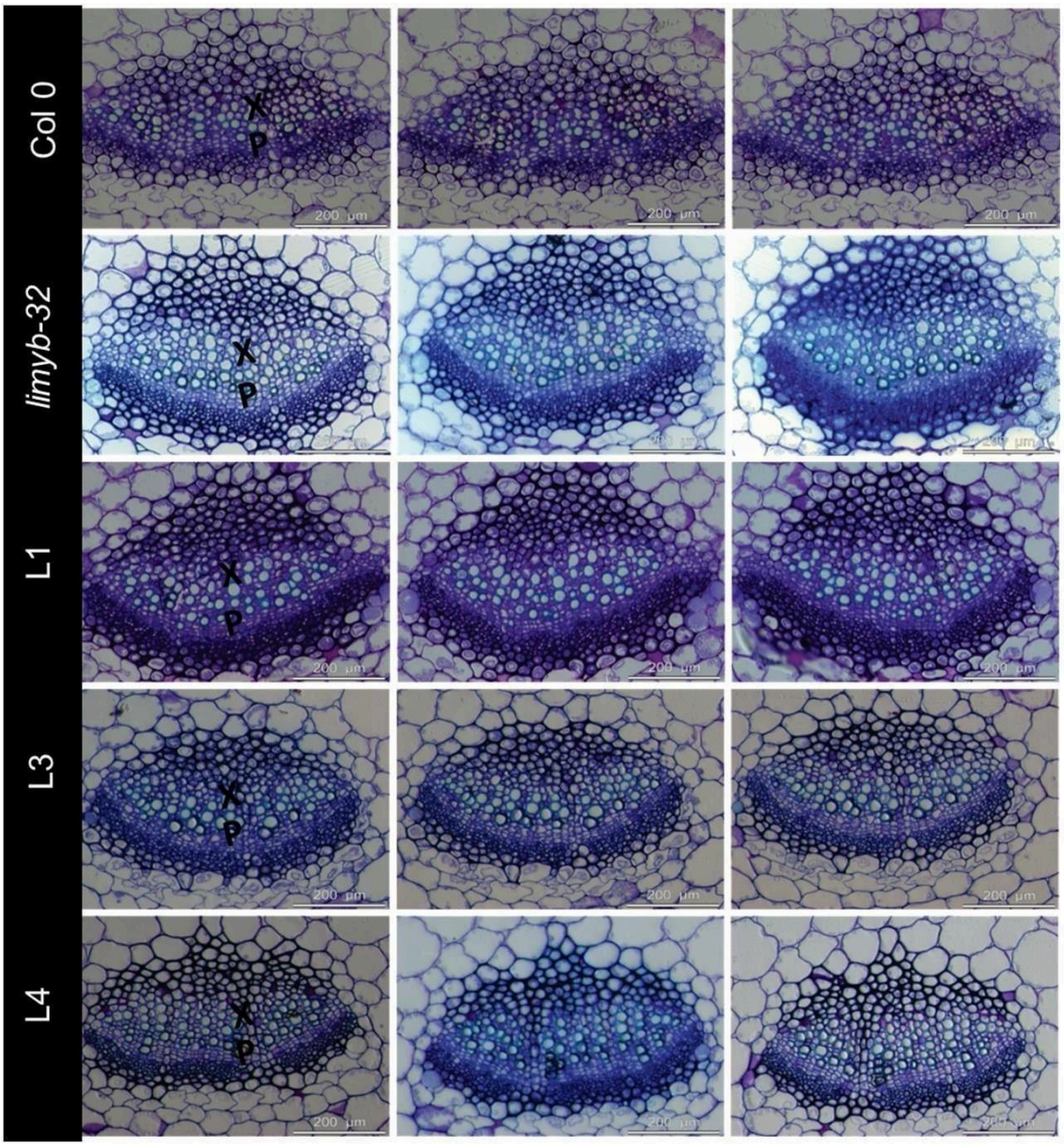

Figure 8. Histological analysis of lignin deposition in LIMYB-overexpressing transgenic Arabidopsis plants. Transverse petiole leaf sections were photographed with Toluidine Blue Oby microscopy to show lignin deposition in the ultrastructure of the xylem of Col- 0, three transgenic lines L1, L3, L4, and the *limyb-32* knockout line.

Table 1 - Primers used in Materials and methods

Primers for RT-qPCR		
	Fwd Primer	**Rvs Primer**
RT-qPCR Luci. Fire	GCGAAGGTTGTGGATCTGGA	CGTCTTCGTCCCAGTAAGCT
RT-qPCR Actina	ATGTCGTGAGCCATCCTGTC	ACACCGGATTCGTGCGGCAT
QRT-POD	ACATTCAAGATCTCATCGCTC	ACTCATCGACGTAGAACGT
QRT-4CL2	AGTCAGGAGCATGTGGTA	GTTGCCACGGATGCATAT
Primers for cloning of gene		
LIMYB At5g05800B	AAAAAGCAGGCTTCACAATGAGG CCAAAAGCAGT	AGAAAGCTGGGTCCTATGTTG TAGTAGGAATAGG
Primers for cloning of promoters		
pRPL28e-TGW-Fwd(1)	GGGGACAACTTTGTATAGAAAAG TTGTCCCCAACCTCCCAGAATATG ACG	GGGGACTGCTTTTTTGTACAAA CTTGCTTCAAATACCTACCTTC ACCACAC
pRL18-TGW-FWD(1)	GGGGACAACTTTGTATAGAAAAG TTGTCGGAAGATGAGTATACGTA AATA	GGGGACTGCTTTTTTGTACAAA CTTGCAATTGAGATCCGATTA ACCTAA
pRL18-TGW-FWD(2)	GGGGACAACTTTGTATAGAAAAG TTGTCGTGTACCAGTAAAATGTTG TTG	
pRL18-TGW-FWD(3)	GGGGACAACTTTGTATAGAAAAG TTGTCGACCATAATCATATTCATT GAAGTG	
POD-TGW-FWD (1)	GGGGACAACTTTGTATAGAAAAG TTGTCTCAGCCCAAGGATCAATC	GGGGACTGCTTTTTTGTACAAA CTTGCTCTGTTCATCTCTATCT GTGTT
POD-TGW-FWD (2)	GGGGACAACTTTGTATAGAAAAG TTGTCCAAGAATTAGAAAGAAGG GAGAG	
4CL2-TGW-FWD(1)	GGGGACAACTTTGTATAGAAAAG TTGTCAGGATCAATGGAACAACC A	GGGGACTGCTTTTTTGTACAAA CTTGCCTGAAACAGAGCATGA TGATC
Primers for RT-PCR		
RT FWD Actin	ATGGCTGAGGCTGATGATATTCA ACC	CCGTACAGATCCTTCCTGATAT CCACA
RTCalCuV_CompB2	TTCATGGACACCAGGAGA	TACACGTGTCCTATGGAGTC

General Conclusion

Plants need highly coordinated mechanisms to overcome environmental adversities involving biotic and abiotic factors. Although they have systems objectively focused on specific answers, strategies for connecting the pathways for an effective response are necessary. In RNA-mediated antiviral immunity, two mechanisms are essential for protection against RNA or DNA viruses, PTGS and TGS. While PTGS is used as a defense that neutralizes both RNA and DNA viruses by intercepting mRNA for suppression or degradation, TGS is targeted at DNA viruses. TGS uses chromatin methylation for heterochromatin formation. These strategies are targeted by geminivirus proteins, which inhibit or hijack components of the host's antiviraldefense, or by activating or inhibiting the expression of endogenous suppressors. Another strategy limiting geminivirus infection has been recently demonstrated as the classical plant PTI, functioning similarly to the defense against non-viral pathogens. Thus, in addition to silencing strategies, geminiviruses also inhibit steps from the host's innate immunity to make the infection successful (Chapter I).

In this investigation, we have also provided several lines of evidence that begomovirus-derived nucleic acids function as viral PAMPs and activate the NIK1-mediated antiviral signaling, which leads to the suppression of global translation as a defense mechanism that prevents the translation of viral mRNAs. First, we showed that treatment of Arabidopsis seedlings with RNA from begomovirus-infected plants, but not from mock-inoculated plants, repressed the expression of translation-related marker genes in a manner dependent on NIK1 and NIK2 receptors (Chapter II). Likewise, DNA from infected plants, but not from mock- inoculated plants, activates NIK1/NIK2 mediated signaling by repressing the marker genes, ribosomal protein genes, and translation regulatory genes. Furthermore, both RNA and DNA from infected plants induced rapid phosphorylation of NIK1, RPL10 phosphorylation and repressed the expression of the photosynthesis-related marker genes (Chapter III). The viral PAMPs-induced activation of the NIK1/RPL10/LIMYB signaling module required the function of NIK1 and NIK2, but not the PTI receptor FLS2 and co-receptor BAK1, indicating that most likely a yet-to-be-identified viral PAMP-sensing receptor activates NIK1.

Geminivirus infection has also been shown to activate the ETI response, such as cell death, HR, ROS, and SA accumulation. Although many studies show that PTI and ETI responses are activated by geminiviruses, few studies have focused on discovering the elicitor molecules of these processes, which may prove to be a crucial factor in setting up

strategies in the field of genetic engineering to enhance plant resistance to pathogens. Furthermore, as viruses are mandatory intracellular parasites and may not have access to the apoplast, it remains to be determined how PRRs would detect viruses, PAMPs, and viral agents to better understand thesteps at the beginning of triggering the immune response.

By combining the results of RNA-seq and ChIP-seq on LIMYB-overexpressing lines and promoter transactivation assays in protoplasts, we defined the LIMYB upregulon and downregulon and demonstrated that the NIK1/RPL10/LIMYB signaling circuit also controls photosynthesis and growth (Chapter III). LIMYB overexpression repressed photosynthetic-apparatus-related genes, which leads to a decrease in photosynthesis rate, stomatal conductance, transpiration, electron transport rate, and quantum efficiency. Furthermore, T474D ectopic expression in Col-0, but not in the *limyb* knockout line, recapitulated the repression of translation- and photosynthesis-related marker genes and decreased photosynthetic function. Finally, we also showed that treatment with both bacterial and viral PAMPs, known to activatethe NIK1/RPL10/LIMYB signaling, also caused the repression of photosynthesis-related marker genes in Col-0, but not in nik1/nik2 double mutant and *limyb* mutant. Remarkably, ourresults indicated that the NIK1/RPL10/LIMYB signaling module is activated by abiotic stresses, including high temperature and osmotic stress. Both stress treatments promoted a rapidNIK1 phosphorylation, followed by RPL10 phosphorylation and repression of the translation- and photosynthesis-related marker genes. Therefore, the NIK1/RPL10/LIMYB signaling circuit is capable of perceiving multiple signals and thus coordinates translation and photosynthesis in plant cells. The coordinated repression of photosynthesis and translation via the stress-activated NIK1/RPL10/LIMYB signaling module may adjust the plant growth patternin response to the changing environment.

We have provided several lines of evidence that NIK1 may function as co-receptor from several transmembrane stress-sensing receptors. First, NIK1 undergoes phosphorylation under multiple abiotic and biotic signals activating the NIK1/RPL10/LIMYB signaling circuit, which coordinates the regulation of translation and photosynthesis in plant cells. Conceptually, signaling receptors recognize stimulus with high specificity and affinity, which precludes one single receptor from being activated by multiple signals. Second, NIK1 has been demonstratedto be capable of forming a high centrality hub, to which converge the interactions of several different receptors. Third, NIK1 shared structural and biochemical properties with BAK1, which has been shown to function as co-receptor of several transmembrane receptors. Finally, we have shown that the bacterial PAMP flg22 induces

NIK1 phosphorylation and activation via an activated immune complex FLS2-BAK1. The bacterial PAMP flg22, but not viral PAMPs, requires the immune complex FLS2-BAK1 for mediating NIK1 phosphorylation and activation. A yet-to-be-determined viral pattern recognition receptor may likely sense viral PAMPs to mediate NIK1 activation in response to viral infection. Thus, we propose that NIK1 forms a central signaling hub that integrates signals from multiple stress-sensing receptors to control growth under stress conditions. NIK1 activation by pathogen and environmental signals leads to coordinate suppression of photosynthesis and translation via the repressing transcriptional activity of LIMYB.

We also show here that, in addition to the repressive function, LIMYB also functions as a transcriptional activator, which induces the expression of genes associated with phenylpropanoid biosynthesis, involved in lignin deposition (Chapter IV). LIMYB-overexpressing lines displayed a higher activity of 4CL2 and POD, resulting in increased lignin content compared to control lines. This phenotype was recapitulated in T474D-expressing lines, indicating that LIMYB-mediated lignin deposition was associated with NIK1 activation. Similar to the responses of PTI and ETI, which have shown increased lignin content in cell wall composition, the NIK1/RPL10/LIMYB signaling module may operate as a complementary mechanism of host defense against non-viral pathogens, providing a physical and spatial barrier to contain the traffic of pathogens.